CT 733-SS1
Don. 2013

xx(209427.1)

Centro de Investigación y de Estudios Avanzados

del Instituto Politécnico Nacional

Unidad Guadalajara

Un Nuevo Enfoque en el Modelado de Líneas de Transmisión Multiconductoras para el Análisis de Transitorios en el Dominio del Tiempo

Tesis que presenta

Juan Carlos Escamilla Sánchez

Para obtener el grado de

Doctor en Ciencias

En la Especialidad de

Ingeniería Eléctrica

Director de Tesis

Dr. Pablo Moreno Villalobos

CINVESTAV del IPN Unidad Guadalajara, Guadalajara, Jalisco, Diciembre 2012.

CLASIF.. CT 00637
ADQUIS.. CT-733-SSI
FECHA: 16-07-2013
PROCED.. Don.-2013
$

ID: 20°1077-2001

Centro de Investigación y de Estudios Avanzados

del Instituto Politécnico Nacional

Unidad Guadalajara

A New Approach for Modeling Multiconductor Transmission Lines for Time Domain Transients Analysis

A thesis presented by·

Juan Carlos Escamilla Sánchez

to obtain the degree of:
Doctor of Sciences

in the subject of:
Electrical Engineering

Thesis Advisors:
Dr. Pablo Moreno Villalobos

CINVESTAV del IPN Unidad Guadalajara, Guadalajara, Jalisco, December 2012.

Un Nuevo Enfoque en el Modelado de Líneas de Transmisión Multiconductoras para el Análisis de Transitorios en el Dominio del Tiempo

Tesis de Doctorado en Ciencias en Ingeniería Eléctrica

Por:

Juan Carlos Escamilla Sánchez

Ingeniero Electricista
Escuela Superior de Ingeniería Mecánica y Eléctrica del IPN 2000 - 2004

Maestro en Ciencias en Ingeniería Eléctrica
SEPI-ESIME del IPN 2005-2008

Becario del CONACYT, expediente **219759**

Director de Tesis
Dr. Pablo Moreno Villalobos

CINVESTAV del IPN Unidad Guadalajara, Diciembre 2012

A New Approach for Modeling Multiconductor Transmission Lines for Time Domain Transient Analysis

Doctor of Science Thesis
in Electrical Engineering

By:

Juan Carlos Escamilla Sánchez

Electrical Engineering
Escuela Superior de Ingeniería Mecánica y Eléctrica del IPN 2000 - 2004

Master of Sciences in Electrical Engineering
SEPI-ESIME del IPN 2005-2008

Scholarship granted by CONACYT, No. **219759**

Thesis Advisor
Dr. Pablo Moreno Villalobos

CINVESTAV del IPN Unidad Guadalajara, December 2012.

Acknowledgements

I would like to thank to:

God.

My parents and brothers.

All the professors who have helped me in my stay at Cinvestav. Specially to Dr. Pablo Moreno and Dr. J. Luis Naredo for their patience, support and friendship.

Dr. Pablo Gómez for his invaluable suggestions and friendship.

CONACYT, for the scholarship.

Dedicated to my girlfriend Laura, Thank you for spending your live with me.

Index

List of Figures

Resumen

El análisis de transitorios electromagnéticos en líneas de transmisión requiere modelos capaces de reproducir los efectos producidos por la dependencia con respecto a la frecuencia de los parámetros eléctricos. Los modelos en el dominio del tiempo presentan algunos problemas para considerar estos efectos, mientras que en el dominio de la frecuencia esto se realiza directamente. Los modelos en el dominio de la frecuencia de líneas o cables son muy precisos; sin embargo presentan dificultades para considerar no linealidades y no es posible incluirlos en programas de simulación en el dominio del tiempo del tipo EMTP.

En este trabajo se presentan dos nuevos modelos de línea de transmisión multiconductora con parámetros eléctricos dependientes de la frecuencia para el análisis de transitorios electromagnéticos en el dominio del tiempo. Ambos modelos se basan en el método de características. En contraste con el método tradicional de características, los modelos presentados en este trabajo no requieren de la discretization espacial a lo largo de la línea. En ambos modelos, la dependencia frecuencial de los parámetros eléctricos se incluye por medio de la resistencia transitoria.

En el primer modelo, para obtener los voltajes y corrientes en los extremos de la línea de transmisión se determinan, por medio de interpolación lineal en el eje de propagación, los valores de voltajes y corrientes modales necesarios. Por otro lado en el segundo modelo, se aplica a cada modo por separado un método interpolación de segundo orden sobre el eje del tiempo. Este último modelo se usa también para el análisis de sistemas de transmisión subterráneos.

Abstract

Electromagnetic transient analysis in transmission lines requires models capable of reproducing the effects of the frequency dependence of the electrical parameters. Models in time domain present some problems considering these effects while in the frequency domain this is straightforward. Frequency domain models of lines and cables are very accurate; however, they present difficulties in dealing with nonlinearities and are impractical for interfacing them with time domain simulation programs such as EMTP.

In this work, two models for multiconductor transmission lines with frequency dependent electrical parameters, for time domain electromagnetic transient analysis are presented. The models are based on the method of characteristics. In contrast with the regular method of characteristics, the models presented in this work do not require the spatial discretization along the line. In both methods, the frequency dependence of the electrical parameters is included by means of a transient resistance.

In the first model for obtaining voltages and currents at the transmission line ends a linear interpolation method on the propagation axis is applied to determine the required values of modal voltages and currents. On the other hand, in the second model a second order interpolation on the time axis for each mode is performed in a separated way to calculate modal voltages, currents and convolution terms. This latter model is also used in the analysis of underground transmission systems.

1 Introduction

1.1 Background

An electromagnetic transient occurs when there is a sudden energy interchange between inductances and capacitances of the electrical power system. This change can be caused by direct or indirect lightning impacts, switching operations, faults etc. [1].

Electromagnetic transients produce overvoltages and overcurrents which propagate through the power system. Overvoltages can produce serious damage to electrical apparatus and systems. On the other hand overcurrents produce excessive heating in electrical appliances deteriorating the protecting insulation. Therefore, determination of the magnitude and characteristics of these quantities is very important in order to know how they affect the electrical equipment and the system in general [1, 2].

Transmission lines (TLs) are the largest part of the power system and through them the energy is transmitted to the distribution system to be sent to the consumption centers. The energy transmission should be done complying with several quality factors defined by each electrical company. Thus, it is very important to know the waveform and the magnitude of transient voltages and currents on a TL, since those variables could affect the operation of the system. Besides, with this information protections for all implicated electrical appliances can be designed, increasing the reliability of the system.

There are methods and models in the frequency and time domain for the analysis of electromagnetic transients on transmission lines. The first techniques used for these analyses were of a graphical type, two of the most known are Bergeron's method, which was developed for hydraulic system, and Bewley's method, best known as Lattice Diagram [2]. These methods do not directly consider losses or the frequency dependence of the electrical parameters of the line. H. W. Dommel developed in 1968 a

program in the time domain based on Bergeron's method, well known today as the "Electromagnetic Transients Program" (EMTP) [3]. Later on, alternative versions arose such as the "Electromagnetic Transients for Direct Current" (EMTDC) and the "Alternative Transient Program" (ATP).

The first models of single phase lines where the frequency dependence of the electrical parameters was considered appeared in the early 70's. These models were presented by Budner and Snelson in 1970 [4] and 1972 [5], respectively, and were based on introducing convolution operations in the transmission line equations. In 1975 H. W. Dommel and Meyer used in the EMTP the technique developed by Snelson solving the convolutions by means of the trapezoidal rule [5].

In 1975 A. Dabuleanu and A. Semlyen proposed a recursive solution for the convolutions; with this development, and using the modal domain, the analysis was extended to the multiconductor case [6].

In 1982, J. Martí developed a model where the frequency dependence of the propagation function and the characteristic impedance is considered. The characteristic impedance is taken into account by means of a rational approximation based on the Foster representation with poles and zeros obtained with Bode's method. This model considers the transformation matrix as real and constant [7]. In a subsequent work L. Martí presented a model that included the frequency dependence of the transformation matrix for the case of underground cables [8].

In 1998 Gustavsen and Semlyen proposed a method in the phase domain. In this work the characteristic impedance and the propagation function were modeled by using the vector fitting technique, where all the elements of each column of the transformation matrix are fitted using the same poles [9]. Another model in the phase domain was proposed by Morched, Gustavsen and Tartibi in 1999; this model arose from the necessities of modeling the high frequency dependence of the electrical parameters. The most important advantage of this last model is the adequate fitting of the characteristic admittance and the propagation function by means of rational approximations [10]. This model is considered today the most advanced and accurate one in the time domain.

In 2009 A. Ambrosio presented a method in time domain for modeling transmission lines with frequency dependent parameters [11]. The model is based on the method of characteristics [12]. The frequency dependence is included in the model by means of the transient resistance, which is expressed in terms of a sum of rational functions. The modal analysis is used to extend the method to multiconductor lines.

In general, in order to consider the skin effect due to the presence of non ideal conductors in the line it is necessary to approximate the frequency behavior of the electrical parameters. The approximation procedures besides being complex, produce errors in the results. It is shown in [13] that, even with an advanced line model, some errors still appear when high frequency dependence is considered. Using techniques in the frequency domain avoids those problems because it is no necessary to make approximations in considering the frequency dependence of electrical parameters. Moreover, with the development of numerical transformation techniques it is possible to obtain reliable results in time domain. However, when modeling systems with non-linear elements is needed, the methods in the frequency domain present difficulties since these techniques have been developed for linear time invariant systems [13, 14]. A procedure that makes used of the Superposition Theorem was presented by S. J. Day *et al.* in 1965 [15] and has been used for modeling some non-linear conditions in frequency domain techniques, but there are still some disadvantages in these methods [13].

1.2 Scope

As it was mentioned previously, there are many works which are related to the analysis and modeling of transmission lines. Neither the models in frequency domain nor the models in time domain can be used for modeling all kinds of transmission lines. Both domains present different disadvantages and restrictions. It is for this reason that these topics are still being investigated and this makes necessary to establish a general methodology that does not present the problems that are common in the models used nowadays.

In this work two models for multiconductor transmission lines with frequency dependent electrical parameters are presented. The models are based on the time domain solution of the telegrapher's equations using the method of characteristics. Rational approximations obtained by means of the vector fitting technique are used to include the frequency dependence of the electrical parameters. One of the methods is also used in cables modeling. The techniques presented in this thesis are validated by means of several examples and the results are compared with a method in the frequency domain and with simulations using the J. Marti Model and the ULM (Universal line model).

1.3 Review of J. Martí Model

In this section the model developed by J. Martí is described. The technique is based on the concept of weighting functions presented in the work by Meyer and Dommel [4, 7]. To avoid reflections at the end of the line an impedance whose frequency response is equal to that of the characteristic impedance is connected. This consideration allows to obtain the weighting functions $a_1(t)$ and $a_2(t)$, where $a_1(t)$ will have just the first spike and $a_2(t) = 0$. The response of the weighting functions and the equivalent network are shown in the Fig (1.1) and Fig. (1.2), respectively.

In order to obtain the weighting function, the backward and forward traveling functions in the frequency domain are obtained [7]:

$$F_K(w) = V_K(w) + Z_{eq}(w) I_K(w) \tag{1.1}$$

$$F_m(w) = V_m(w) + Z_{eq}(w) I_m(w) \tag{1.2}$$

$$B_K(w) = V_K(w) - Z_{eq}(w) I_K(w) \tag{1.3}$$

$$B_m(w) = V_m(w) - Z_{eq}(w) I_m(w) \tag{1.4}$$

Where F_K and F_m are the forward traveling function, B_K and B_m are the backward traveling function, Z_{eq} is the characteristic impedance. Considering that, the general solutions in the frequency domain is defined as follows [1]:

$$V_K(w) = \cosh[\gamma(w)\ell] V_m(w) - Z_c(w) \sinh[\gamma(w)\ell] I_m(w) \tag{1.5a}$$

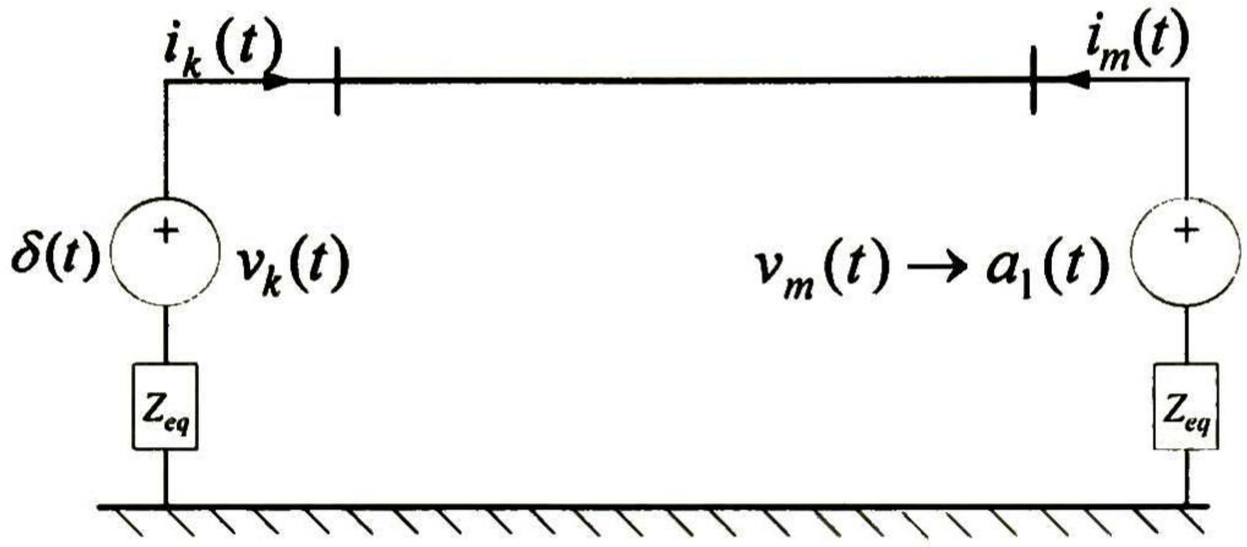

Figure 1.1 Equivalent network.

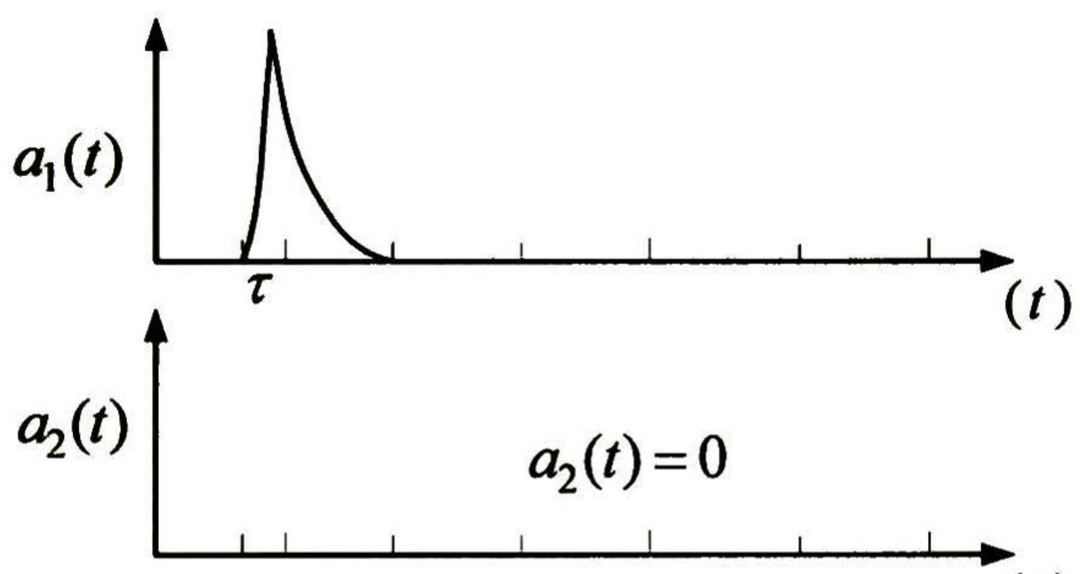

Figure 1.2. Weighting functions response.

$$I_K(w) = \frac{1}{Z_c(w)} \sinh\left[\gamma(w)\,\ell\right] V_m(w) - \cosh\left[\gamma(w)\,\ell\right] I_m(w) \qquad (1.5b)$$

where

$$Z_C(w) = \sqrt{Z(w)Y(w)} \text{ and } \gamma(w) = \sqrt{\frac{Z(w)}{Y(w)}} \qquad (1.6a), (1.6b)$$

by comparison of (1.1)-(1.4) with the general solution defined in (1.5) the next expressions are obtained:

$$B_K(w) = A_1(w) F_m(w) \qquad (1.7a)$$

$$B_m(w) = A_1(w) F_K(w) \qquad (1.7b)$$

where

$$A_1(w) = e^{-\gamma(w)\ell} = \frac{1}{\cosh[\gamma(w)\ell] + \sinh[\gamma(w)\ell]} \tag{1.8}$$

Expressing in time domain eqns. (1.7) gives:

$$b_k(t) = \int_{\tau}^{\infty} f_m(t-u)\, a_1(u)du \tag{1.9a}$$

$$b_m(t) = \int_{\tau}^{\infty} f_k(t-u)\, a_1(u)du \tag{1.9b}$$

As long as the time step Δt is smaller than τ, the values b_k and b_m can be defined from the past history terms of the function F_m and F_K. With these considerations and expressing eqns. (1.3) and (1.4) in time domain gives:

$$v_k(t) = e_k(t) + b_k \tag{1.10a}$$

$$v_m(t) = e_m(t) + b_m \tag{1.10b}$$

being e_k and e_m the voltages across $Z_{eq.}$ Equations (1.10) represent a model with a Norton's equivalent circuit for each TL end, as shown in Fig. (1.3).

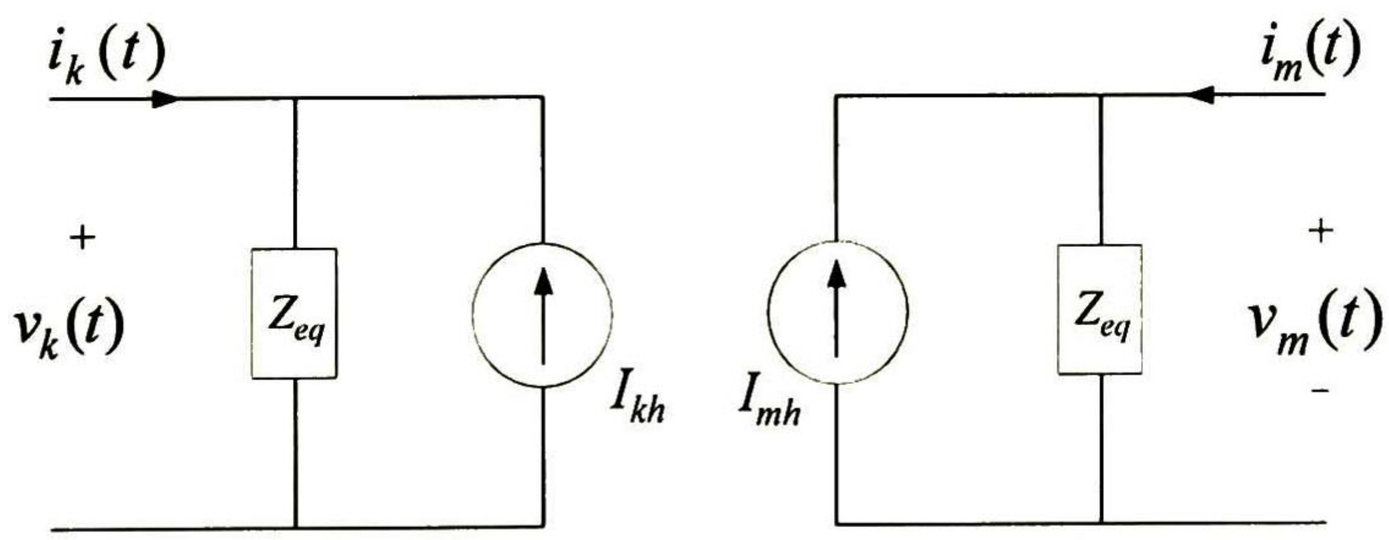

Figure 1.3. Norton´s circuit model.

1.3.1 Synthesis of the Characteristic Impedance and Propagation Function

The synthesis of the characteristic admittance is obtained by means of a Foster realization, as shown in Fig. (1.4).

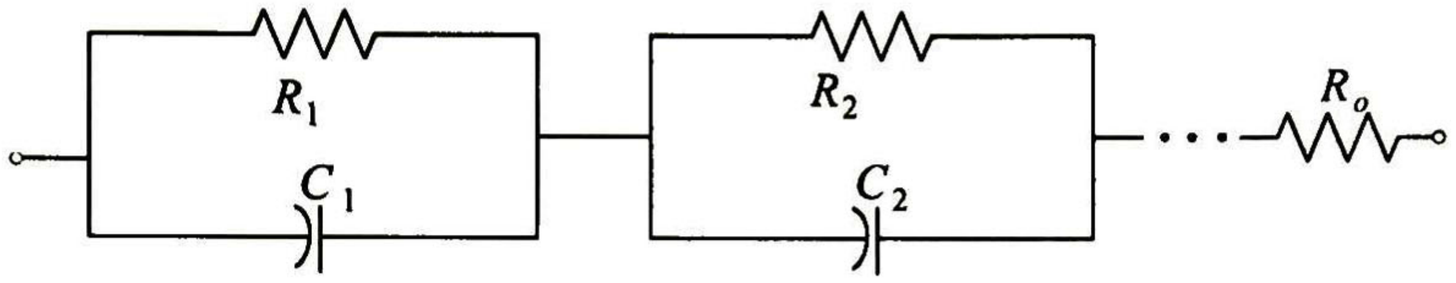

Figure 1.4. Foster representation.

where $R_o = k_o$, $R_i = k_i/p_i$, $C_i = 1/k_i$. For i=1, 2, …, n. The values p_i and k_i are the poles and residues obtained from the expansion in partials fractions of Z_{eq} as follows.

$$Z_{eq}(s) = k_o + \frac{k_1}{s+p_1} + \frac{k_2}{s+p_2} + \ldots + \frac{k_i}{s+p_i} \tag{1.11}$$

In order to obtain the current sources of Fig. (1.3), the evaluation of the weighting function of the history terms given by eqns. (1.9) is required. Recursive evaluation of the convolution integrals was adopted by J. Martí to approximate $a_1(t)$. According to Fig. (1.2) it can be seen that:

$$a_1(t) = p(t-\tau) \tag{1.12}$$

Expressing (1.12) in frequency domain gives:

$$A_1(w) = P(w)e^{-jw\tau} \tag{1.13}$$

The function $P(w)$ can be expanded in rational function as follows:

$$P_a(s) = \frac{N(s)}{D(s)} = H\frac{(s+z_1)(s+z_2)\ldots(s+z_n)}{(s+p_1)(s+p_2)\ldots(s+p_m)} \tag{1.14}$$

Substituting (1.14) in (1.13) and expressing the result in time domain the next expression is obtained:

$$a_1(t) = \left(K_1 e^{-p_1(t-\tau)} + K_2 e^{-p_2(t-\tau)} \ldots + K_m e^{-p_m(t-\tau)}\right)u(t-\tau) \tag{1.15}$$

This result allows evaluation of the history integrals in a recursive way.

1.4 Review of the Universal line Model

This technique is the most general model in the time domain for overhead and underground transmission lines. The model is developed in the phase domain and includes the frequency dependence of the electrical parameters. The model requires the synthesis of the characteristic admittance and the propagation function which present fast variation; this complicates the synthesis of these parameters. The propagation function is first fitted in the modal domain and with these results it is then fitted in the phase domain, whereas the characteristics admittance is fitted directly in the phase domain [10].

The relation between the voltages and currents at the ends of lines are defined by the next expression:

$$\mathbf{Y}_c\mathbf{v}-\mathbf{i}=2\mathbf{i}_i=2\mathbf{H}\,\mathbf{i}_{far} \tag{1.16}$$

where i_i and i_{far} are the incident and reflected currents respectively, Y_c and H are defined as follows:

$$\mathbf{H}=\exp\left(-\sqrt{\mathbf{YZ}}\ell\right) \tag{1.17a}$$

$$\mathbf{Y}_c=\mathbf{Z}^{-1}\sqrt{\mathbf{ZY}} \tag{1.17b}$$

The matrices Z and Y are the series impedance and the shunt admittance matrices per unit length. Applying modal decomposition to the H matrix the following expression is obtained:

$$\mathbf{H}(w)=\mathbf{T}e^{-\Lambda(w)\ell}\,\mathbf{T}^{-1}=\sum_{k=1}^{n}\mathbf{\Gamma}_k(w)e^{-\lambda_k(w)t}=\sum_{k=1}^{n}\mathbf{H}_k^{'}(w)e^{-jw\tau_k} \tag{1.18}$$

where T is the eigenvectors matrix. Γ_k is obtained from the product of the *kth* column of T times the *kth* row of $\mathbf{T}^{-1}$. From the combination of (1.18) and (1.16) and expressing the result in time domain gives:

$$\mathbf{Y}_c\mathbf{V}-\mathbf{i}=2\sum_{k=1}^{n}\mathbf{H}_k^{'}(t-\tau_k)\,i_{far} \tag{1.19}$$

The modal contribution of **H** can be defined as follows:

$$\mathbf{H}_k(w) = \mathbf{\Gamma}_k(w)e^{-\lambda_k(w)\ell} = \mathbf{\Gamma}_k(w)e^{-\lambda_k'(w)\ell}e^{jw\tau_k} \tag{1.20}$$

Using the vector fitting technique for the fitting of these functions and applying delay times to fit **H** in phase domain gives:

$$\mathrm{H}_{ij}(jw_1) = \sum_{k=1}^{n}\left[\sum_{k=1}^{N_k}\frac{c_{mkij}}{jw_1 - p_{mk}}\right]e^{-jw_1\tau_k} \tag{1.21a}$$

where N_k is the number of poles for the *kth* mode. Expressing (1.21a) in matrix form gives the following:

$$\mathbf{AX} = \mathbf{B} \tag{1.21b}$$

where **X** are the residues matrix, the columns and rows of **A** and **B** correspond to the frequency points and to the elements of **H,** respectively. The poles p_{mk} are included in the *ith* and *jth* element of the fitted **H**-matrix.

1.5 Review of the Characteristics Model with Spatial Discretization

The time domain equations for an overhead multiconductor transmission line with frequency dependent electrical parameters can be expressed as follows [12, 34].

$$\frac{\partial}{\partial\xi}\mathbf{U} + \mathbf{A}\frac{\partial}{\partial t}\mathbf{U} + \mathbf{BU} + \mathbf{W} = \mathbf{0} \tag{1.22}$$

where

$$\mathbf{A} = \begin{bmatrix} \mathbf{0} & \mathbf{C}^{-1} \\ \mathbf{D}^{-1} & \mathbf{0} \end{bmatrix} \qquad \mathbf{B} = \begin{bmatrix} \mathbf{C}^{-1}\mathbf{G} & \mathbf{0} \\ \mathbf{0} & \mathbf{D}^{-1}\mathbf{R}_x \end{bmatrix} \tag{1.23a), (1.23b}$$

$$\mathbf{U} = \begin{bmatrix} \mathbf{V} \\ \mathbf{I} \end{bmatrix} \qquad \mathbf{W} = \begin{bmatrix} \mathbf{0} \\ \mathbf{D}^{-1}\mathbf{\Psi} \end{bmatrix} \tag{1.24a), (1.24b}$$

The parameters **C** and **G** are defined in section 2.2; **D**, $\mathbf{R}_x$ and $\mathbf{\Psi}$ are defined in Appendix B. In order to find a solution for **V** and **I**, (1.22) should be modified performing a time domain modal analysis. Applying modal analysis as it is shown in [34] the next equations system for the *jth* mode are obtained:

$$\left(\frac{\partial}{\partial t}+\gamma_j\frac{\partial}{\partial \xi}\right)V_{mj}(\xi,t)+Z_{wj}\left(\frac{\partial}{\partial t}+\gamma_j\frac{\partial}{\partial \xi}\right)I_{mj}(\xi,t)$$
$$+\gamma_j\sum_{k=1}^{n}\tilde{R}_{jk}I_{mk}(\xi,t)+\gamma_j Z_{wj}\tilde{G}_j V_{mj}(\xi,t)=0 \qquad (1.25a)$$

$$\left(\frac{\partial}{\partial t}-\gamma_j\frac{\partial}{\partial \xi}\right)V_{mj}(\xi,t)-Z_{wj}\left(\frac{\partial}{\partial t}-\gamma_j\frac{\partial}{\partial \xi}\right)I_{mj}(\xi,t)$$
$$-\gamma_j\sum_{k=1}^{n}\tilde{R}_{jk}I_{mk}(\xi,t)+\gamma_j Z_{wj}\tilde{G}_j V_{mj}(\xi,t)=0 \qquad (1.25b)$$

where sub-index j indicates corresponding elements for the *jth* mode. In Fig. (1.5) a new coordinates system given by two families of lines known as "characteristics" is shown. These families of lines are solutions of:

$$\gamma_j=\pm\frac{dx}{dt} \qquad (1.26)$$

Along the characteristic lines the terms in parenthesis of (1.25) become total derivatives, hence it can be written:

$$dV_{mj}+Z_{wj}dI_{mj}+dx_j\sum_{k=1}^{n}\tilde{R}_{jk}I_{mk}+dx_j Z_{wj}\tilde{G}_j V_{mj}+dx_j\psi_{mj}=0 \qquad (1.27a)$$

$$dV_{mj}-Z_{wj}dI_{mj}+dx_j\sum_{k=1}^{n}\tilde{R}_{jk}I_{mk}-dx_j Z_{wj}\tilde{G}_j V_{mj}+dx_j\psi_{mj}=0 \qquad (1.27b)$$

Equations (1.26) and (1.27) are an Ordinary Differential Equations system that represents the Partial Differential Equations system given by (1.22). In Fig. (1.5), Vel_{mj} are the propagation velocities of each mode and $V_{mj}^{D,E,F}$ are the corresponding modal voltages.

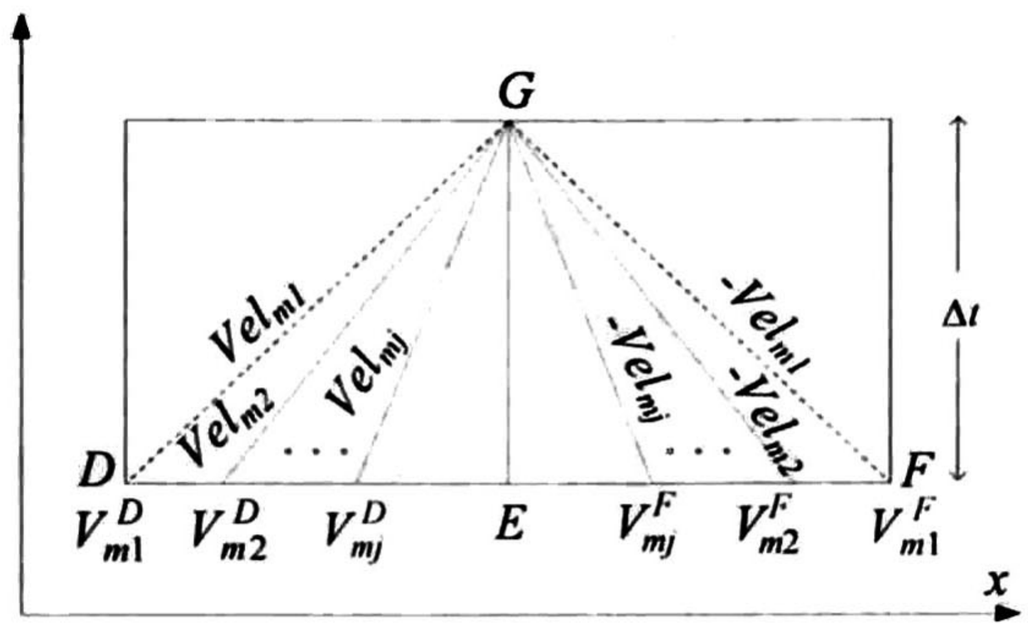

Figure 1.5. Characteristics curve diagram for the interior points of the line.

Applying the central finite differences method to (1.27) according to Fig. (1.5) and expressing the result in matrix form the next equations for $\mathbf{V}_m$ and $\mathbf{I}_m$ at interior points of the line are obtained:

$$\mathbf{I}_m^G = -\frac{1}{2} inv(\mathbf{Z}_q)\Big[\mathbf{H}_6(\alpha_1-\alpha_3)\left(\mathbf{V}_m^D-\mathbf{V}_m^F\right)+\mathbf{Z}_1(\alpha_1+\alpha_3)\left(\mathbf{I}_m^D-\mathbf{I}_m^F\right)+2\alpha_2\mathbf{Z}_1\mathbf{I}_m^E - \frac{\Delta x}{2}(\alpha_1+\alpha_3)\left(\Psi_m^D+\Psi_m^F\right)-\Delta x\Psi_m^G\Big] \tag{1.28a}$$

$$\mathbf{V}_m^G = \frac{1}{2} inv(\mathbf{H}_5)\Big[\mathbf{H}_6(\alpha_1+\alpha_3)\left(\mathbf{V}_m^D+\mathbf{V}_m^F\right)+2\mathbf{H}_6\alpha_2\,\mathbf{V}_m^E+\mathbf{Z}_1(\alpha_1-\alpha_3)\left(\mathbf{I}_m^D-\mathbf{I}_m^F\right) + \frac{\Delta x}{2}(\alpha_3-\alpha_1)\left(\Psi_m^D+\Psi_m^F\right)\Big] \tag{1.28b}$$

where

$$\mathbf{H}_5 = \mathbf{I}_\mathbf{I} + \frac{\Delta x Z_w \mathbf{G}}{2} \tag{1.29a}$$

$$\mathbf{H}_6 = \mathbf{I}_\mathbf{I} - \frac{\Delta x Z_w \mathbf{G}}{2} \tag{1.29b}$$

$$\mathbf{Z}_1 = \mathbf{Z}_w - \frac{\Delta x \tilde{\mathbf{R}}_{Xm}}{2} \tag{1.30a}$$

$$\mathbf{Z}_2 = \mathbf{Z}_w + \frac{\Delta x \tilde{\mathbf{R}}_{Xm}}{2} \tag{1.30b}$$

$$\mathbf{Z}_q = \mathbf{Z}_2 - \frac{\Delta t\,\Delta \mathbf{x}}{2}\sum_{i=1}^{N}\frac{\mathbf{T}_V^{-1}\mathbf{K}_i p_i \mathbf{T}_I}{1+\Delta t\, p_i} \tag{1.31a}$$

$$\mathbf{\Psi}_m^{G'} = -\sum_{i=1}^{N}\left[\frac{\mathbf{\Psi}_m^{G-\Delta t}}{1+\Delta t\, p_i}\right] \tag{1.31b}$$

$\mathbf{I_1}$ is the identity matrix; the variables $V_{mj}^{D,E,F}$ $I_{mj}^{D,E,F}$ and $\psi_{mj}^{D,E,F}$ are calculated using a second order interpolation method.

1.5.1 Boundary Points

For the solution of $\mathbf{V}_m$ and $\mathbf{I}_m$ at the ends of the line, it is necessary to establish boundary conditions. It is important to note that, at the beginning of the line, only the equation corresponding to characteristics with negative slope is available; on the other hand, at the end of the line only the equation corresponding to characteristics with positive slope is available. With these conditions it is possible to obtain a Norton's circuit model that represents the ends of the line. Applying the central finite differences method to (1.27) according to Fig. (1.6) the solution for the boundaries of the line is obtained. Expressing the result in matrix form gives:

$$\mathbf{H}_5\mathbf{V}_m^S - \mathbf{Z}_q\mathbf{I}_m^S = \mathbf{V}_{HSm} \tag{1.32a}$$

$$\mathbf{H}_5\mathbf{V}_m^L + \mathbf{Z}_q\mathbf{I}_m^L = \mathbf{V}_{HLm} \tag{1.32b}$$

where

$$\mathbf{V}_{HSm} = \mathbf{H}_6\mathbf{V}_m^F - \mathbf{Z}_1\mathbf{I}_m^F + \frac{\Delta x}{2}\left(\mathbf{\Psi}_m^{G'} + \mathbf{\Psi}_m^F\right) \tag{1.33a}$$

$$\mathbf{V}_{HLm} = \mathbf{H}_6\mathbf{V}_m^D + \mathbf{Z}_1\mathbf{I}_m^D - \frac{\Delta x}{2}\left(\mathbf{\Psi}_m^{G'} + \mathbf{\Psi}_m^D\right) \tag{1.33b}$$

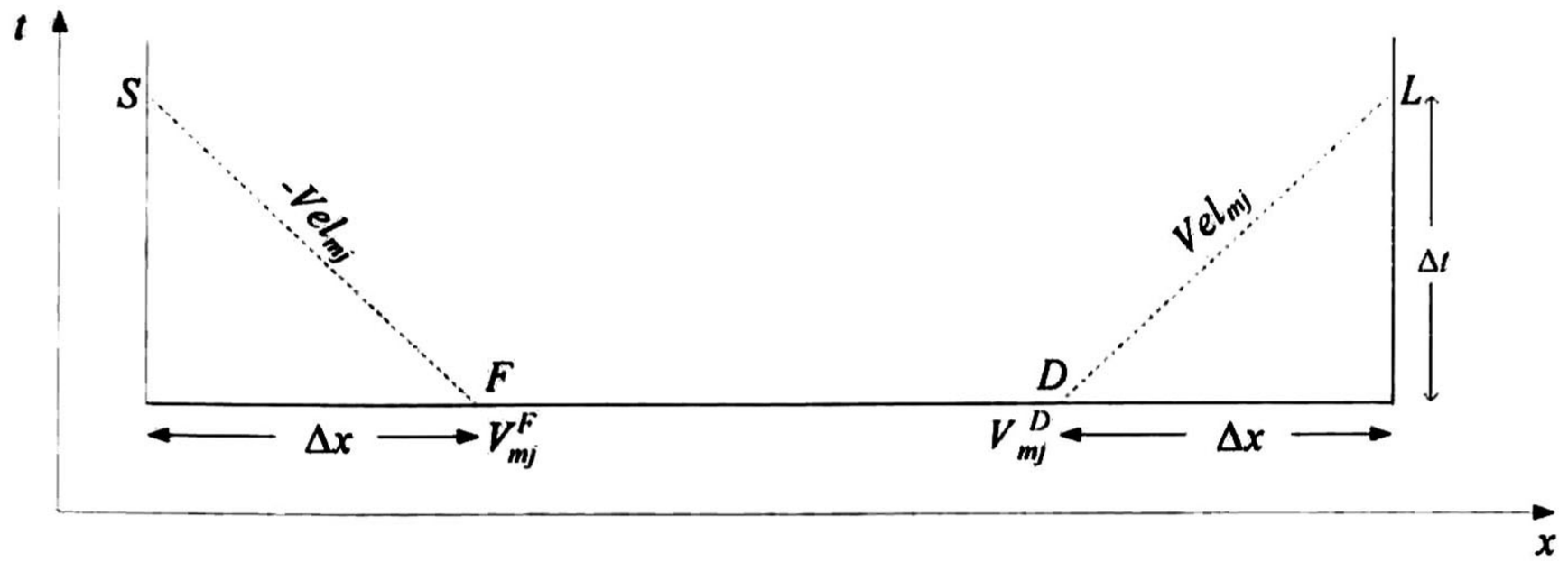

Figure 1.6. Characteristics curve diagram for the boundaries line.

Equations (1.33) represent history terms delayed a time step, Δt. Applying the modal transformation matrices to (1.32) the next equation in phase domain is obtained:

$$\mathbf{I}^S = \mathbf{Y}_Q \mathbf{V}^S + \mathbf{I}^F_{HS}, \; \mathbf{I}^L = \mathbf{Y}_Q \mathbf{V}^L_{\bullet} + \mathbf{I}^D_{HL} \qquad \text{(1.34a), (1.34b)}$$

where

$$\mathbf{I}^L = -\mathbf{T}_I \, \mathbf{I}^L_m \qquad \text{(1.35a)}$$

$$\mathbf{I}^S = \mathbf{T}_I \, \mathbf{I}^S_m \qquad \text{(1.35b)}$$

$$\mathbf{V}^L = \mathbf{T}_V \, \mathbf{V}^L_m \qquad \text{(1.36a)}$$

$$\mathbf{V}^S = \mathbf{T}_V \, \mathbf{V}^S_m \qquad \text{(1.36b)}$$

$$\mathbf{I}^F_{HS} = -\mathbf{T}_I \mathbf{Z}_q^{-1} \mathbf{V}_{HSm} \qquad \text{(1.37a)}$$

$$\mathbf{I}^D_{HL} = -\mathbf{T}_I \mathbf{Z}_q^{-1} \mathbf{V}_{HLm} \qquad \text{(1.37b)}$$

$$\mathbf{Y}_Q = \mathbf{T}_I \mathbf{Z}_q^{-1} \mathbf{H}_5 \mathbf{T}_V^{-1} \qquad \text{(1.38)}$$

From equation (1.34) the Norton's equivalent circuits for the source and load boundaries are obtained as shown in Fig. 1.7.

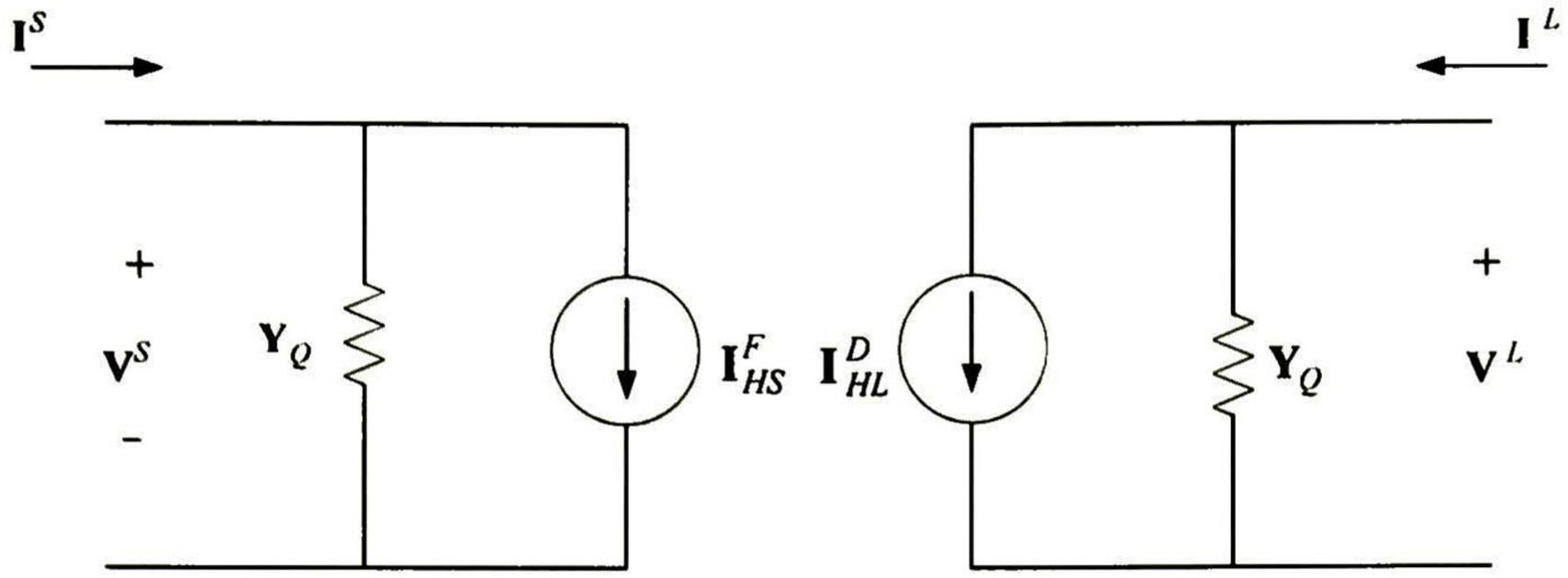

Figure 1.7. Norton's circuit model for the source and load boundary.

1.6 Review of Frequency Domain Modeling of MTL

In this section a review of the frequency domain modeling of Multiconductor Transmission lines is presented. The procedure consists of first solving the transmission line equations and after that finding a circuit model for the transmission line.

1.6.1 Solution of the Multiconductor Transmission Line Equations

The equations that describe the transmission line behavior in the frequency domain are:

$$-\frac{d\mathbf{V}(z,s)}{dz}=\mathbf{Z}(s)\mathbf{I}(z,s), \quad -\frac{d\mathbf{I}(z,s)}{dz}=\mathbf{Y}(s)\mathbf{V}(z,s) \qquad (1.39a,b)$$

where $\mathbf{V}(z,s)$ and $\mathbf{I}(z,s)$ are the voltage and current vectors, respectively; $\mathbf{Z}(s)$ and $\mathbf{Y}(s)$ are the per unit length impedance and admittance matrices; s is the Laplace variable. Taking a second derivative of (1.39a):

$$-\frac{d^2\mathbf{V}(z,s)}{dz^2}=\mathbf{Z}(s)\frac{d\mathbf{I}(z,s)}{dz} \qquad (1.40)$$

using (1.39b) yields:

$$\frac{d^2\,\mathbf{V}(z,s)}{dz^2}=\mathbf{A}(s)\,\mathbf{V}(z,s) \qquad (1.41a)$$

where

$$\mathbf{A}(s) = \mathbf{Z}(s)\mathbf{Y}(s) \tag{1.41b}$$

Assuming that $\mathbf{A}(s)$ is diagonalizable:

$$\mathbf{A}(s) = \mathbf{T}_V\, \boldsymbol{\lambda}\, \mathbf{T}_V^{-1} \tag{1.42}$$

where $\boldsymbol{\lambda} = \boldsymbol{\lambda}(s)$ is the eigenvalues diagonal matrix of $\mathbf{A}(s)$ and $\mathbf{T}_V = \mathbf{T}_V(s)$ is a matrix whose columns are the corresponding eigenvectors.

Substituting (1.42) into (1.41a) and left multiplying by $\mathbf{T}_V^{-1}$ the next expression is obtained:

$$\frac{d^2\left[\mathbf{T}_V^{-1}\mathbf{V}(z,s)\right]}{dz^2} = \boldsymbol{\lambda}\,\mathbf{T}_V^{-1}\mathbf{V}(z,s) \tag{1.43}$$

Defining modal voltages vector as:

$$\mathbf{V}_m(z,s) = \mathbf{T}_V^{-1}\mathbf{V}(z,s) \tag{1.44}$$

it can be written:

$$\frac{d^2\,\mathbf{V}_m(z,s)}{dz^2} = \boldsymbol{\lambda}\,\mathbf{V}_m(z,s) \tag{1.45}$$

Equation (1.45) is formed by n decoupled ordinary differential equations whose general solution for the *ith* mode is:

$$V_{mi}(z,s) = V_{Fmi}(s)e^{-\gamma_i z} + V_{Bmi}(s)e^{\gamma_i z} \tag{1.46}$$

where $V_{Fmi}(s)$ and $V_{Bmi}(s)$ are integration constants and γ_i is the propagation constant defined as:

$$\gamma_i = \sqrt{\lambda_i} = \alpha_i + j\beta_i \tag{1.47}$$

where α_i is the attenuation constant in Nep/m and β_i the phase constant in rad/m.

Grouping the n solutions to (1.46), it can be written in compact form as:

$$\mathbf{V}_m(z,s) = \exp(-\boldsymbol{\Gamma} z)\,\mathbf{V}_{Fm}(s) + \exp(+\boldsymbol{\Gamma} z)\,\mathbf{V}_{Bm}(s) \tag{1.48}$$

where

$$\exp(\pm\boldsymbol{\Gamma}z)=\begin{bmatrix} e^{\pm\gamma_1 z} & 0 & & 0 \\ 0 & e^{\pm\gamma_2 z} & 0 & \\ & & & 0 \\ 0 & & 0 & e^{\pm\gamma_n z} \end{bmatrix} \tag{1.49}$$

$$\boldsymbol{\Gamma}=\begin{bmatrix} \gamma_1 & \cdots & 0 \\ & & \\ 0 & \cdots & \gamma_n \end{bmatrix}=\sqrt{\boldsymbol{\lambda}} \tag{1.50}$$

Using (1.44) it can be written in the phase domain as follows:

$$\mathbf{V}(z,s)=\exp(-\boldsymbol{\Psi}z)\mathbf{V}_F(s)+\exp(+\boldsymbol{\Psi}z)\,\mathbf{V}_B(s) \tag{1.51}$$

where

$$\exp(\pm\boldsymbol{\Psi}z)=\mathbf{T}_V\exp(\pm\boldsymbol{\Gamma}z)\,\mathbf{T}_V^{-1} \tag{1.52a}$$

$$\boldsymbol{\Psi}=\mathbf{T}_V\,\boldsymbol{\Gamma}\,\mathbf{T}_V^{-1}=\sqrt{\mathbf{A}(s)} \tag{1.52b}$$

The solution for the currents can be obtained from (1.39a), then

$$\mathbf{I}(z,s)=-\mathbf{Z}(s)^{-1}\frac{d\,\mathbf{V}(z,s)}{dz} \tag{1.53}$$

Substituting (1.51) gives:

$$\mathbf{I}(z,s)=-\mathbf{Z}(s)^{-1}\frac{d}{dz}\left[\exp(-\boldsymbol{\Psi}z)\,\mathbf{V}_F(s)+\exp(+\boldsymbol{\Psi}z)\,\mathbf{V}_B(s)\right] \tag{1.54}$$

Performing the derivative and rearranging gives the follows:

$$\mathbf{I}(z,s)=\mathbf{Y}_0\left[\exp(-\boldsymbol{\Psi}z)\,\mathbf{V}_F(s)-\exp(+\boldsymbol{\Psi}z)\,\mathbf{V}_B(s)\right] \tag{1.55}$$

where

$$\mathbf{Y}_0=\mathbf{Z}^{-1}\boldsymbol{\Psi} \tag{1.56}$$

1.6.2 Admittance model.

In order to obtain an admittance model of a transmission line the boundary conditions should be used. At the receiving end of the line, $z = 0$, as shown in Fig. 1.8, from (1.51) and (1.55) gives:

$$\mathbf{V}(0) = \mathbf{V}_L = \mathbf{V}_F + \mathbf{V}_B \tag{1.57a}$$

$$\mathbf{I}(0) = \mathbf{I}_L = \mathbf{Y}_0 \left[\mathbf{V}_F - \mathbf{V}_B \right] \tag{1.57b}$$

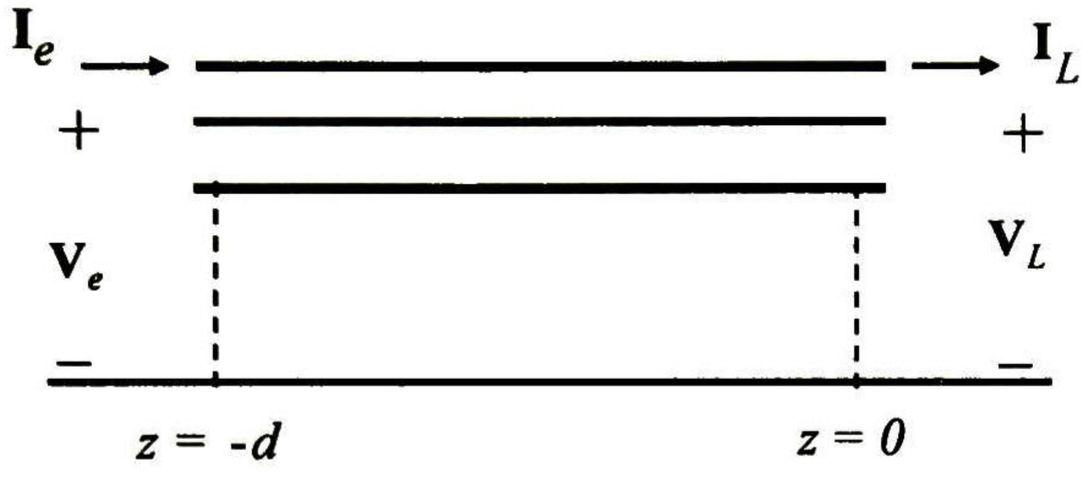

Figure. 1.8. Boundary conditions of a transmission line.

from (1.57)

$$\mathbf{V}_F = \tfrac{1}{2}(\mathbf{V}_L + \mathbf{Z}_0 \mathbf{I}_L) \tag{1.58a}$$

$$\mathbf{V}_B = \tfrac{1}{2}(\mathbf{V}_L - \mathbf{Z}_0 \mathbf{I}_L) \tag{1.58b}$$

For the sending end, $z = -d$:

$$\mathbf{V}(-d) = \mathbf{V}_e = \exp(\Psi d)\, \mathbf{V}_F + \exp(-\Psi d)\, \mathbf{V}_B \tag{1.59a}$$

$$\mathbf{I}(-d) = \mathbf{I}_e = \mathbf{Y}_0 \left[\exp(\Psi d)\, \mathbf{V}_F - \exp(+\Psi d)\, \mathbf{V}_B \right] \tag{1.59b}$$

Combining (1.58) and (1.59) it can be found:

$$\begin{bmatrix} \mathbf{I}_e \\ \mathbf{I}_r \end{bmatrix} = \begin{bmatrix} \mathbf{A} & -\mathbf{B} \\ -\mathbf{B} & \mathbf{A} \end{bmatrix} \begin{bmatrix} \mathbf{V}_e \\ \mathbf{V}_r \end{bmatrix} \tag{1.60}$$

where

$$\mathbf{A} = \mathbf{Y}_0 \, coth(\Psi d) \tag{1.61a}$$

$$\mathbf{B} = \mathbf{Y}_0 \, csch(\Psi d) \tag{1.61b}$$

$$\mathbf{I}_r = -\mathbf{I}_L \tag{1.61c}$$

$$\mathbf{V}_r = \mathbf{V}_L \tag{1.61d}$$

Figure 1.9 shows the admittance model defined by (1.60). This model can be used to form the bus admittance of a network. The excitations are the Laplace transforms of the time domain sources. After solving the network time domain waveforms are obtained using the Inverse Numerical Laplace Transform [19].

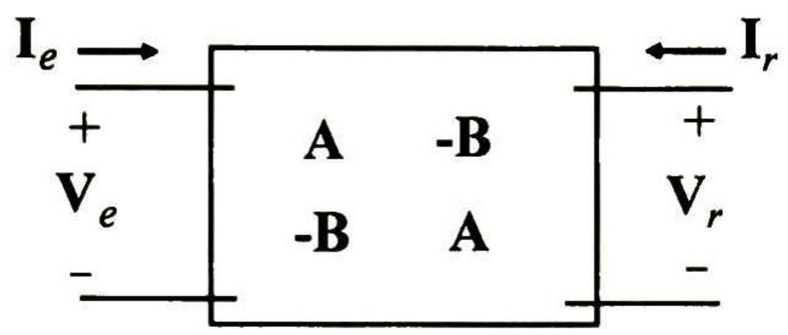

Figure 1.9. Admittance model of a transmission line.

2 Multiconductor Transmission Line Modeling

2.1 Introduction

Transmission lines are the most common elements in electrical power systems. The electric energy is transmitted to the user through them and it can be transmitted either in the form of direct current or alternating current. Moreover depending of its design the line can be overhead or underground.

Due to the importance of transmission lines, it has been necessary the development of mathematical models that represent their behavior. These models are characterized by the next parameters: the resistance **R**, that represents the series losses, the inductance **L**, that represents the magnetic flux generated by the current flowing through the conductors, the capacitance **C**, that represents the displacement currents among conductors in the transversal plane and the conductance **G**, that represents the transverse currents flowing among conductors.

The models of transmission lines used for electromagnetic transients analysis can be of lumped or distributed parameters. In order to consider the propagation of waves on transmission lines and correctly reproduce the behavior of electromagnetic transients it is necessary to develop models with distributed parameters.

In Section 2.2 in order to introduce the basis of the new method a model for multiconductor transmission lines without frequency dependence is first presented, it is based in the well known method of characteristics and modal analysis [12].

In Section 2.3 the frequency dependence of the electrical parameters is included in the model by means of a rational approximation of the transient resistance [16].

Finally, a number of line configurations are used to validate the model and the results are compared to those from a frequency domain method [15] and from the ATP//EMTP [3].

2.2 Multiconductor Transmission Line with Constant Electrical Parameters

The telegrapher's equations have been used for the analysis of transient state; these equations govern the behavior of the transmission line. In time domain these equations can be expressed as follows:

$$\frac{\partial \mathbf{V}(\xi,t)}{\partial \xi} + \mathbf{L}\frac{\partial \mathbf{I}(\xi,t)}{\partial t} + \mathbf{R}\,\mathbf{I}(\xi,t) = \mathbf{0} \tag{2.1}$$

$$\frac{\partial \mathbf{I}(\xi,t)}{\partial \xi} + \mathbf{C}\frac{\partial \mathbf{V}(\xi,t)}{\partial t} + \mathbf{G}\,\mathbf{V}(\xi,t) = \mathbf{0} \tag{2.2}$$

Where **L**, **C**, **R** and **G** are the electrical parameters described previously, $\mathbf{V}(\xi,t)$ and $\mathbf{I}(\xi,t)$ are the voltages and currents of the line respectively. Independent variables t and ξ represent time and distance, respectively. For aerial lines the conductance **G** is negligible but this is not the case for underground cables modeling. Multiplying (2.1) and (2.2) by $\mathbf{L}^{-1}$ and $\mathbf{C}^{-1}$ respectively, the next equation in matrix form is obtained [12].

$$\frac{\partial}{\partial \xi}\mathbf{U} + \mathbf{A}\frac{\partial}{\partial t}\mathbf{U} + \mathbf{B}\mathbf{U} = \mathbf{0} \tag{2.3}$$

where

$$\mathbf{A} = \begin{bmatrix} \mathbf{0} & \mathbf{C}^{-1} \\ \mathbf{L}^{-1} & \mathbf{0} \end{bmatrix} \tag{2.4a}$$

$$\mathbf{B} = \begin{bmatrix} \mathbf{C}^{-1}\mathbf{G} & \mathbf{0} \\ \mathbf{0} & \mathbf{L}^{-1}\mathbf{R} \end{bmatrix} \tag{2.4b}$$

$$\mathbf{U} = \begin{bmatrix} \mathbf{V}(\xi,t) \\ \mathbf{I}(\xi,t) \end{bmatrix} \tag{2.4c}$$

The diagonalization of the **LC** and **CL** products are defined as follows:

$$\mathbf{T}_V^{-1}\mathbf{L}\mathbf{C}\mathbf{T}_V = \mathbf{\Lambda} \tag{2.5a}$$

and

$$\mathbf{T}_I^{-1}\mathbf{C}\mathbf{L}\mathbf{T}_I = \mathbf{\Lambda} \tag{2.5b}$$

where $\mathbf{T}_V$ and $\mathbf{T}_I$ are the transformation matrices of voltages and currents, respectively. $\mathbf{\Lambda}$ is a diagonal matrix whose elements correspond to the inverses of the square of the velocities of each mode. Using (2.5) it can be defined the following diagonal modal matrices.

$$\tilde{\mathbf{L}} = \mathbf{T}_V^{-1}\mathbf{L}\mathbf{T}_I \tag{2.6a}$$

and

$$\tilde{\mathbf{C}} = \mathbf{T}_I^{-1}\mathbf{C}\mathbf{T}_V \tag{2.6b}$$

Therefore it can be written:

$$\tilde{\mathbf{L}}\tilde{\mathbf{C}} = \mathbf{\Lambda} \tag{2.6c}$$

Consider now the matrices of left and right eigenvector, $\mathbf{M_L}$ and $\mathbf{M_R}$ respectively, of **A**:

$$\mathbf{M_L} = \frac{1}{\sqrt{2}}\begin{bmatrix} \mathbf{T}_V^{-1} & \mathbf{Z}_W\mathbf{T}_I^{-1} \\ \mathbf{T}_V^{-1} & -\mathbf{Z}_W\mathbf{T}_I^{-1} \end{bmatrix} \tag{2.7a}$$

and

$$\mathbf{M_R} = \frac{1}{\sqrt{2}}\begin{bmatrix} \mathbf{T}_V & \mathbf{Z}_W\mathbf{T}_V \\ \mathbf{T}_I\mathbf{Y}_W & -\mathbf{T}_I\mathbf{Y}_W \end{bmatrix} \tag{2.7b}$$

where $\mathbf{Z}_W = \sqrt{\tilde{\mathbf{L}}\tilde{\mathbf{C}}^{-1}}$ and $\mathbf{Y}_W = \sqrt{\tilde{\mathbf{C}}\tilde{\mathbf{L}}^{-1}}$ Using (2.7) the eigenvalues matrix of **A** are obtained as follows:

$$\mathbf{M_L}\mathbf{A}\mathbf{M_R} = \begin{bmatrix} \mathbf{\Gamma} & \mathbf{0} \\ \mathbf{0} & -\mathbf{\Gamma} \end{bmatrix} \tag{2.8}$$

where

$$\boldsymbol{\Gamma} = \sqrt{\tilde{\mathbf{C}}^{-1}\tilde{\mathbf{L}}^{-1}} = \sqrt{\boldsymbol{\Lambda}^{-1}} \tag{2.9}$$

For obtaining a system of ordinary differential equations the telegrapher's equations must be transformed to the characteristics domain. Premultiplying (2.3) times (2.7a) the next equations are obtained:

$$\mathbf{Z}_W\tilde{\mathbf{C}}\left(\frac{\partial}{\partial t}+\boldsymbol{\Gamma}\frac{\partial}{\partial \xi}\right)\mathbf{V}_m(\xi,t)+\tilde{\mathbf{L}}\left(\frac{\partial}{\partial t}+\boldsymbol{\Gamma}\frac{\partial}{\partial \xi}\right)\mathbf{I}_m(\xi,t)+\tilde{\mathbf{R}}\mathbf{I}_m(\xi,t)+\mathbf{Z}_W\tilde{\mathbf{G}}\,\mathbf{V}_m(\xi,t)=\mathbf{0} \tag{2.10a}$$

$$\mathbf{Z}_W\tilde{\mathbf{C}}\left(\frac{\partial}{\partial t}-\boldsymbol{\Gamma}\frac{\partial}{\partial \xi}\right)\mathbf{V}_m(\xi,t)-\tilde{\mathbf{L}}\left(\frac{\partial}{\partial t}-\boldsymbol{\Gamma}\frac{\partial}{\partial \xi}\right)\mathbf{I}_m(\xi,t)-\tilde{\mathbf{R}}\mathbf{I}_m(\xi,t)+\mathbf{Z}_W\tilde{\mathbf{G}}\,\mathbf{V}_m(\xi,t)=\mathbf{0} \tag{2.10b}$$

where

$$\tilde{\mathbf{R}} = \mathbf{T}_V^{-1}\mathbf{R}\mathbf{T}_I \tag{2.10c}$$

and

$$\tilde{\mathbf{G}} = \mathbf{T}_I^{-1}\mathbf{G}\mathbf{T}_V \tag{2.10d}$$

Multiplying (2.10a) and (2.10b) times $\left(\mathbf{Z}_W\tilde{\mathbf{C}}\right)^{-1}$ and considering that $\left(\mathbf{Z}_W\tilde{\mathbf{C}}\right)^{-1}=\boldsymbol{\Gamma}$ and $\left(\mathbf{Z}_W\tilde{\mathbf{C}}\right)^{-1}\tilde{\mathbf{L}}=\mathbf{Z}_W$ the next equations for the *jth* mode are obtained:

$$\begin{aligned}\left(\frac{\partial}{\partial t}+\gamma_j\frac{\partial}{\partial \xi}\right)V_{mj}(\xi,t)+Z_{wj}\left(\frac{\partial}{\partial t}+\gamma_j\frac{\partial}{\partial \xi}\right)I_{mj}(\xi,t)\\ +\gamma_j\sum_{k=1}^{n}\tilde{R}_{jk}I_{mk}(\xi,t)+\gamma_j Z_{wj}\tilde{G}_j V_{mj}(\xi,t)=0\end{aligned} \tag{2.11a}$$

$$\begin{aligned}\left(\frac{\partial}{\partial t}-\gamma_j\frac{\partial}{\partial \xi}\right)V_{mj}(\xi,t)-Z_{wj}\left(\frac{\partial}{\partial t}-\gamma_j\frac{\partial}{\partial \xi}\right)I_{mj}(\xi,t)\\ -\gamma_j\sum_{k=1}^{n}\tilde{R}_{jk}I_{mk}(\xi,t)+\gamma_j Z_{wj}\tilde{G}_j V_{mj}(\xi,t)=0\end{aligned} \tag{2.11b}$$

where γ_j and Z_{wj} are the modal propagation velocity and characteristic impedance, V_{mj} and I_{mj} are the modal voltage and current. $\tilde{R}_{jk}$ is the element j,k of matrix $\tilde{\mathbf{R}}$ and

$\tilde{G}_j$ is the element j,j of $\tilde{\mathbf{G}}$. Index j takes the values 1, 2, 3, ...,n where n is the number of modes in the system.

Solutions for the expression $\gamma_j = \pm\frac{dx}{dt}$ represent families of lines in the x-t plane; these lines are well known as characteristic and they are shown in the Fig. (2.1) [12]. Along these lines the condition $\left(\frac{\partial}{\partial t} \pm \gamma_j \frac{\partial}{\partial \xi}\right) = \pm\frac{d}{dt}$ holds. Substituting these terms in (2.11a) and (2.11b) and multiplying by dt the next equations are obtained:

$$dV_{mj}(\xi,t) + Z_{wj} dI_m(\xi,t) + dx_j \sum_{k=1}^{n} \tilde{R}_{jk} I_{mk}(\xi,t) + dx_j Z_{wj} \tilde{G}_j V_{mj}(\xi,t) = 0 \qquad (2.12)$$

$$dV_{mj}(\xi,t) - Z_{wj} dI_{mj}(\xi,t) + dx_j \sum_{k=1}^{n} \tilde{R}_{jk} I_{mk}(\xi,t) - dx_j Z_{wj} \tilde{G}_j V_{mj}(\xi,t) = 0 \qquad (2.13)$$

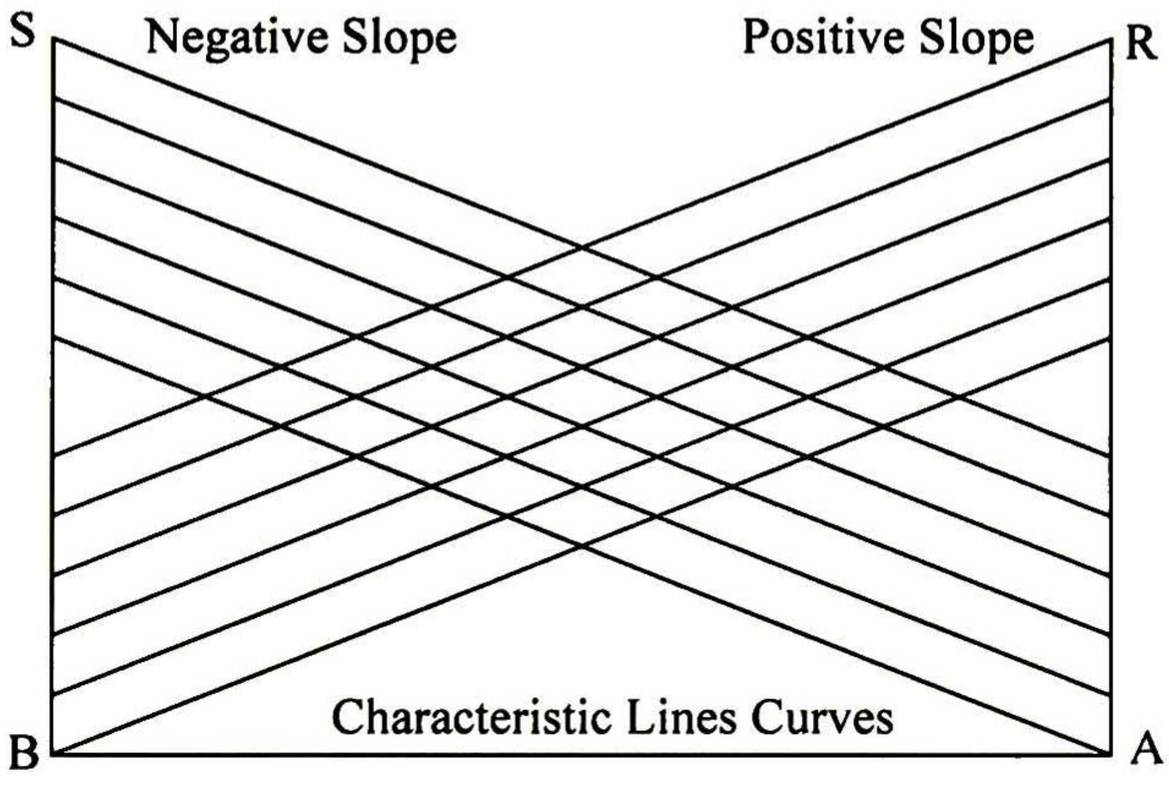

Figure 2.1. Characteristics diagram.

Equations (2.12) and (2.13) are an Ordinary Differential Equations system that represents the Partial Differential Equations system given by (2.1) and (2.2). The central finite differences method is used to integrate (2.12) and (2.13), the values in S and R are approximated using the values at a travel time (τ), as is shown in Fig. (2.2).

From Fig. (2.2), Vel_{mj}^{A} and Vel_{mj}^{B} are the velocities of propagation of each mode and V_{mj}^{A} and V_{mj}^{B} are the voltages of each mode. Equations (2.12) and (2.13) correspond to the positive and negative slopes of the characteristics. Applying the central finite differences method to (2.12) and (2.13) respectively gives:

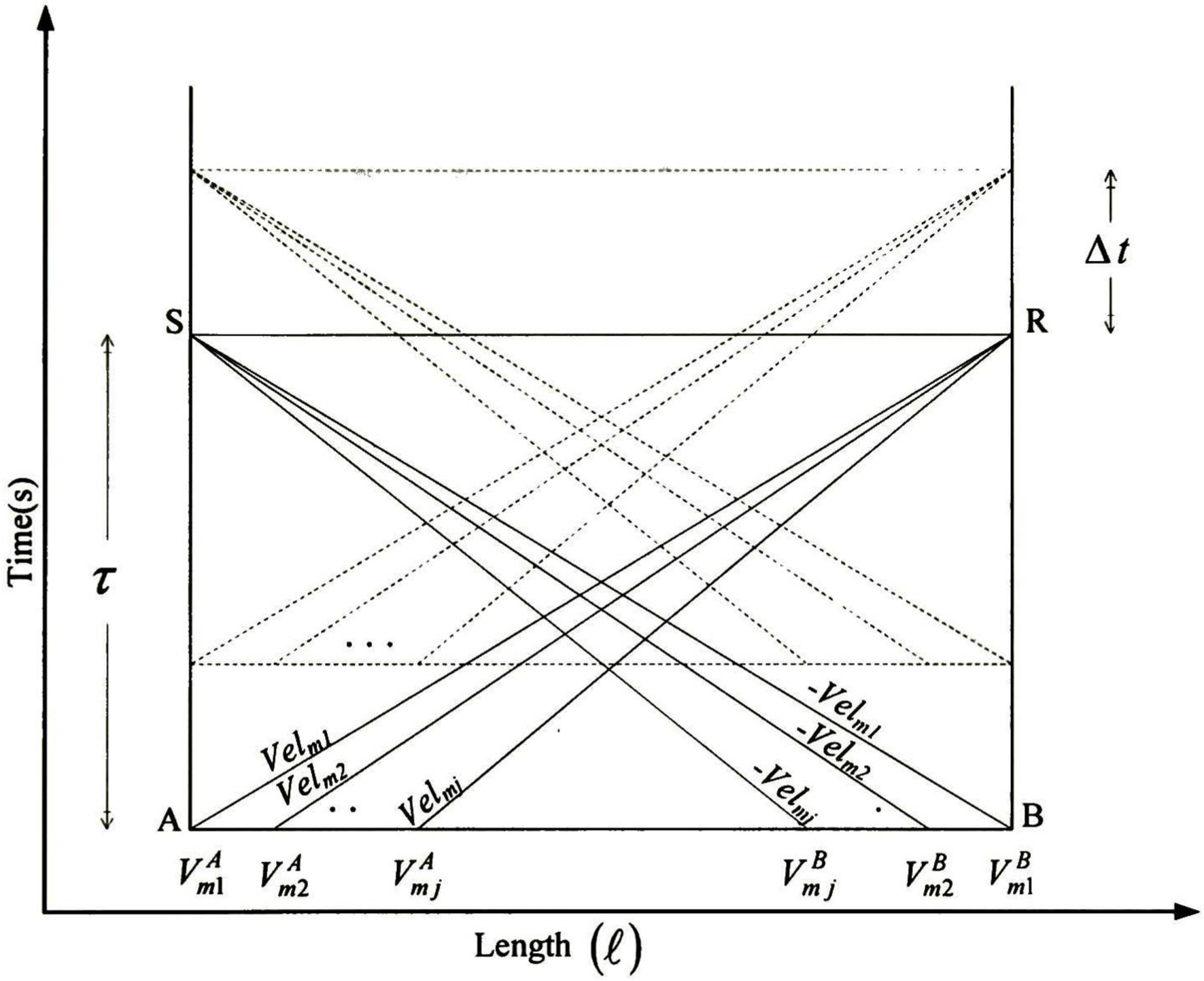

Figure 2.2. Modal voltages in the characteristic curves diagram.

$$H_5 V_{mj}^{R} - H_6 V_{mj}^{A} + Z_2 I_{mj}^{R} - Z_1 I_{mj}^{A} = 0 \tag{2.14}$$

$$H_5 V_{mj}^{S} - H_6 V_{mj}^{B} - Z_2 I_{mj}^{S} + Z_1 I_{mj}^{B} = 0 \tag{2.15}$$

where

$$H_5 = \left(1 + \frac{\ell Z_{wj} \tilde{G}_j}{2}\right) \tag{2.16a}$$

$$H_6 = \left(1 - \frac{\ell Z_{wj} \tilde{G}_j}{2}\right) \tag{2.16b}$$

$$Z_1 = \left(Z_{wj} - \frac{\ell \tilde{R}_j}{2}\right) \tag{2.17a}$$

$$Z_2 = \left(Z_{wj} + \frac{\ell \tilde{R}_j}{2}\right) \tag{2.17b}$$

The values V_{m1}^A, V_{m1}^B and I_{m1}^A, I_{m1}^B are known, using these values the rest of the modal voltages and currents between the extremes A and B are calculated with the linear interpolation method of Lagrange as is shown in appendix A.

Representing (2.14) and (2.15) in matrix form and substituting (A.6) and (A.7) the next equation systems are obtained:

$$\mathbf{H}_5 \mathbf{V}_m^R + \mathbf{Z}_2 \mathbf{I}_m^R = \mathbf{V}_{Hm}^A \tag{2.18a}$$

$$\mathbf{H}_5 \mathbf{V}_m^S - \mathbf{Z}_2 \mathbf{I}_m^S = \mathbf{V}_{Hm}^B \tag{2.18b}$$

where

$$\mathbf{V}_{Hm}^A = \mathbf{H}_6 \left(\alpha_2 \mathbf{V}_m^A + \alpha_1 \mathbf{V}_m^B\right) + \mathbf{Z}_1 \left(\alpha_2 \mathbf{I}_m^A + \alpha_1 \mathbf{I}_m^B\right) \tag{2.19a}$$

$$\mathbf{V}_{Hm}^B = \mathbf{H}_6 \left(\alpha_1 \mathbf{V}_m^A + \alpha_2 \mathbf{V}_m^B\right) - \mathbf{Z}_1 \left(\alpha_1 \mathbf{I}_m^A + \alpha_2 \mathbf{I}_m^B\right) \tag{2.19b}$$

The right hand sides of (2.18) involve voltages and currents delayed a travel time, hence they represent "*history terms*". With the transformation matrices $\mathbf{T}_V$ and $\mathbf{T}_I$ (2.18a) and (2.18b) can be expressed in phase domain as follows:

$$\mathbf{I}^{R'} = \mathbf{Y}_{phase} \mathbf{V}^{R'} + \mathbf{I}_H^A \tag{2.20a}$$

$$\mathbf{I}^S = \mathbf{Y}_{phase} \mathbf{V}^S + \mathbf{I}_H^B \tag{2.20b}$$

where

$$\mathbf{I}^{R'} = -\mathbf{T}_I \mathbf{I}_m^R \tag{2.21a}$$

$$\mathbf{I}^S = \mathbf{T}_I \mathbf{I}_m^S \tag{2.21b}$$

$$\mathbf{V}^{R'} = \mathbf{T}_V \, \mathbf{V}_m^R \tag{2.22a}$$

$$\mathbf{V}^{S} = \mathbf{T}_V \, \mathbf{V}_m^S \tag{2.22b}$$

$$\mathbf{I}_H^A = -\mathbf{T}_I \mathbf{Z}_2^{-1} \mathbf{V}_{Hm}^A \tag{2.23a}$$

$$\mathbf{I}_H^B = -\mathbf{T}_I \mathbf{Z}_2^{-1} \mathbf{V}_{Hm}^B \tag{2.23b}$$

$$\mathbf{Y}_{phase} = \mathbf{T}_I \mathbf{Z}_2^{-1} \mathbf{H}_5 \mathbf{T}_V^{-1} \tag{2.24}$$

Equations (2.20) represent Norton's equivalent circuits for the transmission line ends, as shown in Fig. (2.3).

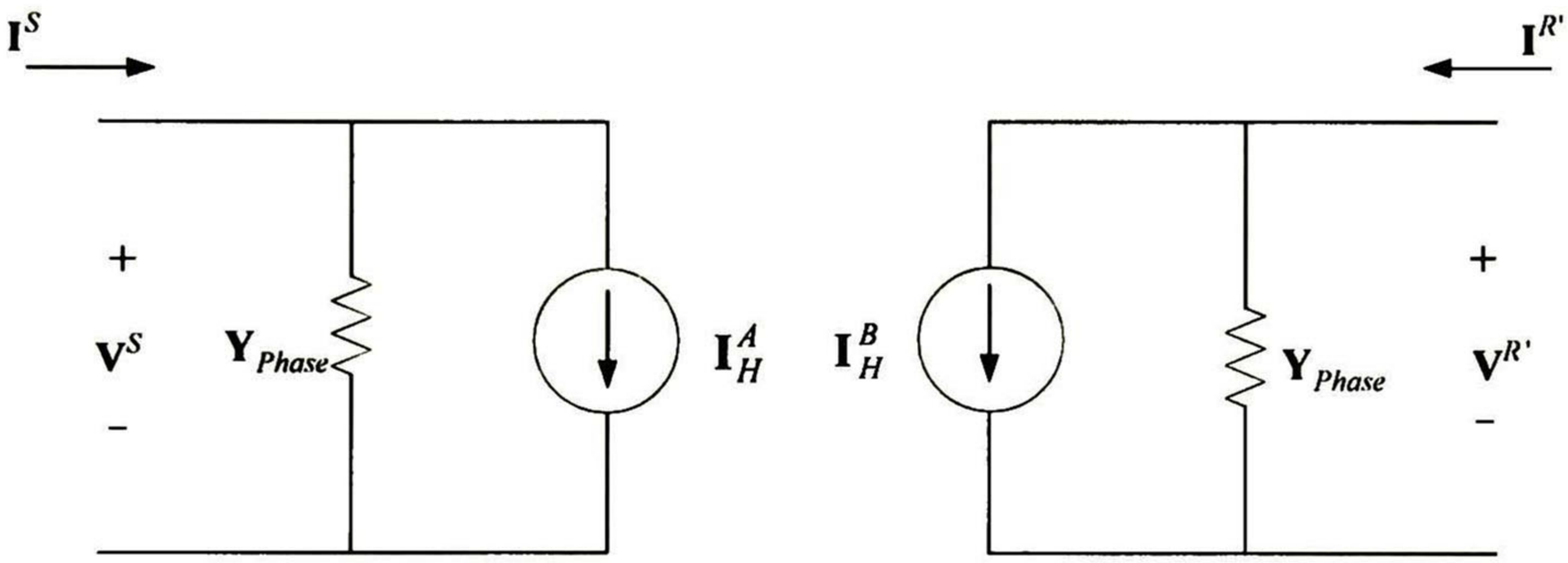

Figure 2.3. Norton's circuits at the end and at the beginning of the line.

2.3 Multiconductor Transmission Line with Frequency Dependent Electrical Parameters

The equations in time domain for multiconductor transmission lines with frequency dependent electrical parameters can be expressed as follows [17].

$$\frac{\partial \mathbf{V}}{\partial \xi} + \mathbf{L}_0 \frac{\partial \mathbf{I}}{\partial t} + \frac{\partial}{\partial t} \int_0^t \mathbf{R}'(t-\tau)\mathbf{I}(\tau)\,d\tau = \mathbf{0} \tag{2.25}$$

$$\frac{\partial \mathbf{I}}{\partial \xi} + \mathbf{C} \frac{\partial \mathbf{V}}{\partial t} + \frac{\partial}{\partial t} \int_0^t \mathbf{G}'(t-\tau)\mathbf{V}(\tau)\,d\tau = \mathbf{0} \tag{2.26}$$

Where $\mathbf{L}_0$, $\mathbf{C}$, $\mathbf{G}'$ and $\mathbf{R}'$ are the geometrical inductance, the capacitance, the shunt transient conductance and series transient resistance of the line, respectively, $\mathbf{V}$ and $\mathbf{I}$ were defined in section 2.2.

In (2.25) the elements of the transient resistance matrix are fitted with a sum of rational functions and the convolution term is solved using a recursive scheme, as is shown in appendix B. According to the appendix B and considering that **G** does not depend on frequency the telegrapher's equations become of the following form:

$$\frac{\partial \mathbf{V}}{\partial \xi} + \mathbf{D}\frac{\partial \mathbf{I}}{\partial t} + \mathbf{R}_x \mathbf{I} + \mathbf{\Psi} = \mathbf{0} \tag{2.27a}$$

$$\frac{\partial \mathbf{I}}{\partial \xi} + \mathbf{C}\frac{\partial \mathbf{V}}{\partial t} + \mathbf{G}\mathbf{V} = \mathbf{0} \tag{2.27b}$$

where **D**, $\mathbf{R}_x$ and $\mathbf{\Psi}$ are defined in appendix B; **C** and **G** were defined in section 2.2. Multiplying the equations (2.27a) and (2.27b) by $\mathbf{D}^{-1}$ and $\mathbf{C}^{-1}$ respectively, gives the following:

$$\frac{\partial}{\partial \xi}\mathbf{U} + \mathbf{A}\frac{\partial}{\partial t}\mathbf{U} + \mathbf{B}\mathbf{U} + \mathbf{W} = \mathbf{0} \tag{2.28}$$

where

$$\mathbf{A} = \begin{bmatrix} \mathbf{0} & \mathbf{C}^{-1} \\ \mathbf{D}^{-1} & \mathbf{0} \end{bmatrix} \tag{2.29a}$$

$$\mathbf{B} = \begin{bmatrix} \mathbf{C}^{-1}\mathbf{G} & \mathbf{0} \\ \mathbf{0} & \mathbf{D}^{-1}\mathbf{R} \end{bmatrix} \tag{2.29b}$$

$$\mathbf{U} = \begin{bmatrix} \mathbf{V} \\ \mathbf{I} \end{bmatrix} \tag{2.30a}$$

$$\mathbf{W} = \begin{bmatrix} \mathbf{0} \\ \mathbf{D}^{-1}\mathbf{\Psi} \end{bmatrix} \tag{2.30b}$$

Diagonalization of **DC** and **CD** products are defined by:

$$\mathbf{T}_V^{-1}\mathbf{D}\mathbf{C}\mathbf{T}_V = \mathbf{\Lambda} \tag{2.31a}$$

and

$$\mathbf{T}_I^{-1}\mathbf{C}\mathbf{D}\mathbf{T}_I = \mathbf{\Lambda} \tag{2.31b}$$

where $\mathbf{T}_V$ and $\mathbf{T}_I$ are the modal matrices of voltages and currents respectively. In addition, modal electrical parameters can be expressed as follows:

$$\tilde{\mathbf{D}} = \mathbf{T}_V^{-1}\mathbf{D}\mathbf{T}_I \tag{2.32a}$$

$$\tilde{\mathbf{C}} = \mathbf{T}_I^{-1}\mathbf{C}\mathbf{T}_V \tag{2.32b}$$

and

$$\tilde{\mathbf{D}}\tilde{\mathbf{C}} = \mathbf{\Lambda} \tag{2.32c}$$

The characteristic impedance and admittance matrices are given by:

$$\mathbf{Z}_W = \sqrt{\tilde{\mathbf{D}}\tilde{\mathbf{C}}^{-1}} \tag{2.33a}$$

$$\mathbf{Y}_W = \sqrt{\tilde{\mathbf{C}}\tilde{\mathbf{D}}^{-1}} \tag{2.33b}$$

Moreover from the diagonalization of **A** the propagation velocities are obtained:

$$\mathbf{M}_\mathbf{L}\mathbf{A}\mathbf{M}_\mathbf{R} = \begin{bmatrix} \mathbf{\Gamma} & \mathbf{0} \\ \mathbf{0} & -\mathbf{\Gamma} \end{bmatrix} \tag{2.34}$$

where

$$\mathbf{\Gamma} = \sqrt{\tilde{\mathbf{C}}^{-1}\tilde{\mathbf{D}}^{-1}} = \sqrt{\mathbf{\Lambda}^{-1}} \tag{2.35}$$

The left ($\mathbf{M}_\mathrm{L}$) and right ($\mathbf{M}_\mathrm{R}$) eigenvectors of **A** were defined in (2.7). According to the procedure presented in section 2.2 equation (2.28) is left-multiplied by $\mathbf{M}_\mathrm{L}$ and knowing that along the characteristics:

$$\left(\frac{\partial}{\partial t} + \gamma_j \frac{\partial}{\partial \xi}\right) = + \frac{d}{dt} \tag{2.36a}$$

$$\left(\frac{\partial}{\partial t} - \gamma_j \frac{\partial}{\partial \xi}\right) = - \frac{d}{dt} \tag{2.36b}$$

the following system in modal domain is obtained:

$$\frac{d}{dt}V_{mj} + Z_{wj}\frac{d}{dt}I_{mj} + \frac{dx_j}{dt}\sum_{k=1}^{n}\tilde{R}_{Xjk}I_{mk} + \frac{dx_j}{dt}Z_{wj}\tilde{G}_j V_{mj} + \frac{dx_j}{dt}\psi_{mj} = 0 \tag{2.37a}$$

$$\frac{d}{dt}V_{mj} - Z_{wj}\frac{d}{dt}I_{mj} + \frac{dx_j}{dt}\sum_{k=1}^{n}\tilde{R}_{Xjk}I_{mk} - \frac{dx_j}{dt}Z_{wj}\tilde{G}_j V_{mj} + \frac{dx_j}{dt}\psi_{mj} = 0 \quad (2.37b)$$

where

$$\gamma_j = \pm\frac{dx}{dt} \quad (2.37c)$$

Equations (2.37) are $4n$ equations that represent (2.25) and (2.26). To integrate (2.37) the central finite differences method is used, as shown in Appendix C. Finally it can be obtained in the phase domain:

$$\mathbf{I}^{R'} = \mathbf{Y}_{Phase}^{K}\mathbf{V}^{R'} + \mathbf{I}_{H}^{A} \quad (2.38a)$$

$$\mathbf{I}^{S} = \mathbf{Y}_{Phase}^{K}\mathbf{V}^{S} + \mathbf{I}_{H}^{B} \quad (2.38b)$$

where

$$\mathbf{I}^{R'} = -\mathbf{T}_I\,\mathbf{I}_m^R \quad (2.39a)$$

$$\mathbf{I}^{S} = \mathbf{T}_I\,\mathbf{I}_m^S \quad (2.39b)$$

$$\mathbf{V}^{R'} = \mathbf{T}_V\,\mathbf{V}_m^R \quad (2.40a)$$

$$\mathbf{V}^{S} = \mathbf{T}_V\,\mathbf{V}_m^S \quad (2.40b)$$

$$\mathbf{I}_H^A = -\mathbf{T}_I\mathbf{Z}_K^{-1}\mathbf{V}_{Hm}^A \quad (2.41a)$$

$$\mathbf{I}_H^B = -\mathbf{T}_I\mathbf{Z}_K^{-1}\mathbf{V}_{Hm}^B \quad (2.41b)$$

$$\mathbf{Y}_{Phase}^{K} = \mathbf{T}_I\mathbf{Z}_K^{-1}\mathbf{H}_3\mathbf{T}_V^{-1} \quad (2.42)$$

From (2.38) the Norton's circuits in phase domain are obtained, as shown in Fig. (2.4).

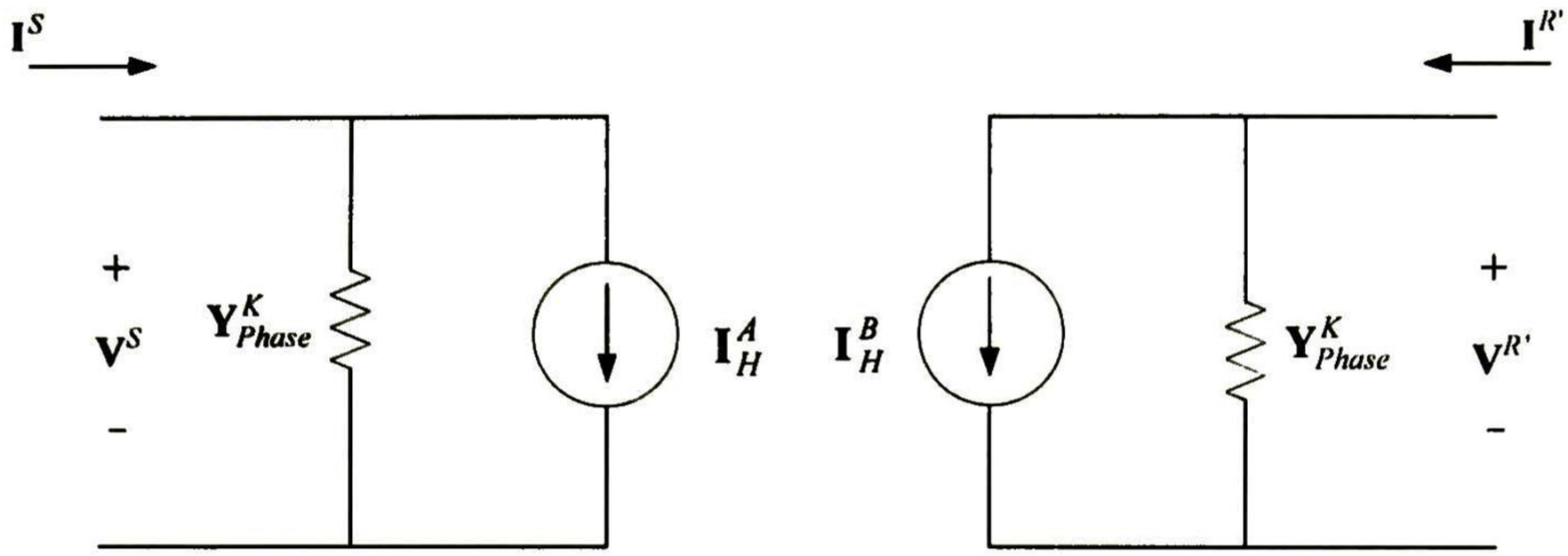

Figure 2.4. Norton's circuits at the end and at the beginning of the line.

2.4 Application Example

Different cases of transient events are used to validate the model. Transient voltages obtained with the developed model are compared with those obtained using a frequency domain method [15] and the ATP/EMTP [3]. Data for the simulation do not belong to an actual specific line, they represent a typical transmission line and are only used to obtain results and to validate the model.

As first application example, a 100 km long 3-phase uniform line is used for the analysis. The line is formed by three conductors in horizontal configuration; the distance between conductors is 3 m. The radius and height of the line are 0.02 m and 15 m respectively, the permeability of the ground and the conductors is 1.2566×10^{-6} H/m, the resistivity of the ground and the conductors are 100 Ω-m and 2.71×10^{-8} Ω-m respectively. At the sending node a 3-phase sinusoidal source is connected; the closing times of the switches for phases A, B and C are 0.002 s, 0.006 s and 0.012 s, respectively. At the end of the line a high resistance is connected to approximate an open circuit. In Figs. (2.5) and (2.7), the magnitudes of the fitted curves of the self and mutual elements of the transient resistance for this line are shown, and Figs. (2.6) and (2.8) show the corresponding phase angles. It is important to note that $\mathbf{R}'$ is a symmetric matrix. On the other hand, Fig. (2.9) shows the transient voltages at the end of the line.

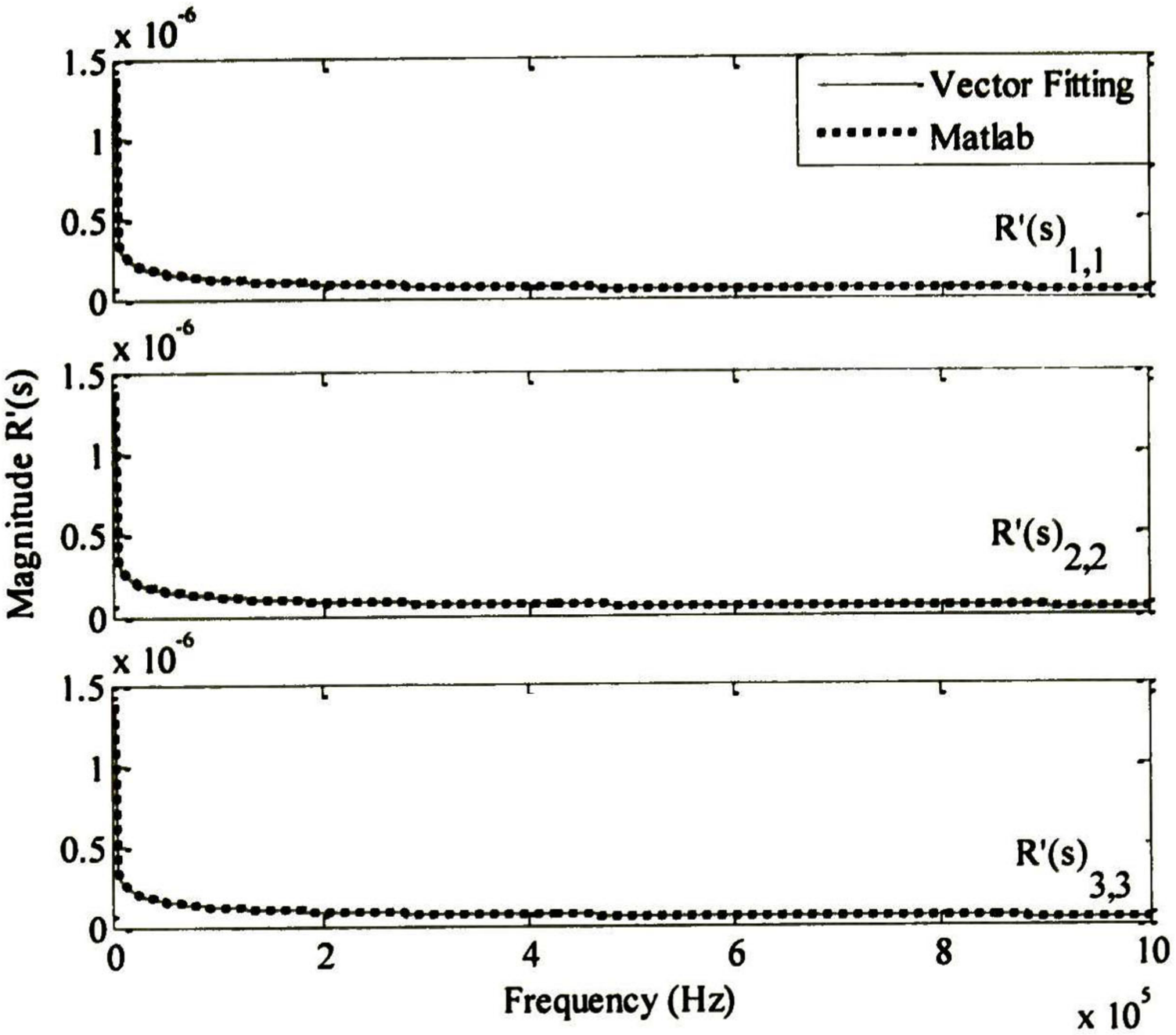

Figure 2.5. Magnitude of the self elements of the transient resistance.

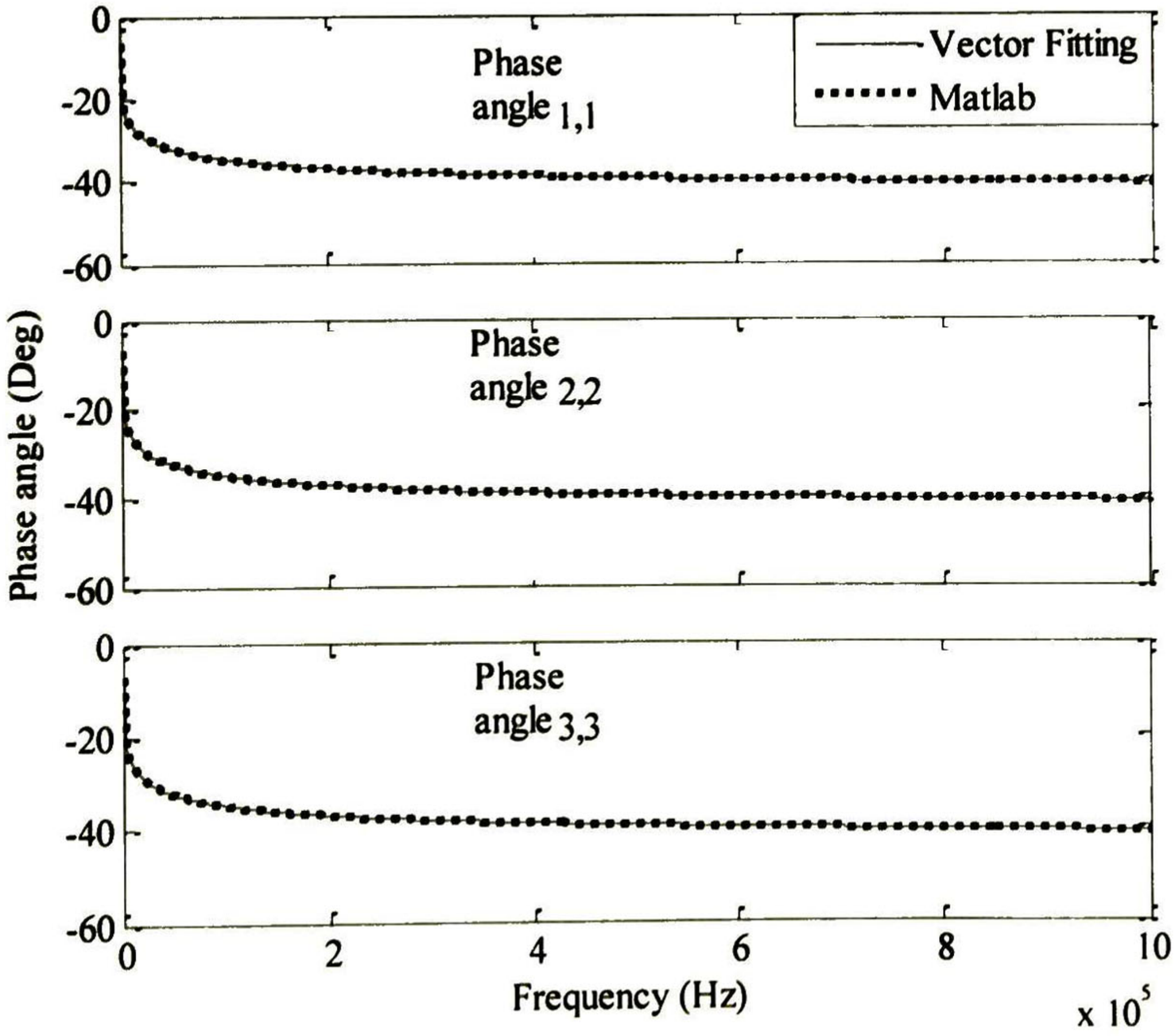

Figure 2.6. Phase angle of the self elements of the transient resistance.

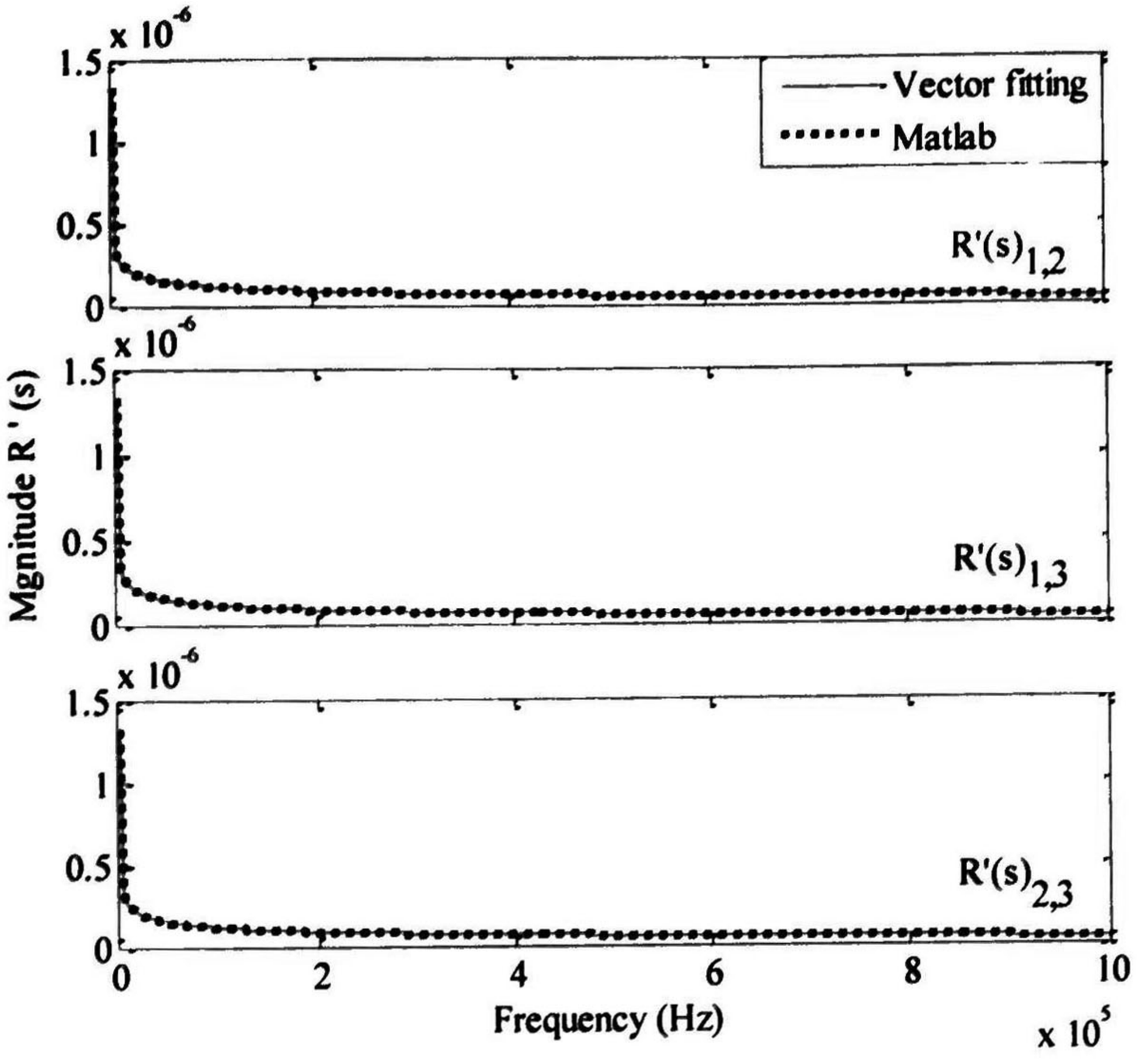

Figure 2.7. Magnitude of the mutual elements of the transient resistance.

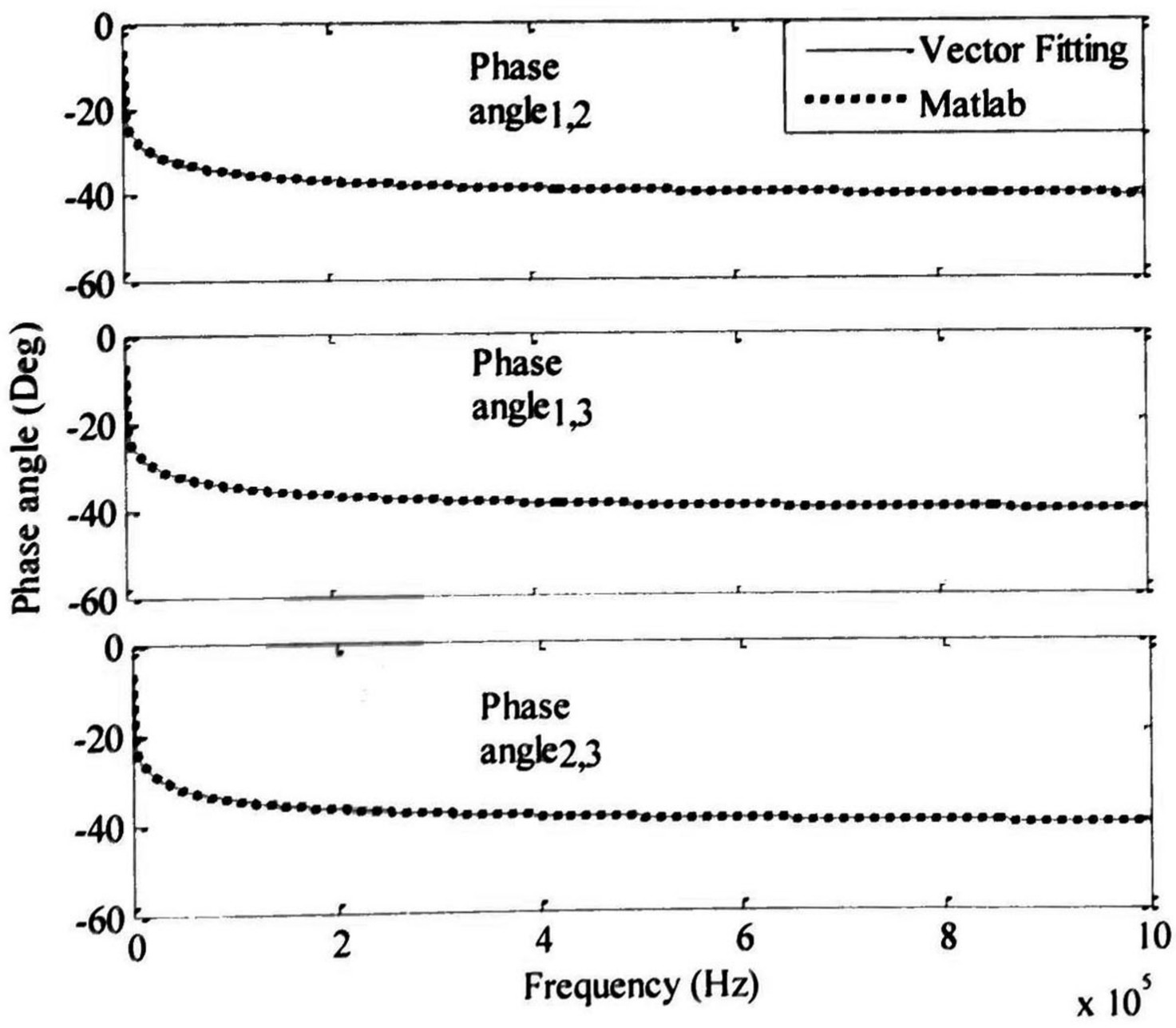

Figure 2.8. Phase angle of the mutual elements of the transient resistance.

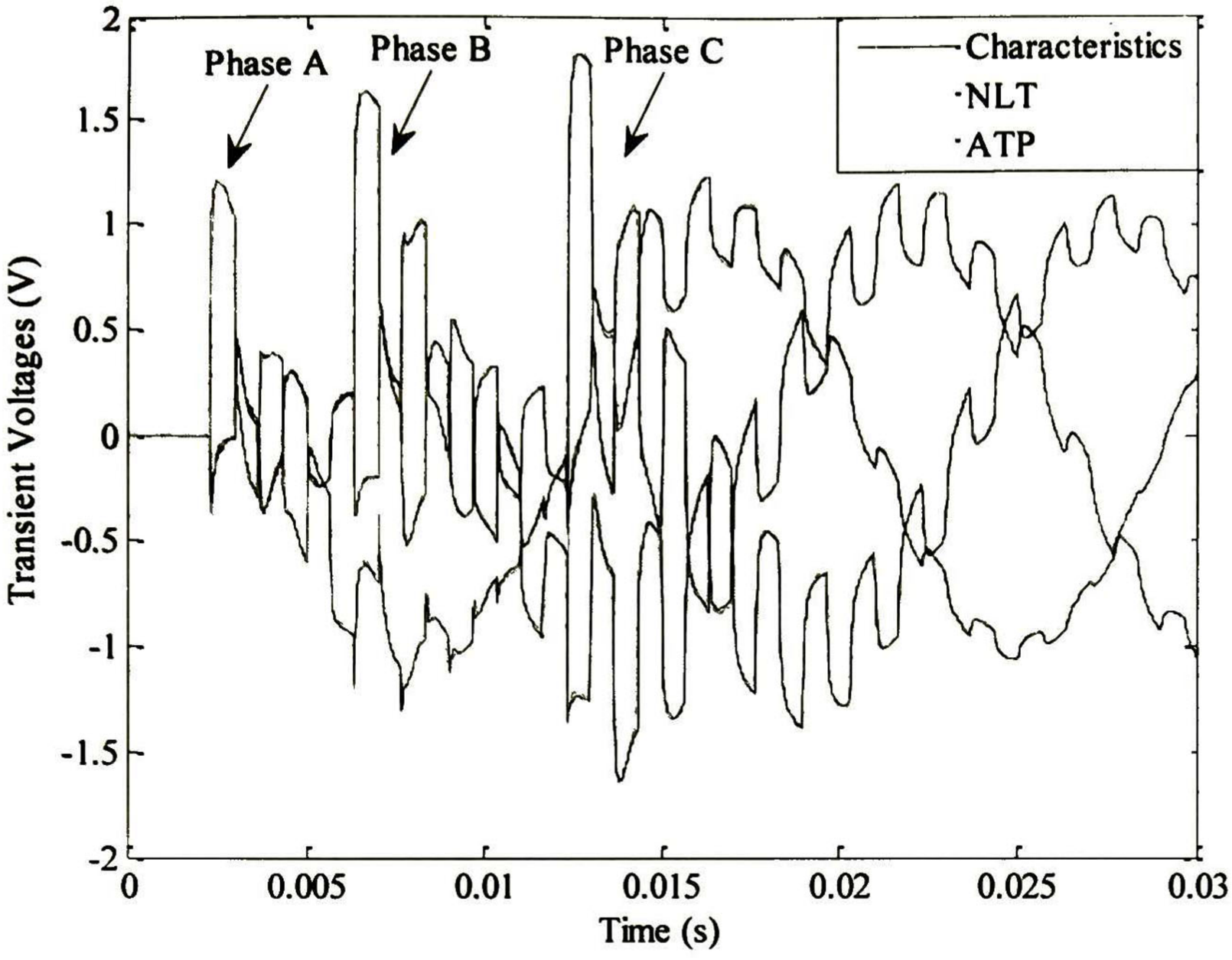

Figure 2.9. Transient voltages at the end of the line.

As a second application example, a system with two parallel 3-phase lines is used, as shown in Fig. (2.10). At the sending nodes of the *A* circuit, a 3-phase sinusoidal source is connected and the times of closing are 0.002 s, 0.006 s and 0.012 s for the phases A, B and C respectively; the receiving end is considered as open circuit.

On the other hand the *B* circuit is not energized; the sending nodes are grounded while the receiving nodes are considered first as open circuits and then as short circuits. In Fig. (2.11) the transient voltages at the receiving node of the *A* circuit are shown.

The induced voltages at the end of the *B* circuit for open circuit are shown in Figs. (2.12). Finally, the transient currents at the receiving node of the *A* and *B* circuits for short circuit termination are shown in Fig. (2.13) and Figs. (2.14), respectively.

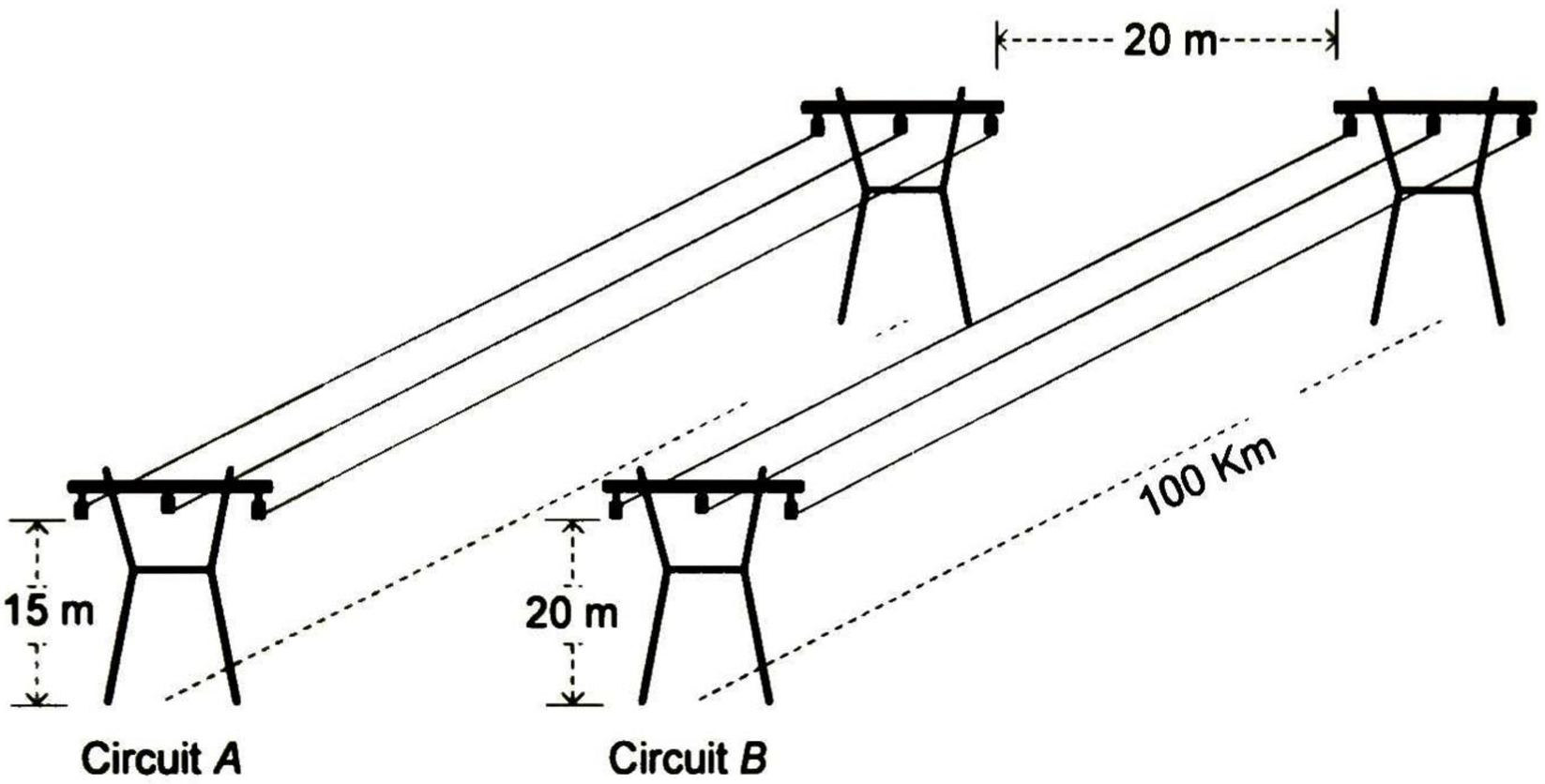

Figure 2.10. Configuration of a circuit of two lines.

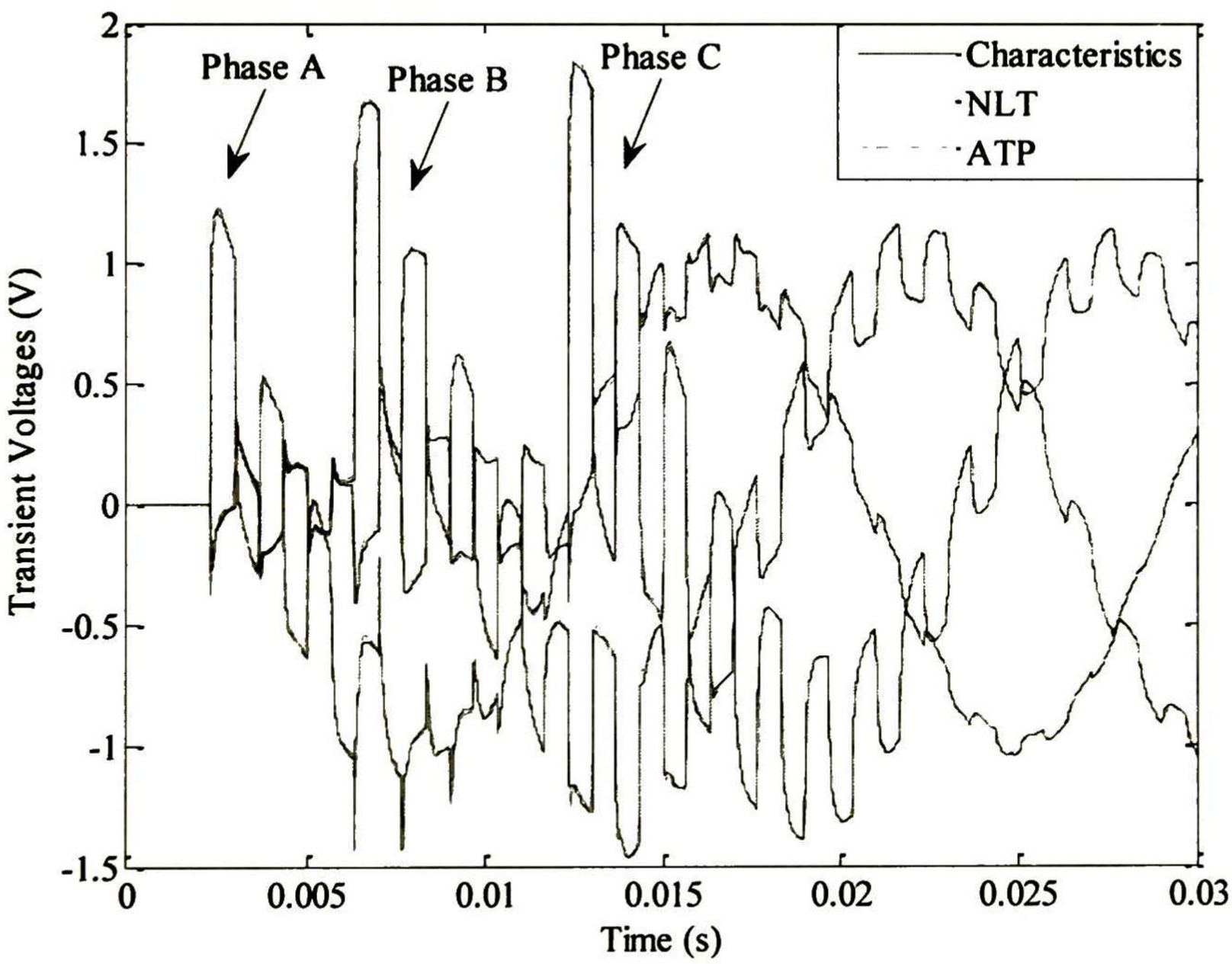

Figure 2.11. Transient voltages at the end of the *A* circuit.

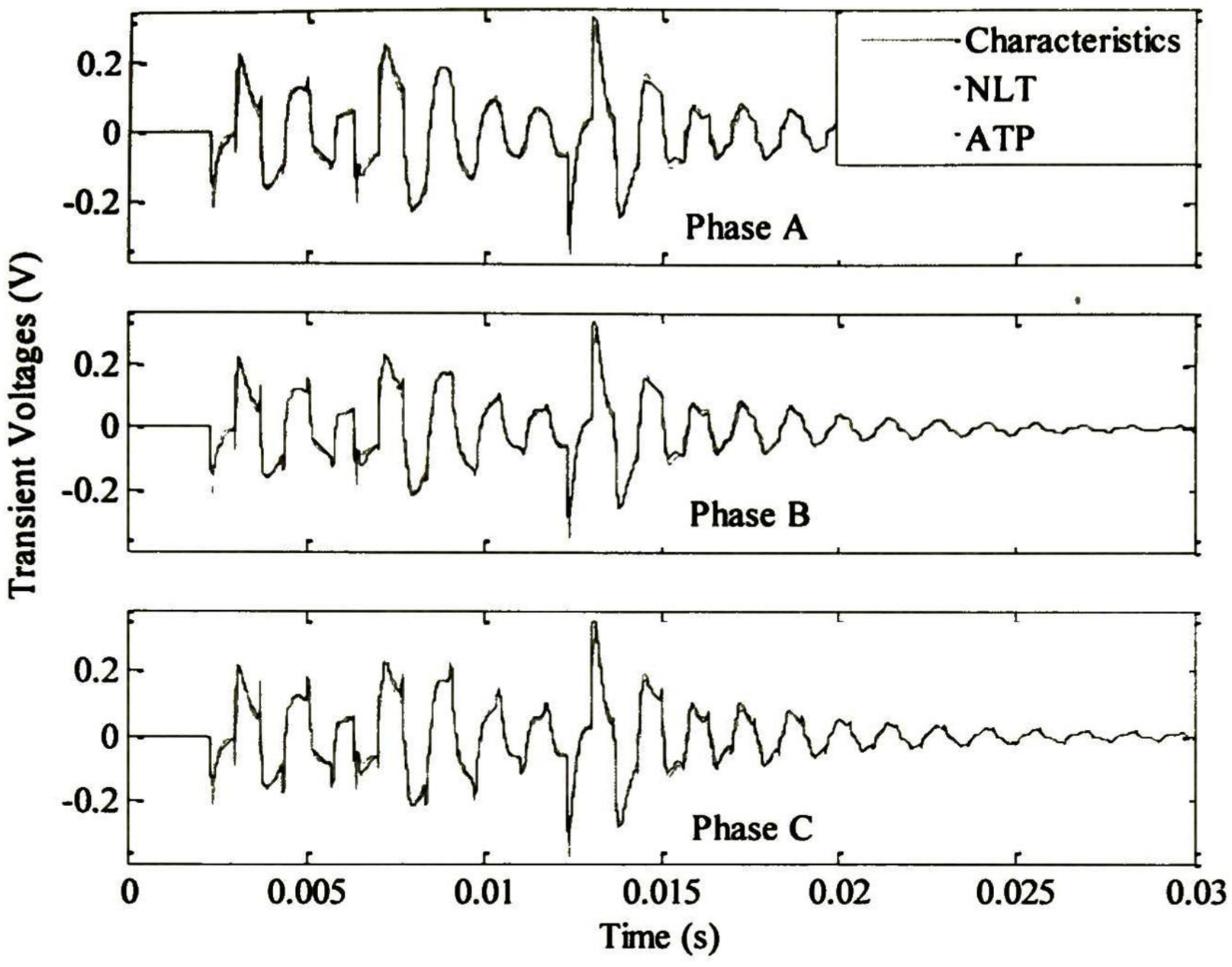

Figure 2.12. Transient induced voltages at the end of the *B* circuit for open circuit.

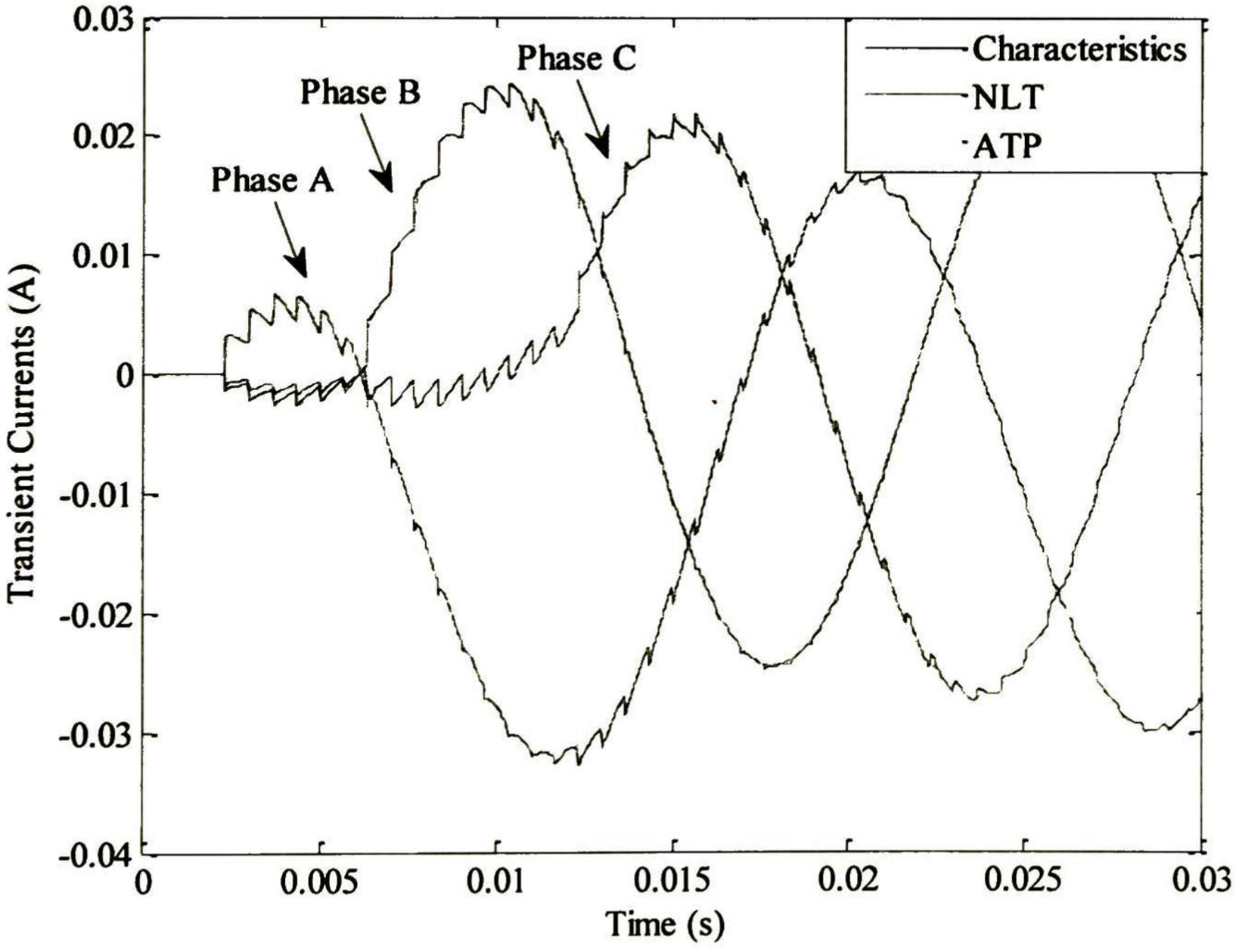

Figure 2.13. Transient currents at the end of the *A* circuit for short circuit.

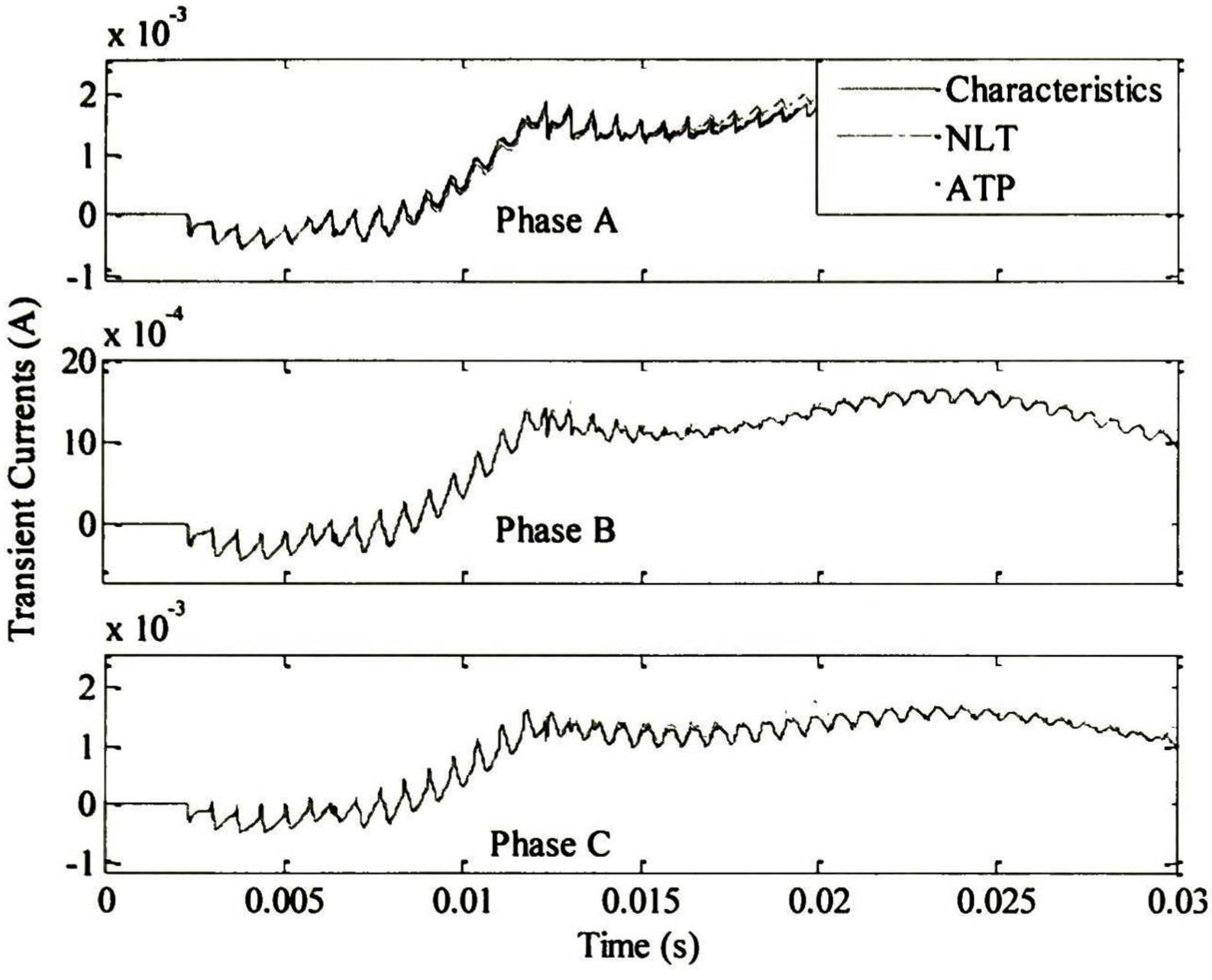

Figure 2.14. Transient induced currents at the end of the *B* circuit for short circuit.

2.5 Conclusions

In this section a model for multiconductor transmission lines with and without frequency dependent electrical parameters for time domain analysis of transient voltages was presented.

Similarly to the Universal model and the Martí model the technique developed in this work does not need to divide the line in segments and the line is represented by Norton's circuits in phase domain.

Both the Universal model and the Martí model require the approximation of two parameters for including the frequency dependence of the electrical parameters. The model presented in this work only requires the approximation of one parameter: the transient resistance.

The parameters approximated in the Universal and the Martí model present fast variations, therefore they are more susceptible to modeling errors. On the other hand, the transient resistance is a smooth function, which is easier to approximate.

The model was validated by comparing its results with those from the Martí model, available in the simulation program ATP/EMTP, and the results from a Numerical Laplace Transform program.

3 Characteristics Model for Transmission Lines Through Decoupled Modes Analysis

3.1 Introduction

In Chapter 2 a characteristic model for Multiconductor Transmission Lines (**MTL**) for time domain transient analysis was presented. The technique is based on the solution in time domain of the telegrapher's equations using the method of characteristics. The interpolation method of Lagrange was used to obtain the values of modal voltages and currents in the propagation axis, as shown in Fig. (2.2).

In this Chapter a different model for multiconductor transmission lines based in the method of characteristics is presented. In contrast with the method presented in Chapter 2, here the interpolations are made in the time axis and modal voltages, modal currents and convolution terms are interpolated in a separate way. To validate the model a number of application examples are used and the results are compared to those from a frequency domain method and from time domain methods.

3.2 Transmission Line with Frequency Dependent Electrical Parameters Through Separated Modes Analysis

As presented in Chapter 2, after using modal analysis an ordinary differential equations system for the *jth*-mode can be obtained:

$$\frac{d}{dt}V_{mj} + Z_{wj}\frac{d}{dt}I_{mj} + \frac{dx_j}{dt}\tilde{R}_{Xj}I_{mj} + \frac{dx_j}{dt}Z_{wj}\tilde{G}_j V_{mj} + \frac{dx_j}{dt}\psi_{mj} = 0 \qquad (3.1a)$$

$$\frac{d}{dt}V_{mj} - Z_{wj}\frac{d}{dt}I_{mj} + \frac{dx_j}{dt}\tilde{R}_{Xj}I_{mj} - \frac{dx_j}{dt}Z_{wj}\tilde{G}_j V_{mj} + \frac{dx_j}{dt}\psi_{mj} = 0 \qquad (3.1b)$$

where

$$\gamma_j = \pm\frac{dx}{dt} \qquad (3.1c)$$

For this model the parameter R_{Xji} is considered as diagonal to enforce the separation of the modes. The central finite differences method is applied to integrate (3.1) according to Fig. (3.1). Each equation system corresponding to the *jth*-mode is evaluated in a separate way. Equation (B.13) is used to replace the convolution terms in points S and R obtaining the following equations:

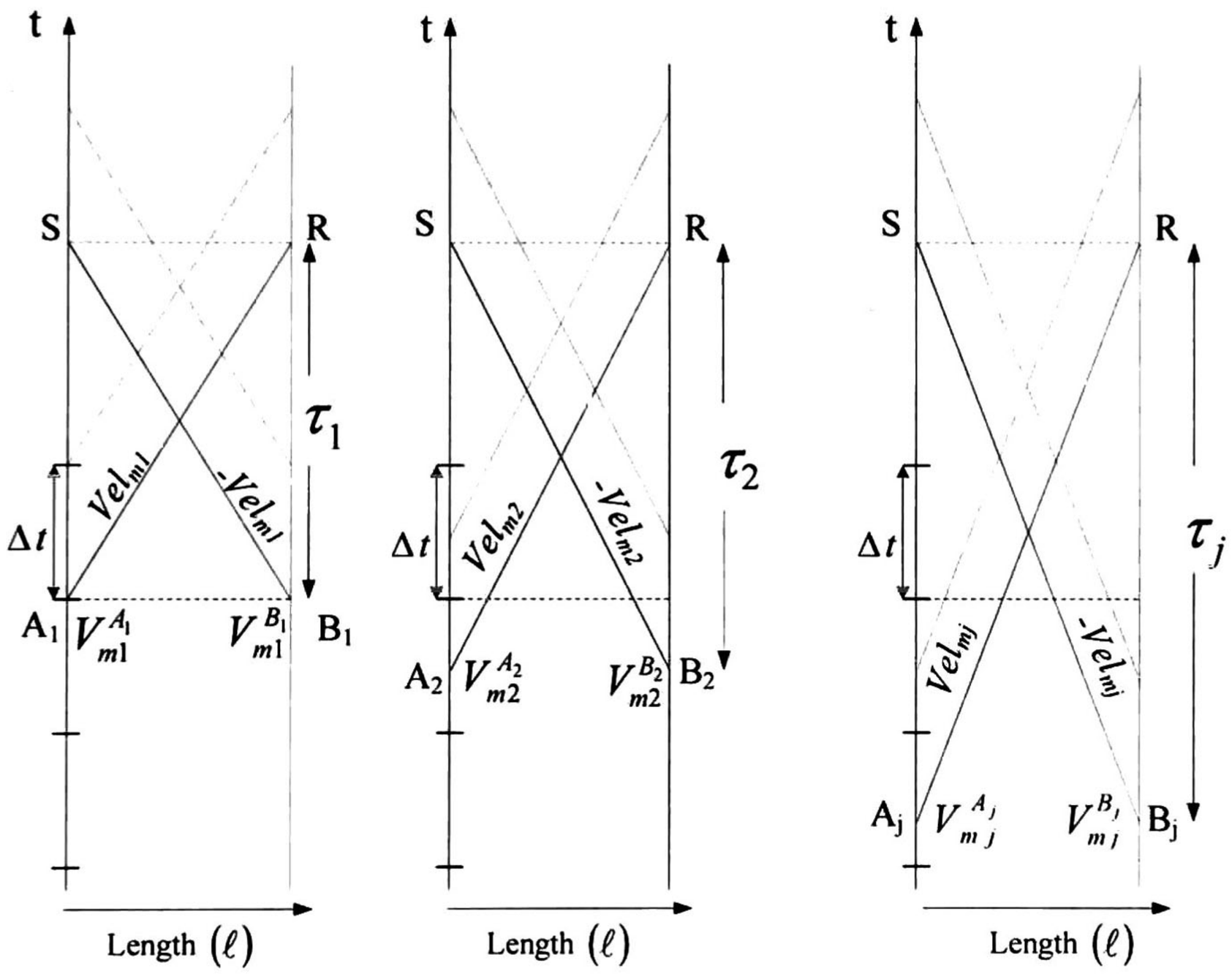

Figure 3.1. Characteristic lines diagrams for the separate modes analysis.

$$H_3 V_{mj}^{R} - H_4 V_{mj}^{A_j} + Z_K I_{mj}^{R} - Z_4 I_{mj}^{A_j} + \frac{\Delta x_j}{2}\left(\psi_{mj}^{A_j} + \psi_{mj}^{R'}\right) = 0 \qquad (3.2a)$$

$$H_3 V_{mj}^{S} - H_4 V_{mj}^{B_j} - Z_K I_{mj}^{S} + Z_4 I_{mj}^{B_j} - \frac{\Delta x_j}{2}\left(\psi_{mj}^{B_j} + \psi_{mj}^{S'}\right) = 0 \qquad (3.2b)$$

The variables Z_4, Z_k, H_3, H_4 and the convolution terms are defined in Appendix C. On the other hand, terms Vel_{mj}, $V_{mj}^{A_j}$ and $V_{mj}^{B_j}$ were defined in Chapter 2. The variables $V_{mj}^{A_j}$, $V_{mj}^{B_j}$, $I_{mj}^{A_j}$, $I_{mj}^{B_j}$ and $\psi_{mj}^{A_j}$, $\psi_{mj}^{B_j}$ are calculated by interpolation with the second order Lagrange method according to Fig. (3.2):

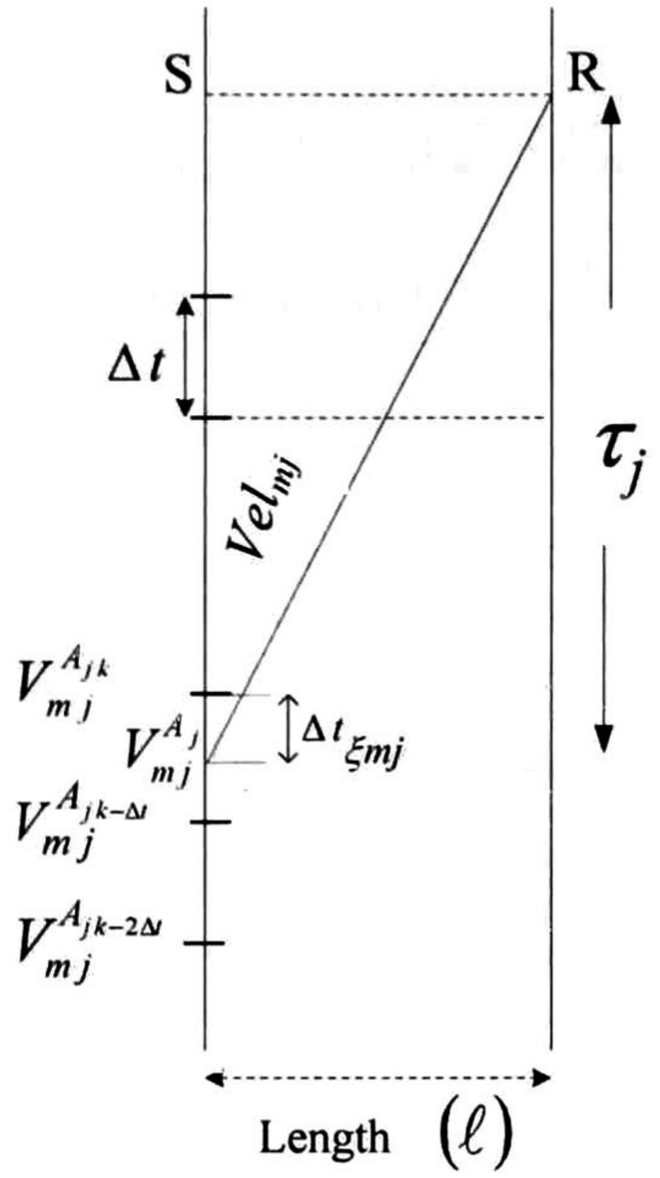

Figure 3.2. Interpolation diagram for the modes voltages of the *jth*-mode.

$$V_{mj}^{A_j} = \alpha_{1j} V_{mj}^{A_{jk}} + \alpha_{2j} V_{mj}^{A_{jk-\Delta t}} + \alpha_{3j} V_{mj}^{A_{jk-2\Delta t}} \tag{3.3a}$$

$$V_{mj}^{B_j} = \alpha_{1j} V_{mj}^{B_{jk}} + \alpha_{2j} V_{mj}^{B_{jk-\Delta t}} + \alpha_{3j} V_{mj}^{B_{jk-2\Delta t}} \tag{3.3b}$$

where

$$\alpha_{1j} = \frac{\Delta t_{\xi mj}{}^2 - 2\Delta t \Delta t_{\xi mj} - \Delta t \Delta t_{\xi mj} + 2\Delta t^2}{2\Delta t^2} \tag{3.4a}$$

$$\alpha_{2j} = \frac{2\Delta t \Delta t_{\xi mj} - \Delta t_{\xi mj}{}^2}{\Delta t^2} \tag{3.4b}$$

$$\alpha_{3j} = \frac{\Delta t_{\xi mj}{}^2 - \Delta t \Delta t_{\xi mj}}{2\Delta t^2} \tag{3.4c}$$

Similar expression to (3.3) for the modal currents and modal convolution terms are obtained. Substituting (3.3) in (3.2) and expressing the result as a function of the "*history terms*" the next equations are obtained:

$$I_{mj}^{R'} = Z_K^{-1} H_3 V_{mj}^{R'} + I_{Hmj}^{A_j} \tag{3.5a}$$

$$I_{mj}^{S} = Z_K^{-1} H_3 V_{mj}^{S} + I_{Hmj}^{B_j} \tag{3.5b}$$

where

$$I_{Hmj}^{A_j} = -Z_K^{-1} V_{Hmj}^{A_j} \tag{3.6a}$$

$$I_{Hmj}^{B_j} = -Z_K^{-1} V_{Hmj}^{B_j} \tag{3.6b}$$

$$V_{Hmj}^{A_j} = H_4\left(\alpha_{1j} V_{mj}^{A_{jk}} + \alpha_{2j} V_{mj}^{A_{jk-\Delta t}} + \alpha_{3j} V_{mj}^{A_{jk-2\Delta t}}\right) + Z_4\left(\alpha_{1j} I_{mj}^{A_{jk}} + \alpha_{2j} I_{mj}^{A_{jk-\Delta t}} + \alpha_{3j} I_{mj}^{A_{jk-2\Delta t}}\right) - \frac{\Delta x_j}{2}\left(\alpha_{1j} \psi_{mj}^{A_{jk}} + \alpha_{2j} \psi_{mj}^{A_{jk-\Delta t}} + \alpha_{3j} \psi_{mj}^{A_{jk-2\Delta t}}\right) - \frac{\Delta x_j}{2} \psi_{mj}^{R'} \tag{3.7a}$$

$$V_{Hmj}^{B_j} = H_4\left(\alpha_{1j} V_{mj}^{B_{jk}} + \alpha_{2j} V_{mj}^{B_{jk-\Delta t}} + \alpha_{3j} V_{mj}^{B_{jk-2\Delta t}}\right) - Z_4\left(\alpha_{1j} I_{mj}^{B_{jk}} + \alpha_{2j} I_{mj}^{B_{jk-\Delta t}} + \alpha_{3j} I_{mj}^{B_{jk-2\Delta t}}\right) + \frac{\Delta x_j}{2}\left(\alpha_{1j} \psi_{mj}^{B_{jk}} + \alpha_{2j} \psi_{mj}^{B_{jk-\Delta t}} + \alpha_{3j} \psi_{mj}^{B_{jk-2\Delta t}}\right) + \frac{\Delta x_j}{2} \psi_{mj}^{S'} \tag{3.7b}$$

The variables $V_{Hmj}^{B_j}$ and $V_{Hmj}^{A_j}$ corresponding to the *jth*-mode represent "*history terms*" delayed a travel time. Expressing (3.5) in matrix form and applying the transformation matrices $\mathbf{T}_V$ and $\mathbf{T}_I$ (3.5) can be expressed in phase domain as follows:

$$\mathbf{I}^{R'} = \mathbf{Y}_{Phs}^{K} \mathbf{V}^{R'} + \mathbf{I}_H^A \tag{3.8a}$$

$$\mathbf{I}^{S} = \mathbf{Y}_{Phs}^{K} \mathbf{V}^{S} + \mathbf{I}_H^B \tag{3.8b}$$

where

$$\mathbf{I}^{R'} = -\mathbf{T}_I \mathbf{I}_m^R, \quad \mathbf{I}^S = \mathbf{T}_I \mathbf{I}_m^S \qquad \text{(3.9a), (3.9b)}$$

$$\mathbf{V}^{R'} = \mathbf{T}_V \mathbf{V}_m^R, \; \mathbf{V}^S = \mathbf{T}_V \mathbf{V}_m^S \qquad \text{(3.10a), (3.10b)}$$

$$\mathbf{I}_H^A = -\mathbf{T}_V \mathbf{Z}_K^{-1} \mathbf{V}_{Hm}^A, \quad \mathbf{I}_H^B = -\mathbf{T}_V \mathbf{Z}_K^{-1} \mathbf{V}_{Hm}^B \qquad \text{(3.11a), (3.11b)}$$

$$\mathbf{Y}_{Phs}^K = \mathbf{T}_I \mathbf{Z}_K^{-1} \mathbf{H}_3 \mathbf{T}_V^{-1} \qquad \text{(3.12a), (3.12b)}$$

In the same form than in Chapter 2, (3.8) represent Norton's equivalent circuits, as shown in Fig. (3.3).

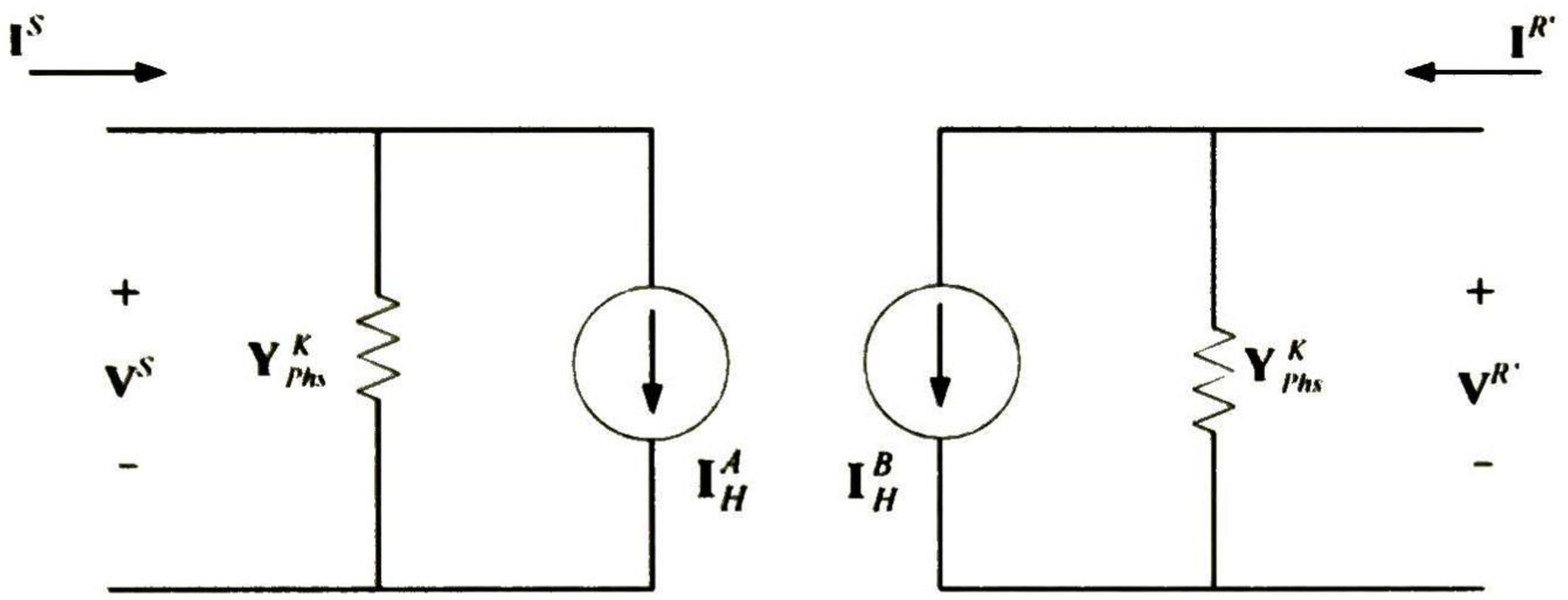

Figure 3.3. Norton's circuits that represent the transmission line.

3.3 Application Examples

The results from the proposed model are compared with those obtained using a FDM (Frequency Domain Method) [18, 19], the Model of J. Martí available in the ATP/EMTP [3] and the ULM (Universal Line Model) available in the EMTP-RV [20]. The FDM is considered as the theoretically exact solution and represents the base of comparison for the simulation results.

a). Energization of a MTL.

As first application example, a system with three parallel 3-phase lines is used, as shown in Fig. (3.4). The length of the lines is 100 km. The radius of the conductors is 0.02 m, the permeability of the ground and the conductors is 1.2566×10^{-6} H/m, the

resistivity of ground and conductors are 100 Ω-m and 2.71×10^{-8} Ω-m, respectively. At the sending node of the *A* circuit, a 3-phase sinusoidal source of 230 kV is connected; the times of closing are 0.002s, 0.006 s and 0.012 s for phases *O*, *P* and *Q*, respectively, and the receiving end is considered as open circuit.

B and *C* circuits are not energized and the sending nodes are grounded while the receiving nodes are considered as open circuits. The elements of R'(s) were fitted with 9 poles for all examples. In Fig. (3.5) the transient voltages at the receiving node of the *P* phase of the *A* circuit are shown. The induced per unit voltages in the *P* phase at the end of the *B* and *C* circuits are shown in Figs. (3.6) and (3.7), respectively. As it can be seen both the ULM and the characteristics model provide for practical purposes results close to those from the FDM.

Consider now the case where the ends of all circuits are connected to ground through 10 Ω resistances. Figures (3.8)-(3.11) show the transient induced currents on the *O* and *P* phases at the ends of the *B* and *C* circuits. In this case the J. Martí model does not provide correct results. This can be attributed to the fact that this model does not take into account the frequency dependence of the transformation matrix.

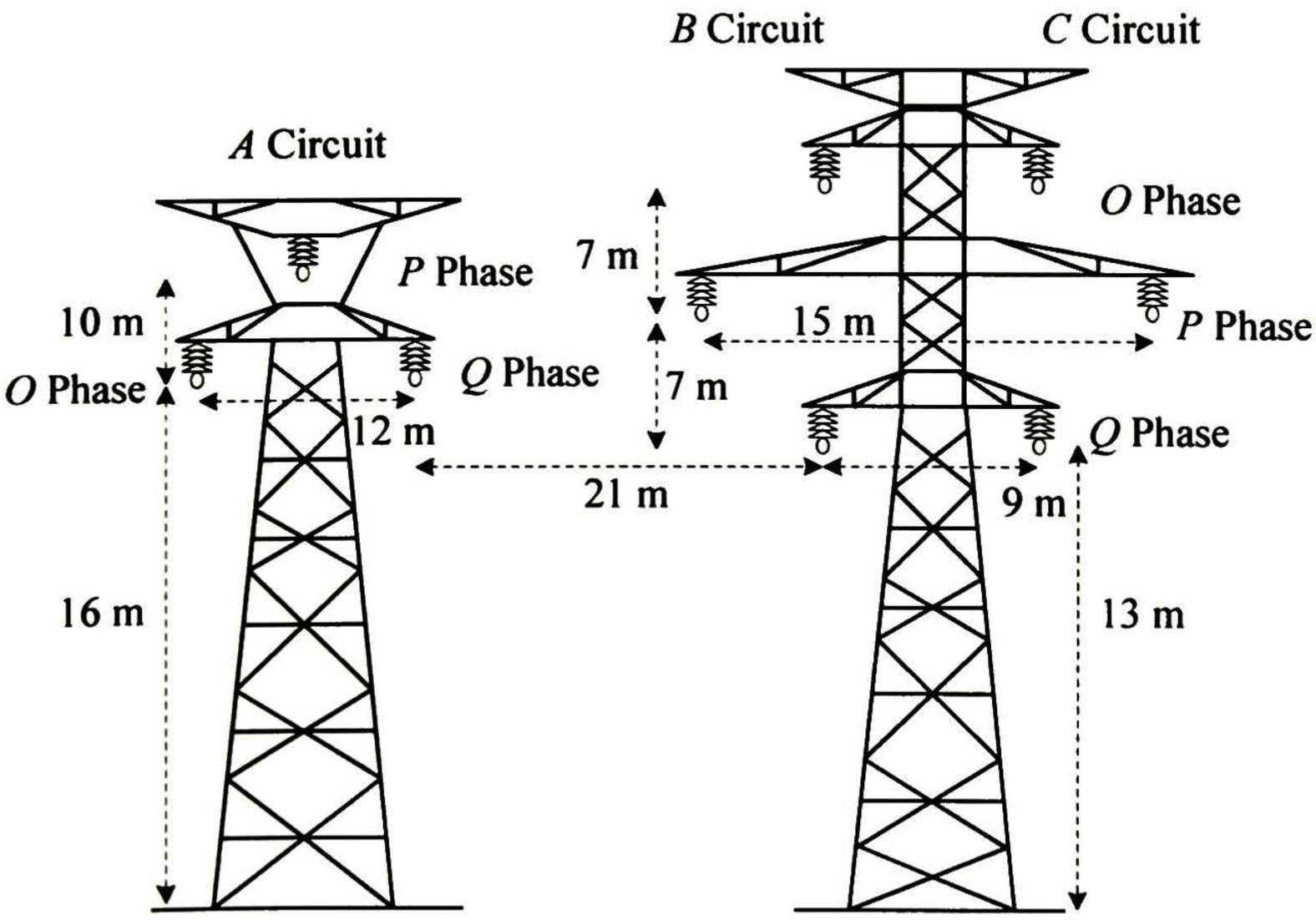

Figure 3.4. Configuration of a MTL with three circuits.

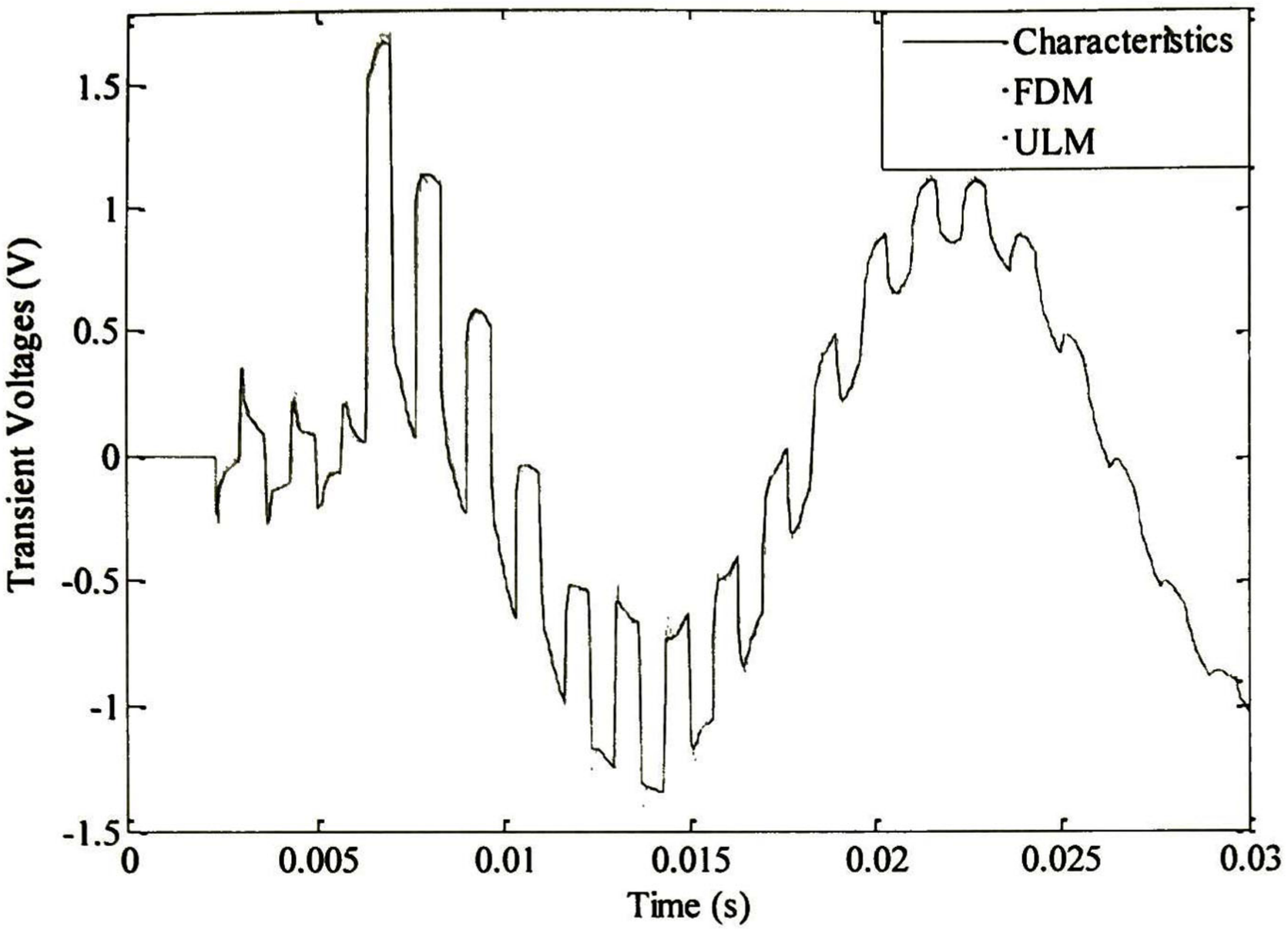

Figure 3.5. Transient voltages in the *P* phase at the end of the *A* circuit.

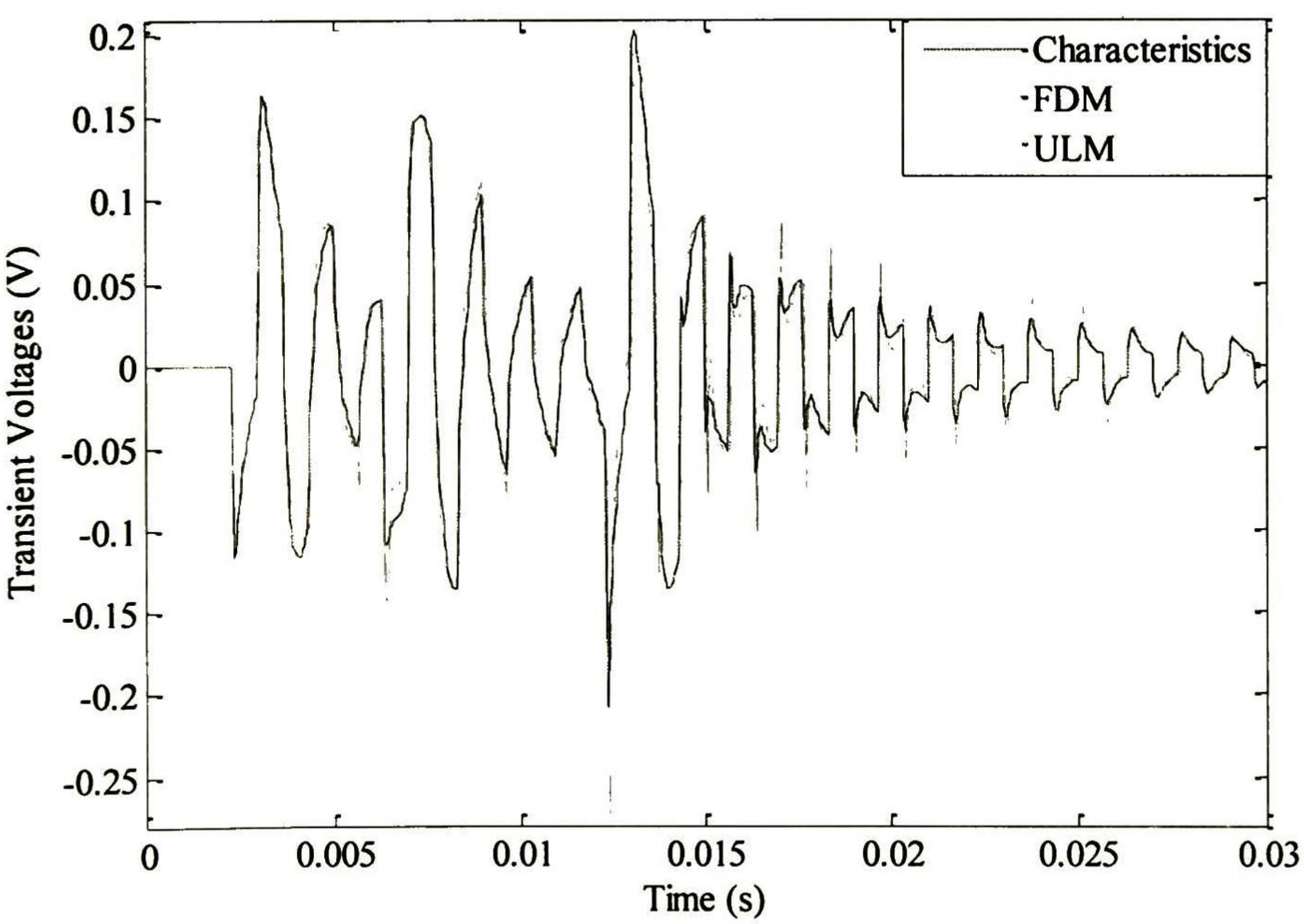

Figure 3.6. Transient induced voltages in the *P* phase at the end of the *B* circuit.

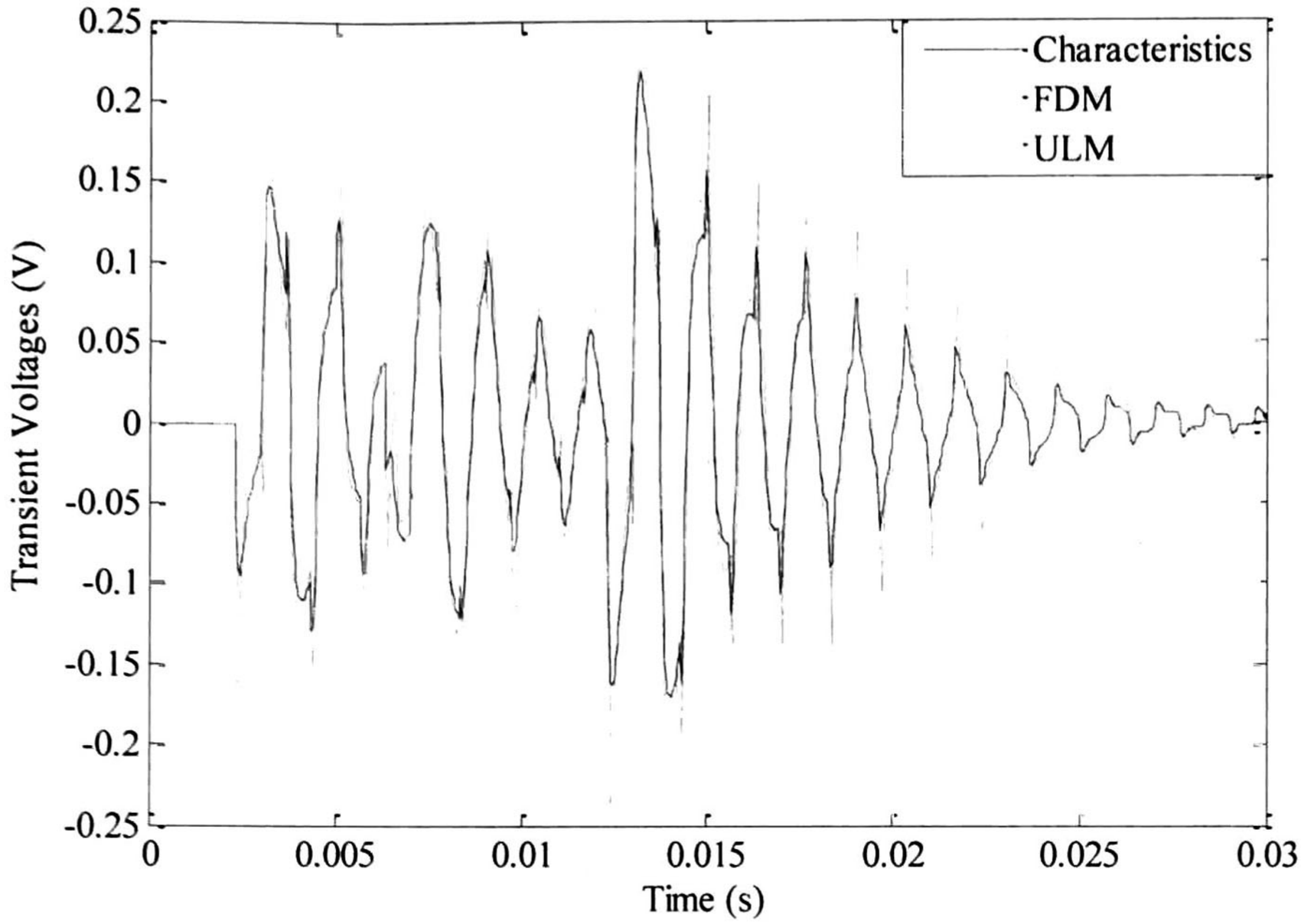

Figure 3.7. Transient induced voltages in the *P* phase at the end of the *C* circuit.

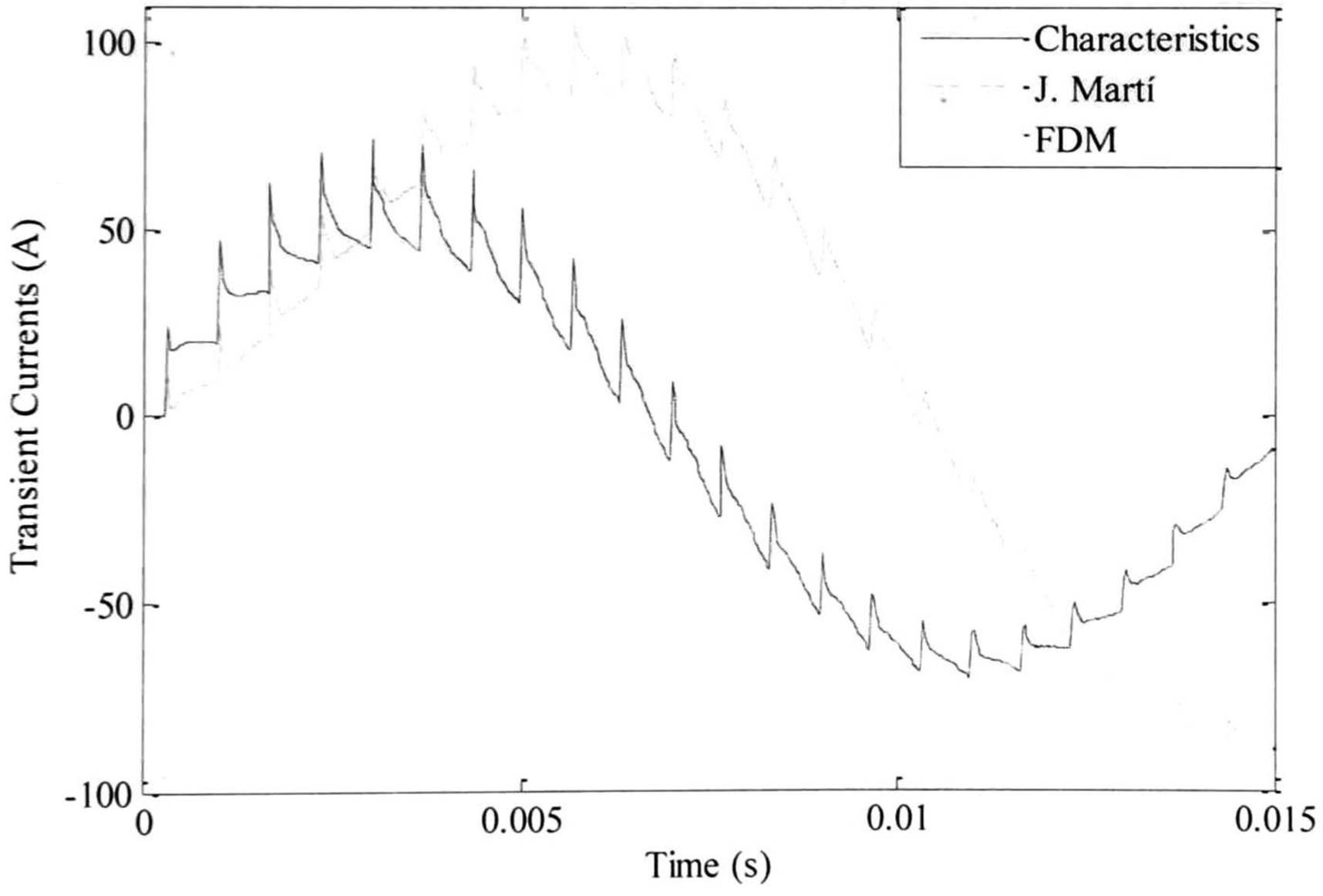

Figure 3.8. Transient induced currents in the *O* phase at the end of the *B* circuit (connected to ground).

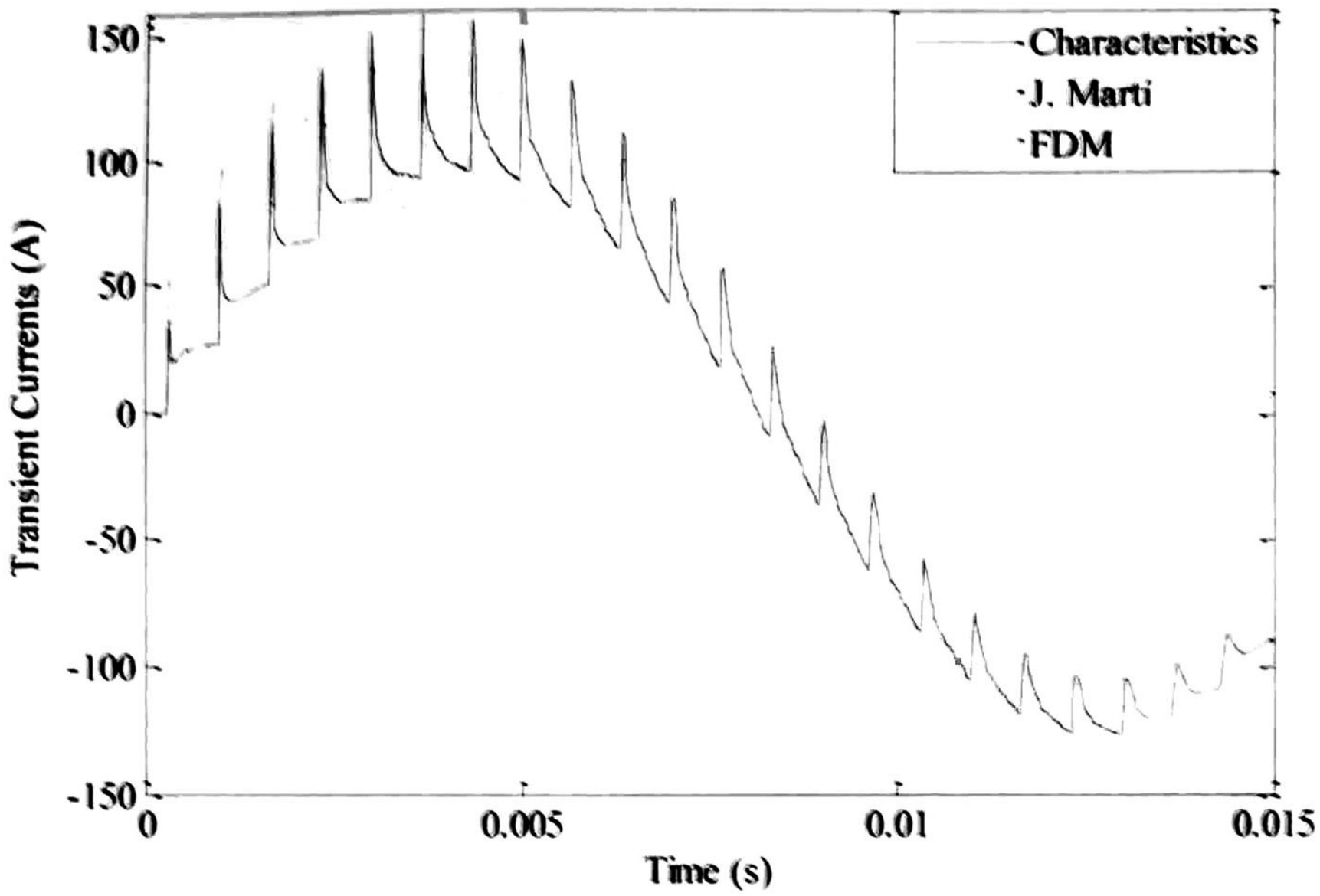

Figure 3.9. Transient induced currents in the *P* phase at the end of the *B* circuit (connected to ground).

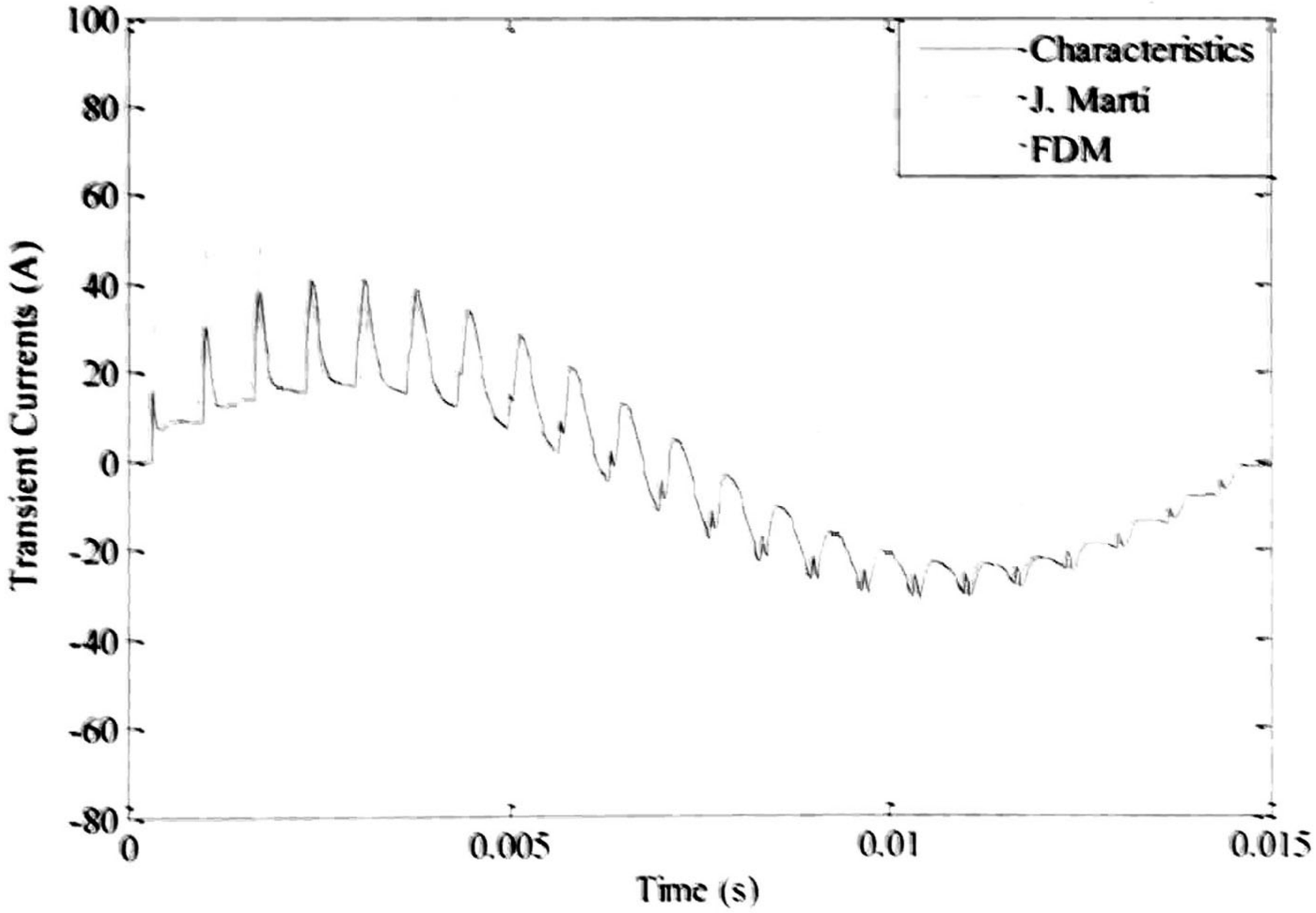

Figure 3.10. Transient induced currents in the *O* phase at the end of the *C* circuit (connected to ground).

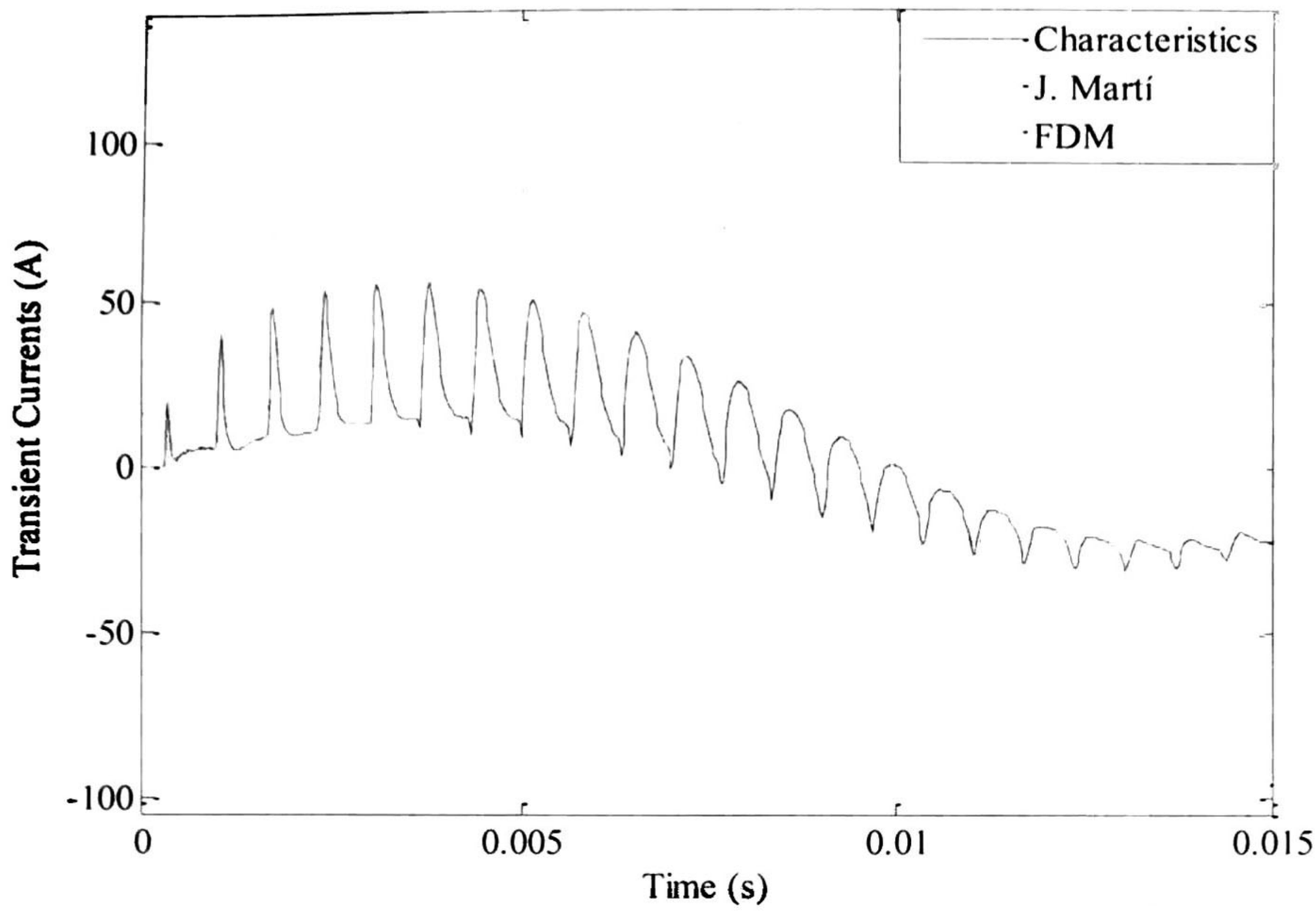

Figure 3.11. Transient induced currents in the *P* phase at the end of the *C* circuit (connected to ground).

b). Field test.

As a second example consider the field measurements published in ref. [21]. The line configuration is shown in Fig. (3.12). The sending nodes of phases B and C and the receiving nodes for all phases are considered as open circuits. Figure (3.13) show the transient voltages at the receiving node of the line.

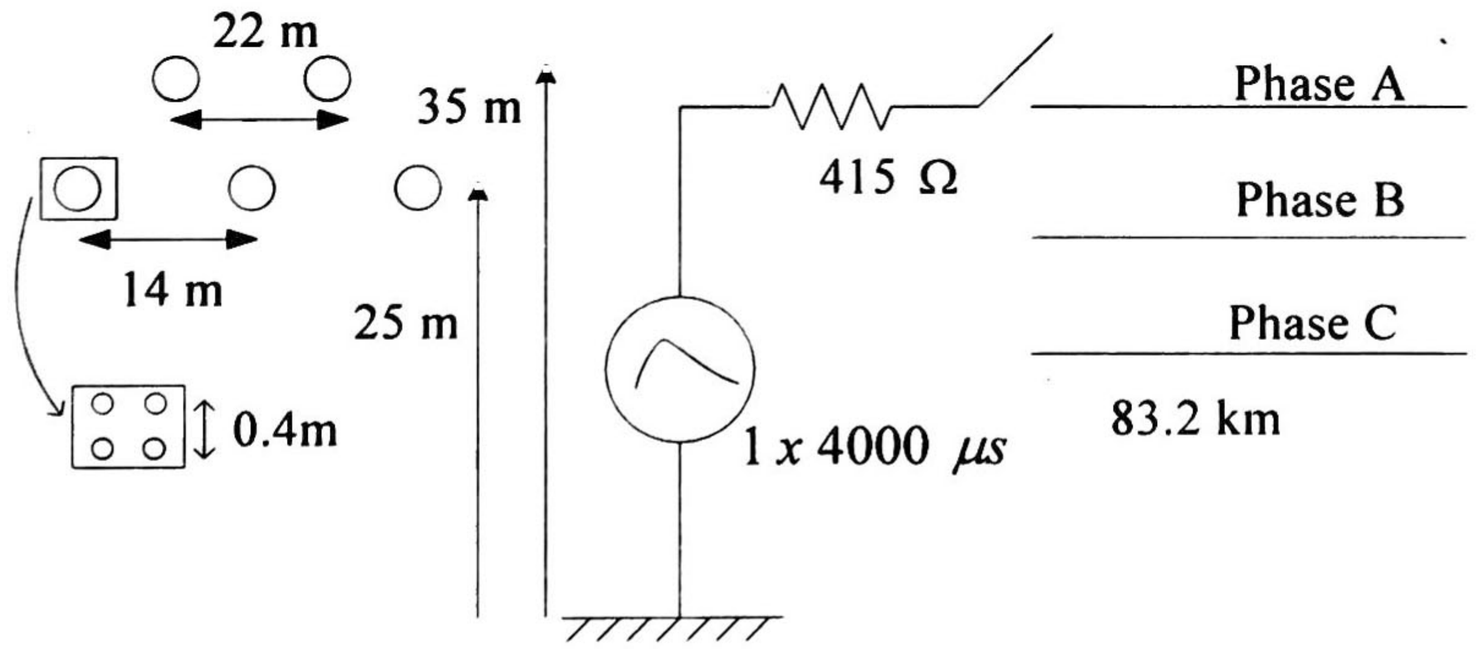

Figure 3.12. Configuration of the line for the field test [21].

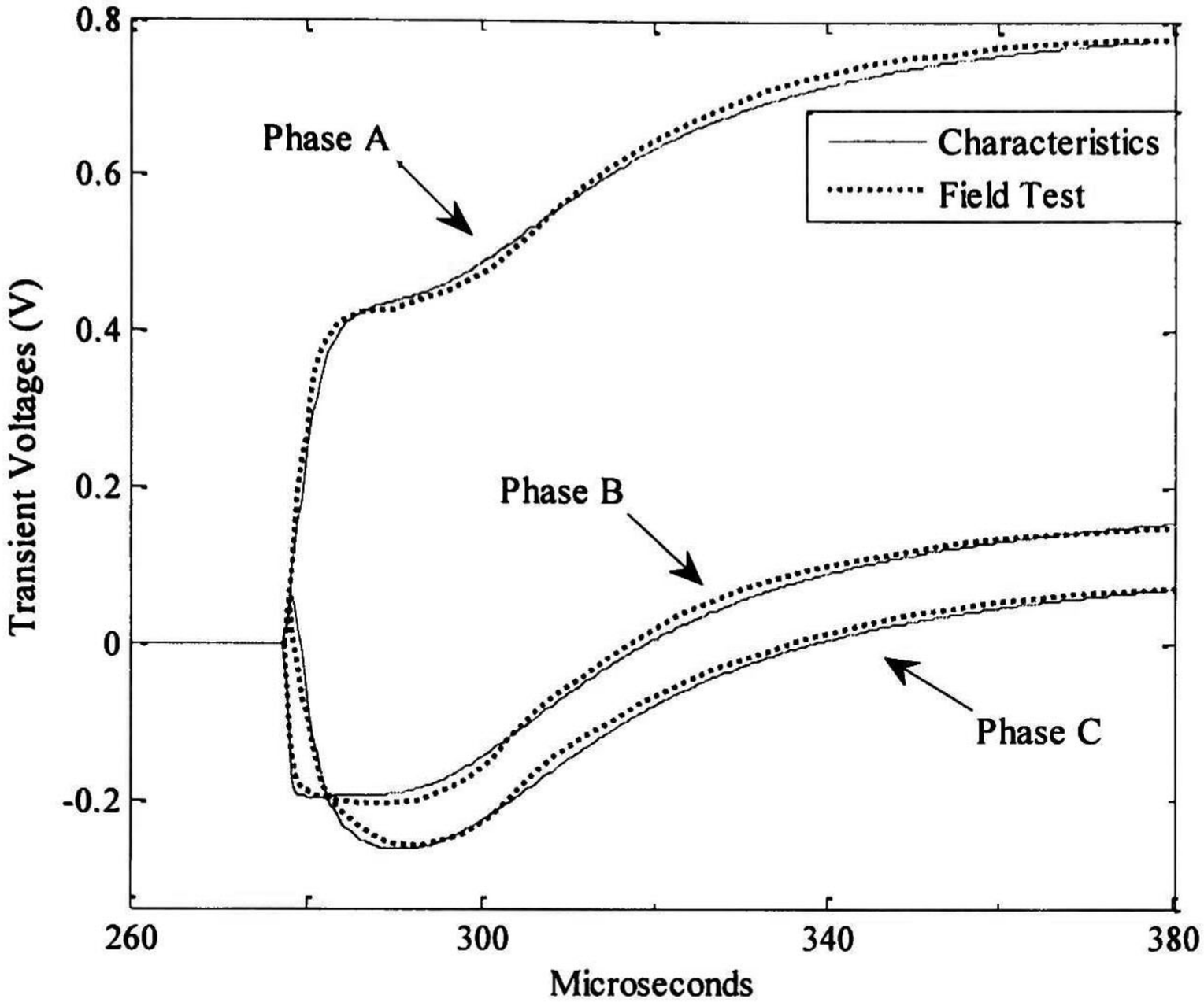

Figure 3.13. Voltages at the receiving nodes.

c). Inclusion of a non-linear element.

The objective of this example is to demonstrate the ability of the proposed line model to manage the inclusion of a non-linear element. Consider the same configuration of Fig. 3.4 but now with a length of 10 km. At the sending node of the *O* phase of the *A* circuit a typical lightning voltage impulse (1.2/50 μs) is injected. The receiving end is considered as open circuit. Circuits *B* and *C* are not energized and sending nodes are grounded while receiving nodes are considered as open circuits.

A simple surge arrester is connected at the receiving node of the *O* phase of the *A* circuit. This arrester is basically a non-linear resistance modeled by means of a piece-wise linear approximation (4 slopes) of its *v-i* characteristic, as shown in Table 1. Transient voltages at the node where the arrester is connected are shown in Fig. 3.14. For comparison purposes results from the ATP/EMTP (J. Marti Model) are also provided. The arrester model in ATP/EMTP used the same piece-wise linear approximation of Table 1. As shown in Fig. 3.14 results from the model proposed here are very close to those from ATP/EMTP.

Table 1 *Surge arrester's data*

Voltage range (p.u.)	Resistance (Ω)
0.0 – 1.0	10,000
1.0 – 1.2	325
1.2 – 1.3	75
1.3 and above	35

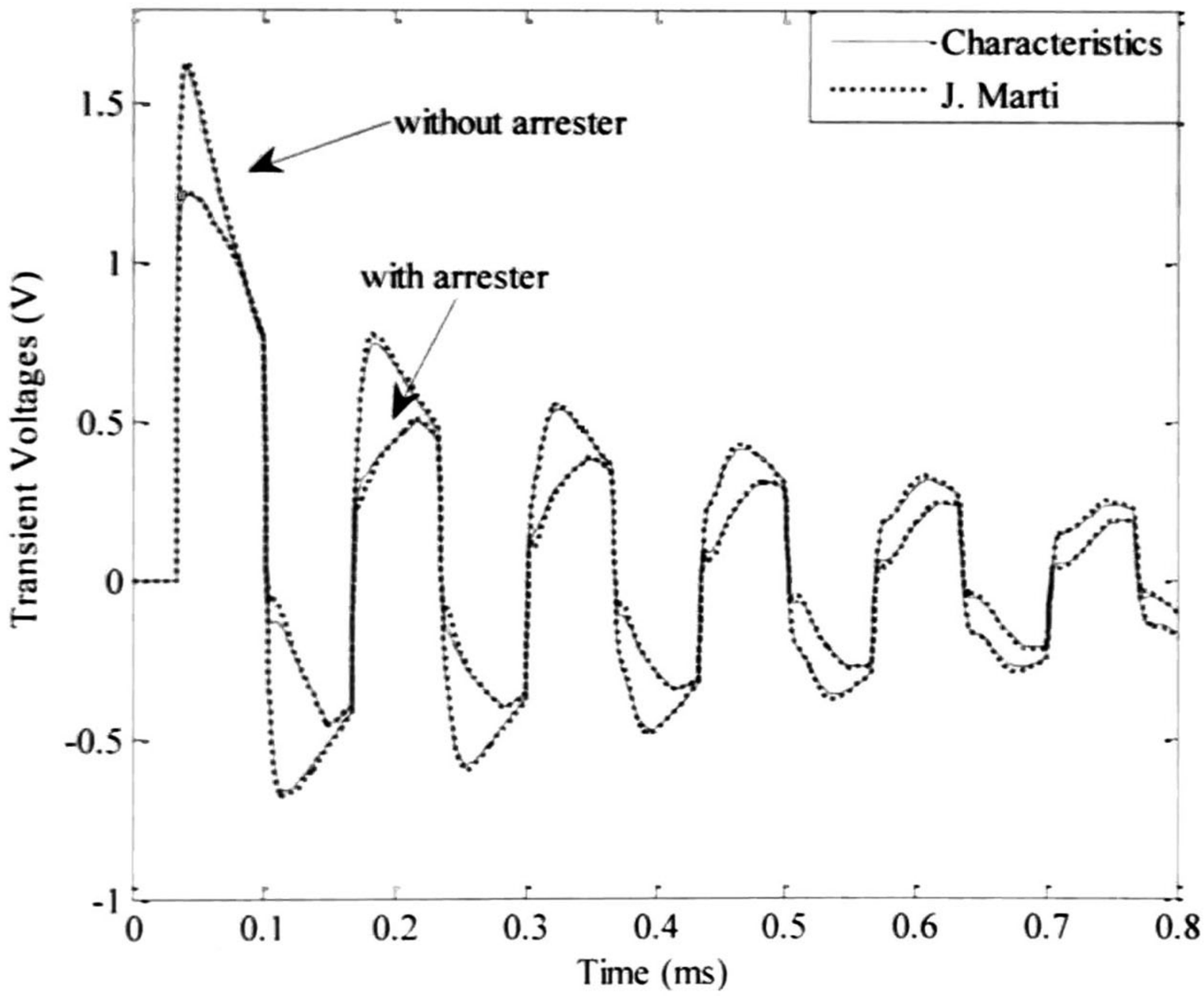

Figure 3.14. Transient voltages at the receiving node of the O phase of the A circuit. with and without arrester

3.4 Conclusions

In this Chapter a second model for overhead MTLs with frequency dependent electrical parameters for time domain transient analysis has been presented. The model requires the approximation of one parameter (the transient resistance) to include the frequency dependence of the electrical parameters.

In contrast with the method presented in section 2, the respective interpolations of the modal voltage, modal current and the convolution terms are made in the time axes and each mode is evaluated in a separate way.

The model does not require the extraction of time delays as is the case of the ULM. Another important contribution is that the model does not need the discretization mesh of the line and it does not present problems with asymmetric line configurations.

Results obtained with the developed model have been compared with those from the J. Martí model, the ULM (Universal Line Model) and a FDM program (Numerical Laplace Transform) and field measurements.

4 Modeling of Underground Transmission Systems

4.1 Introduction

Cable systems are used to transmit electrical energy when the installation of overhead lines is unpractical, unsafe or when they present an unacceptable environmental impact. The main application of underground systems has been in crowed cities where rights-of-way for overhead lines are expensive or even unavailable. Places where cable installations are necessary include zones where overhead lines would be a risk for people as well as for the reliability of the system, or even when this sort of installations do not "match" the style of the place. These zones are for example airports and surroundings, exits of station of public transportations, crossings through areas with water like rivers and lakes, etc.

The models that have been developed for the analysis of overhead lines can be used for cables modeling. However, these models have presented some problems to suitably reproduce voltages and currents in transient state. These problems are due to the fact that the modal velocities of an underground cable system are more dissimilar from each other than those of an overhead transmission line.

From the above, in this Chapter a model for underground transmission systems is developed. The model that was presented in Chapter 3 for overhead transmission systems is extended for modeling buried cables. This model uses second order interpolations on the time axis and the modal voltages, modal currents and convolution terms are interpolated in a separate way. This decreases some problems found in the

model of Chapter 2 produced for the large differences among the modal velocities of the underground systems; however, it does not eliminate the problem completely.

The results obtained with the methodology presented here are compared with those from a frequency domain method.

4.2 Electrical Parameters of Single Phase Cables

For the single phase cable shown in Fig. (4.1) the telegrapher's equations in the frequency domain can be expressed as follows:

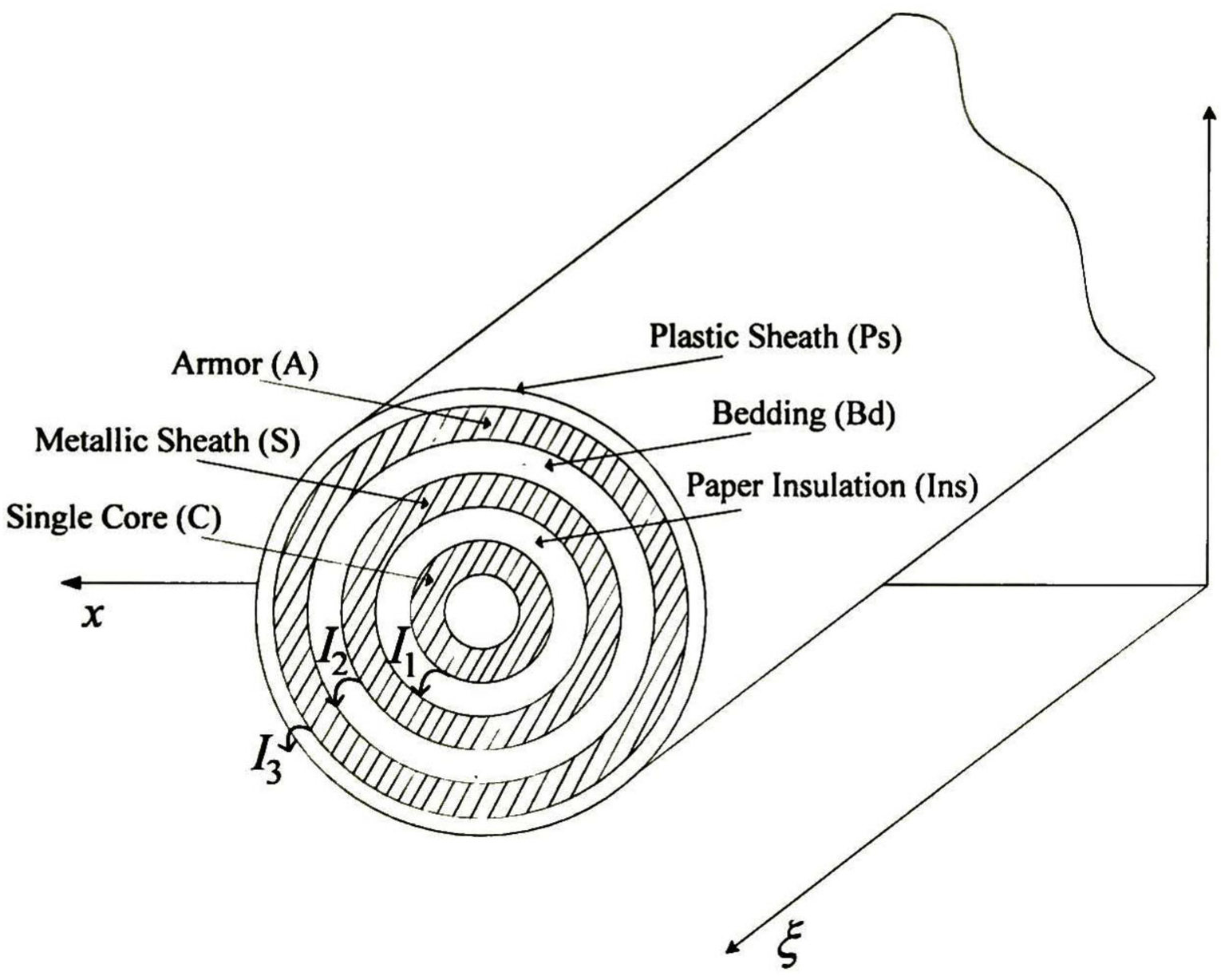

Figure 4.1. Single phase cable with three loops (Core, Metallic sheath and Armor).

$$-\frac{d\mathbf{V}(\xi,t)}{d\xi} = \mathbf{Z}\,\mathbf{I}(\xi,t) \tag{4.1}$$

$$-\frac{d\mathbf{I}(\xi,t)}{d\xi} = \mathbf{Y}\,\mathbf{V}(\xi,t) \tag{4.2}$$

Where **Z** and **Y** are the series impedance and shunt admittance matrices per unit length, respectively.

4.2.1 Impedances Calculation

According to Fig. (4.1) the series impedance is expressed as follows [3]:

$$\mathbf{Z} = \begin{bmatrix} Z_{11} & Z_{12} & 0 \\ Z_{21} & Z_{22} & Z_{23} \\ 0 & Z_{32} & Z_{33} \end{bmatrix} \tag{4.3}$$

where

$$Z_{11} = Z_{Core\_out} + Z_{Core/Sheath\_Insulation} + Z_{Sheath\_in} \tag{4.4a}$$

$$Z_{22} = Z_{Sheath\_out} + Z_{Sheath/Armor\_Insulation} + Z_{Armor\_in} \tag{4.4b}$$

$$Z_{33} = Z_{Armor\_out} + Z_{Armor/Earth\_insulation} + Z_{Earth\_in} \tag{4.4c}$$

being Z_{Core_out}, Z_{Sheath_out} and Z_{Armor_out} the internal impedance per unit length of tubular core, sheath and armor conductor respectively.

The internal impedance per unit length of the tubular core is defined as:

$$Z_{Core\_out} = \sqrt{R_{cd} + Z_{Hz}} \tag{4.5a}$$

where R_{cd} and Z_{Hz} are the direct current resistance and the high frequency impedance given by:

$$R_{cd} = \frac{\rho_{core}}{\pi r_{r-core}^2} \text{ and } Z_{Hz} = \frac{\rho_{core}}{2\pi r_{r-core} p} \tag{4.5b}$$

being ρ_{core} and r_{r-core} the resistivity and the radius of the core and p is the complex penetration depth defined as:

$$p = \sqrt{\frac{\rho_{core}}{jw\mu_u}} \tag{4.5c}$$

where μ_u is the permeability of the core.

On the other hand, Z_{Sheath_out} and Z_{Armor_out} are calculated as follows:

$$Z_{Tube\_out} = \left(\frac{\rho_{Tube}}{2\pi r_{outside}\, p}\right)\left(\frac{K_1(r_{inside}/p)I_0(r_{outside}/p) + K_0(r_{outside}/p)I_1(r_{inside}/p)}{D}\right) \quad (4.6a)$$

where

$$D = K_1(r_{inside}/p)I_1(r_{outside}/p) - K_1(r_{outside}/p)I_1(r_{inside}/p) \quad (4.6b)$$

In (4.6b) I_n and K_n are the Bessel functions of first and second kind, respectively; $r_{outside}$ and r_{inside} are the external an internal radius of the tubular conductor. The expressions for Z_{Sheath_in} and Z_{Armor_in} are given by:

$$Z_{Tube\_in} = \left(\frac{\rho_{Tube}}{2\pi r_{inside}\, p}\right)\left(\frac{K_1(r_{outside}/p)I_0(r_{inside}/p) + K_0(r_{inside}/p)I_1(r_{outside}/p)}{D}\right) \quad (4.6c)$$

For a single phase cable Z_{Earth_in} is not needed, hence the way of calculating this will be explained in the next section. On the other hand, $Z_{Core/Sheath\_Insulation}$, $Z_{Sheath/Armor\_Insulation}$ and $Z_{Armor/Erath\_Insulation}$ are the geometrical impedances of each element of the cable. For example $Z_{Core/Sheath\_Insulation}$ is obtained as follows:

$$Z_{Core/Sheath\_Insulation} = jw\frac{\mu_0\mu_r}{2\pi}\ln\frac{r_{outside-Ins}}{r_{inside-Ins}} \quad (4.7)$$

Where $r_{outside-Ins}$ and $r_{inside-Ins}$ are the outside and inside radius of the insulation, μ_0 and μ_r are the permeability of free space and insulation respectively. For the mutual impedances it is considered that $Z_{12} = Z_{21}$, $Z_{23} = Z_{32}$ and $Z_{13} = Z_{31} = 0$ because there is not common branch between the loops 1 and 3. The mutual impedance is defined as follows:

$$Z_{Tube-mutual} = -\frac{\rho_{Sheat}}{2\pi r_{outside-Sheath}\, r_{inside-Sheath}\, D} \quad (4.8)$$

where $r_{outside-Sheath}$ and $r_{inside-Sheath}$ are the outside and inside radius of the sheath and ρ_{sheath} is the resistivity of the sheath. According to Fig. (4.1) the next conditions are considered:

$$\begin{aligned} V_{core} - V_{sheath} &= V_1 \\ V_{sheath} - V_{armor} &= V_2 \\ V_{armor} &= V_3 \end{aligned} \tag{4.9a}$$

and

$$\begin{aligned} I_{core} &= I_1 \\ I_{core} + I_{sheath} &= I_2 \\ I_{core} + I_{sheath} + I_{armor} &= I_3 \end{aligned} \tag{4.9b}$$

Substituting (4.9) in (4.1) gives:

$$-\frac{d(V_{core} - V_{sheath})}{d\xi} = (Z_{11} + Z_{12})I_{core} + Z_{12}I_{sheath} \tag{4.10a}$$

$$-\frac{d(V_{sheath} - V_{armor})}{d\xi} = (Z_{21} + Z_{22} + Z_{23})I_{core} + (Z_{22} + Z_{23})I_{sheath} + Z_{23}I_{armor} \tag{4.10b}$$

$$-\frac{d(V_{armor})}{d\xi} = (Z_{32} + Z_{33})I_{core} + (Z_{32} + Z_{33})I_{sheath} + Z_{33}I_{armor} \tag{4.10c}$$

Adding (4.10b) and (4.10c) to (4.10a) and adding (4.10c) to (4.10b) equations for V_{core} V_{sheath} are obtained. Finally, the equations systems that are obtained are given by:

$$-\frac{dV_{core}}{d\xi} = Z_{coco}I_{core} + Z_{cosh}I_{sheath} + Z_{coar}I_{armor} \tag{4.11a}$$

$$-\frac{dV_{sheath}}{d\xi} = Z_{shco}I_{core} + Z_{shsh}I_{sheath} + Z_{shar}I_{armor} \tag{4.11b}$$

$$-\frac{dV_{armor}}{d\xi} = Z_{arco}I_{core} + Z_{arsh}I_{sheath} + Z_{arar}I_{armor} \tag{4.11c}$$

where

$$\begin{aligned} Z_{coco} &= Z_{11} + 2Z_{12} + Z_{22} + 2Z_{23} + Z_{33} \\ Z_{shco} &= Z_{\text{cosh}} = Z_{12} + Z_{22} + 2Z_{23} + Z_{33} \\ Z_{coar} &= Z_{arco} = Z_{shar} = Z_{arsh} = Z_{23} + Z_{33} \\ Z_{shsh} &= Z_{22} + 2Z_{23} + Z_{33} \\ Z_{arar} &= Z_{33} \end{aligned} \tag{4.12}$$

Equations (4.11) allow obtaining voltages and currents at each element of the cable. For calculating the geometrical inductance ($\mathbf{L}_g$) and the transient resistance ($\mathbf{Z}_c$) that allows

modeling the cable in time domain it will be necessary to separate the parameters from (4.12). Equations (4.11) are expressed in matrix form as follows:

$$-\begin{bmatrix} \frac{dV_{core}}{d\xi} \\ \frac{dV_{shaeth}}{d\xi} \\ \frac{dV_{armor}}{d\xi} \end{bmatrix} = \mathbf{Z}_{Modified} \begin{bmatrix} I_{core} \\ I_{sheath} \\ I_{armor} \end{bmatrix} \tag{4.13a}$$

where

$$\mathbf{Z}_{Modified} = \begin{bmatrix} Z_{coco} & Z_{\cosh} & Z_{coar} \\ Z_{shco} & Z_{shsh} & Z_{shar} \\ Z_{arco} & Z_{arsh} & Z_{arar} \end{bmatrix} \tag{4.13b}$$

$\mathbf{Z}_{Modified}$ can be expressed as:

$$\mathbf{Z}_{Modified} = \mathbf{Z}_c + s\mathbf{L}_g \tag{4.14a}$$

where:

$$\mathbf{Z}_c = \begin{bmatrix} Z_{C11} & Z_{C12} & Z_{C13} \\ Z_{C21} & Z_{C22} & Z_{C23} \\ Z_{C31} & Z_{C32} & Z_{C33} \end{bmatrix} \tag{4.14b}$$

$$\mathbf{L}_g = \frac{1}{s}\begin{bmatrix} Z_{g11} & Z_{g12} & Z_{g13} \\ Z_{g21} & Z_{g22} & Z_{g23} \\ Z_{g31} & Z_{g32} & Z_{g33} \end{bmatrix} \tag{4.14c}$$

The elements of $\mathbf{Z}_c$ and $\mathbf{Z}_g$ are defined starting from (4.12) as:

$$\begin{aligned} Z_{C11} &= Z_{Core\_out} + Z_{Sheath\_in} + Z_{Sheath\_out} + Z_{Armor\_in} + Z_{Armor\_out} + Z_{Earth\_in} + 2(Z_{12} + Z_{23}) \\ Z_{C12} &= Z_{C21} = Z_{Sheath\_out} + Z_{Armor\_in} + Z_{Armor\_out} + Z_{Earth\_in} + Z_{12} + 2Z_{23} \\ Z_{C13} &= Z_{C31} = Z_{C23} = Z_{C32} = Z_{32} + Z_{Armor\_out} + Z_{Earth\_in} \\ Z_{C22} &= Z_{Sheath\_out} + Z_{Armor\_in} + Z_{Armor\_out} + Z_{Earth\_in} + 2Z_{23} \\ Z_{C33} &= Z_{Armor\_out} + Z_{Earth\_in} \end{aligned} \tag{4.15}$$

$$
\begin{aligned}
Z_{g11} &= Z_{Core/Sheat\_Insulation} + Z_{Sheath/Armor\_Insulation} + Z_{Armor/Earth\_Insulation} \\
Z_{g12} &= Z_{g21} = Z_{Sheath/Armor\_Insulation} + Z_{Armor/Earth\_Insulation} \\
Z_{g13} &= Z_{g31} = Z_{g23} = Z_{g32} = Z_{Armor/Earth\_Insulation} \\
Z_{g22} &= Z_{Sheath/Armor\_Insulation} + Z_{Armor/Earth\_insulation} \\
Z_{g33} &= Z_{Armor/Earth\_insulation}
\end{aligned}
\tag{4.16}
$$

4.2.2 Admittance Calculation

The expression for the shunt conductance (**G**) and shunt capacitance ($\mathbf{C}_g$) for each insulation layer is obtained starting from (4.2) as follows:

$$
-\begin{bmatrix} \frac{dI_1}{d\xi} \\ \frac{dI_2}{d\xi} \\ \frac{dI_3}{d\xi} \end{bmatrix} = \begin{bmatrix} G_1 + jwC_1 & 0 & 0 \\ 0 & G_2 + jwC_2 & 0 \\ 0 & 0 & G_3 + jwC_3 \end{bmatrix} \begin{bmatrix} V_1 \\ V_2 \\ V_3 \end{bmatrix} \tag{4.17}
$$

In the same form in which $\mathbf{Z}_{Modified}$ was obtained, the conditions of equation (4.9) are applied in (4.17) to obtain $\mathbf{Y}_{Modified}$ as follows:

$$
-\begin{bmatrix} \frac{dI_{care}}{d\xi} \\ \frac{dI_{sheath}}{d\xi} \\ \frac{dI_{armor}}{d\xi} \end{bmatrix} = \mathbf{Y}_{Modified} \begin{bmatrix} V_{core} \\ V_{sheath} \\ V_{armor} \end{bmatrix} \tag{4.18}
$$

where

$$
\mathbf{Y}_{Modified} = \mathbf{G} + s\mathbf{C}_g \tag{4.19}
$$

and

$$\mathbf{G} = \begin{bmatrix} G_1 & -G_1 & 0 \\ -G_1 & G_1 + G_2 & -G_2 \\ 0 & -G_2 & G_2 + G_3 \end{bmatrix} \tag{4.20a}$$

$$\mathbf{C}_g = \begin{bmatrix} C_1 & -C_1 & 0 \\ -C_1 & C_1 + C_2 & -C_2 \\ 0 & -C_2 & C_2 + C_3 \end{bmatrix} \tag{4.20b}$$

The shunt capacitance and shunt conductance for a tubular insulation are defined as:

$$C = \frac{2\pi\varepsilon_0\varepsilon_{rn}}{\log \frac{r_{outside}}{r_{inside}}} \quad \text{and} \quad G_n = \frac{C_n\sigma_n}{\varepsilon_0} \tag{4.21a), (4.21b}$$

where ε_0 and ε_{rn} are the permittivity of free space and the *nth*-insulation, σ_n is the conductivity of the *nth*-insulation, $r_{outside}$ and r_{inside} are the outside and inside radius of the tubular insulation.

4.3 Calculation of Electrical Parameters for Three-Phase Cables.

To extend the calculation of the electrical parameters to the case of a three-phase cable system, the magnetic coupling between the cables should be considered. In Fig. (4.2) a system with three cables is shown [3]; they are located at the same depth (h) and the cross section is detailed in Fig. (4.1).

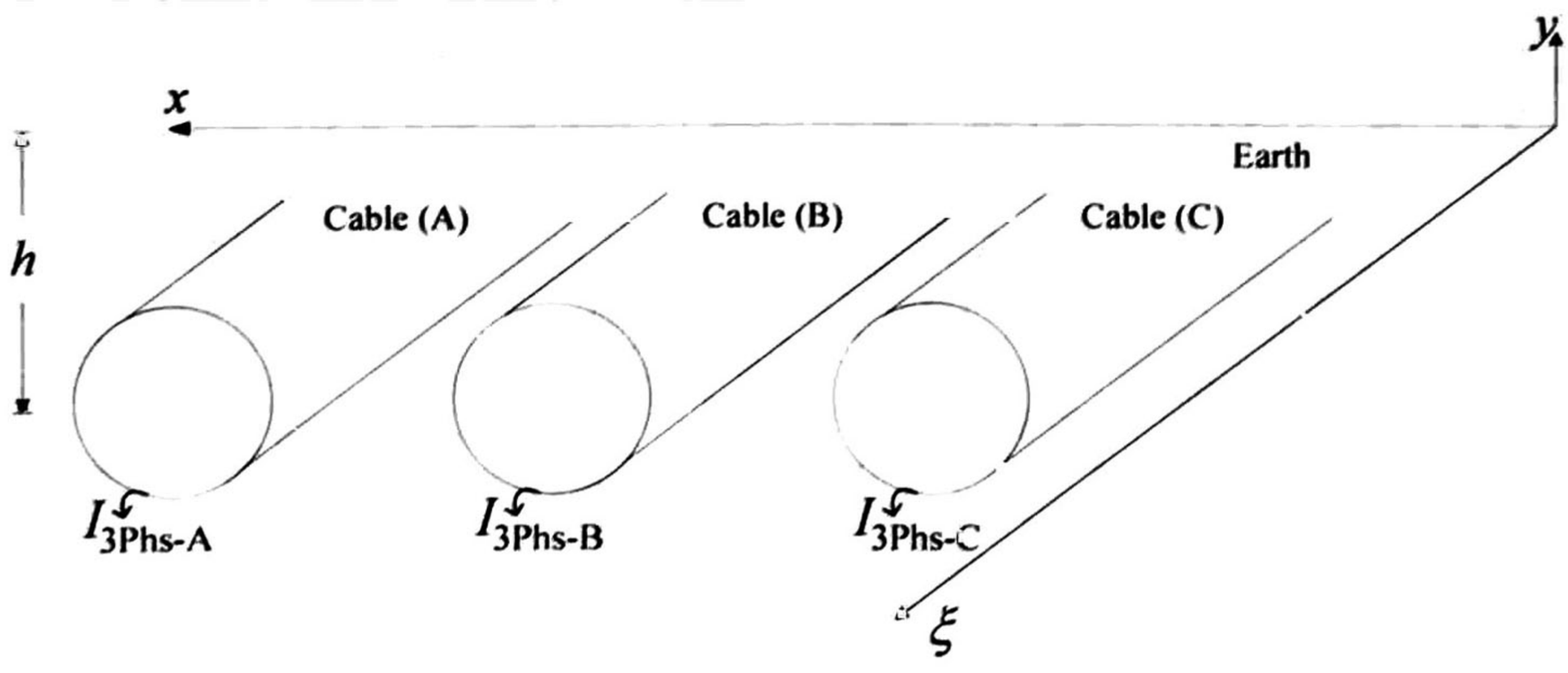

Figure 4.2. Three-phase cable system.

4.3.1 Impedance Calculation.

For the three-phase cable system shown in Fig. (4.2) equation (4.1) becomes of the following form:

$$-\frac{d}{d\xi}\begin{bmatrix}\mathbf{V}_1\\ \mathbf{V}_2\\ \mathbf{V}_3\\ \mathbf{V}_4\\ \mathbf{V}_5\\ \mathbf{V}_6\\ \mathbf{V}_7\\ \mathbf{V}_8\\ \mathbf{V}_9\end{bmatrix}=\begin{bmatrix}\begin{bmatrix}Z_{11}^A & Z_{12}^A & Z_{13}^A\\ Z_{21}^A & Z_{22}^A & Z_{23}^A\\ Z_{31}^A & Z_{32}^A & Z_{33}^A\end{bmatrix} & \begin{bmatrix}0&0&0\\0&0&0\\0&0&Z_{AB}\end{bmatrix} & \begin{bmatrix}0&0&0\\0&0&0\\0&0&Z_{AC}\end{bmatrix}\\ \begin{bmatrix}0&0&0\\0&0&0\\0&0&Z_{BA}\end{bmatrix} & \begin{bmatrix}Z_{11}^B & Z_{12}^B & Z_{13}^B\\ Z_{21}^B & Z_{22}^B & Z_{23}^B\\ Z_{31}^B & Z_{32}^B & Z_{33}^B\end{bmatrix} & \begin{bmatrix}0&0&0\\0&0&0\\0&0&Z_{BC}\end{bmatrix}\\ \begin{bmatrix}0&0&0\\0&0&0\\0&0&Z_{CA}\end{bmatrix} & \begin{bmatrix}0&0&0\\0&0&0\\0&0&Z_{CB}\end{bmatrix} & \begin{bmatrix}Z_{11}^C & Z_{12}^C & Z_{13}^C\\ Z_{21}^C & Z_{22}^C & Z_{23}^C\\ Z_{31}^C & Z_{32}^C & Z_{33}^C\end{bmatrix}\end{bmatrix}\begin{bmatrix}\mathbf{I}_1\\ \mathbf{I}_2\\ \mathbf{I}_3\\ \mathbf{I}_4\\ \mathbf{I}_5\\ \mathbf{I}_6\\ \mathbf{I}_7\\ \mathbf{I}_8\\ \mathbf{I}_9\end{bmatrix} \tag{4.22}$$

being $Z_{BC}=Z_{CB}$, $Z_{AB}=Z_{BA}$ and $Z_{CA}=Z_{AC}$. The couplings are given by the parameters Z_{AB}, Z_{AC}, Z_{BC}. For obtaining a system in terms of each element of the cable (core, sheath and armor) the conditions of equations (4.9) are applied to (4.22). According to the above the next equations system is obtained:

$$-\frac{d}{d\xi}\begin{bmatrix}\mathbf{V}_A\\ \mathbf{V}_B\\ \mathbf{V}_C\end{bmatrix}=\begin{bmatrix}\mathbf{Z}_A & \mathbf{Z}_{AB} & \mathbf{Z}_{AC}\\ \mathbf{Z}_{AB} & \mathbf{Z}_B & \mathbf{Z}_{BC}\\ \mathbf{Z}_{AC} & \mathbf{Z}_{BC} & \mathbf{Z}_C\end{bmatrix}\begin{bmatrix}\mathbf{I}_A\\ \mathbf{I}_B\\ \mathbf{I}_C\end{bmatrix} \tag{4.23}$$

where

$$\mathbf{Z}_A=\begin{bmatrix}Z_{coco}^A & Z_{cosh}^A & Z_{coar}^A\\ Z_{shco}^A & Z_{shsh}^A & Z_{shar}^A\\ Z_{arco}^A & Z_{arsh}^A & Z_{arar}^A\end{bmatrix},\mathbf{Z}_B=\begin{bmatrix}Z_{coco}^B & Z_{cosh}^B & Z_{coar}^B\\ Z_{shco}^B & Z_{shsh}^B & Z_{shar}^B\\ Z_{arco}^B & Z_{arsh}^B & Z_{arar}^B\end{bmatrix},\mathbf{Z}_C=\begin{bmatrix}Z_{coco}^C & Z_{cosh}^C & Z_{coar}^C\\ Z_{shco}^C & Z_{shsh}^C & Z_{shar}^C\\ Z_{arco}^C & Z_{arsh}^C & Z_{arar}^C\end{bmatrix} \tag{4.24a}$$

and

$$\mathbf{Z}_{AB}=\begin{bmatrix}Z_{AB} & Z_{AB} & Z_{AB}\\ Z_{AB} & Z_{AB} & Z_{AB}\\ Z_{AB} & Z_{AB} & Z_{AB}\end{bmatrix}\mathbf{Z}_{AC}=\begin{bmatrix}Z_{AC} & Z_{AC} & Z_{AC}\\ Z_{AC} & Z_{AC} & Z_{AC}\\ Z_{AC} & Z_{AC} & Z_{AC}\end{bmatrix}\mathbf{Z}_{BC}=\begin{bmatrix}Z_{BC} & Z_{BC} & Z_{BC}\\ Z_{BC} & Z_{BC} & Z_{BC}\\ Z_{BC} & Z_{BC} & Z_{BC}\end{bmatrix} \tag{4.24b}$$

The vectors of voltages and currents correspond to elements of each cable, for example the vectors of voltages are given by:

$$\mathbf{V}_A = \begin{bmatrix} V_{Core}^A \\ V_{Sheath}^A \\ V_{Armor}^A \end{bmatrix}, \mathbf{V}_B = \begin{bmatrix} V_{Core}^B \\ V_{Sheath}^B \\ V_{Armor}^B \end{bmatrix}, \mathbf{V}_C = \begin{bmatrix} V_{Core}^C \\ V_{Sheath}^C \\ V_{Armor}^C \end{bmatrix} \tag{4.25}$$

The diagonal matrices $\mathbf{Z}_A$, $\mathbf{Z}_B$ and $\mathbf{Z}_C$ are calculated in the same form to that of $\mathbf{Z}_{Modified}$ in section (4.2.1). $\mathbf{Z}_A = \mathbf{Z}_B = \mathbf{Z}_C$ if the cables have the same geometrical configuration and electrical properties.

The electrical parameters Z_{Earth_in}, Z_{AB}, Z_{AC}, Z_{BC} are the self and mutual earth impedances. Pollaczek defined an expression to calculate these impedances [3, 22]; however, there are difficulties to find the analytical solution for these expressions.

There are some approximations for the solution of Pollaczek expressions (the infinite earth model, Wedepohl and Wilcox approximation and the approximation of Ametani) [22]. In this work, the infinite earth model is used to calculate the earth impedances:

$$Z_{Earth\_in} = \frac{\rho_{Earth} K_0(r_{outside} / p)}{2\pi r_{outside}\, p K_1(r_{outside} / p)} \tag{4.26}$$

$$Z_{Earth-Mutual} = \frac{\rho_{Earth} K_0(d / p)}{2\pi r_1 r_2\, p K_1(r_1 / p) K_1(r_2 / p)} \tag{4.27}$$

where $Z_{Earth-Mutual}$ is the mutual impedance of earth between two cables, $Z_{Earth-in}$ is the self impedance of earth, ρ_{Earth} is the resistivity of the earth, $r_{outside}$ is the total radius of the cable and d is the distance between cables.

For obtaining the geometrical inductance and the transient resistance of the three-phase system, equation (4.22) is expressed as follows:

$$-\frac{d}{d\xi}\mathbf{V}_{ABC} = \mathbf{Z}_{Modified}^{ABC}\mathbf{I}_{ABC} \tag{4.28}$$

where

$$\mathbf{V}_{ABC} = \begin{bmatrix} \mathbf{V}_A \\ \mathbf{V}_B \\ \mathbf{V}_C \end{bmatrix}, \mathbf{I}_{ABC} = \begin{bmatrix} \mathbf{I}_A \\ \mathbf{I}_B \\ \mathbf{I}_C \end{bmatrix} \tag{4.29}$$

$$\mathbf{Z}_{Modified}^{ABC} = \mathbf{Z}_c^{ABC} + s\,\mathbf{L}_g^{ABC} = \begin{bmatrix} \mathbf{Z}_A & \mathbf{Z}_{AB} & \mathbf{Z}_{AC} \\ \mathbf{Z}_{AB} & \mathbf{Z}_B & \mathbf{Z}_{BC} \\ \mathbf{Z}_{AC} & \mathbf{Z}_{BC} & \mathbf{Z}_C \end{bmatrix} \tag{4.30}$$

where $\mathbf{Z}_c^{ABC}$ and $\mathbf{L}_g^{ABC}$ are the transient resistance matrix and geometrical inductance matrix of the system, respectively, which are defined as follows:

$$\mathbf{Z}_c^{ABC} = \begin{bmatrix} \mathbf{Z}_c^A & \mathbf{Z}_{AB} & \mathbf{Z}_{AC} \\ \mathbf{Z}_{BA} & \mathbf{Z}_c^B & \mathbf{Z}_{BC} \\ \mathbf{Z}_{CA} & \mathbf{Z}_{CB} & \mathbf{Z}_c^C \end{bmatrix} \tag{4.31a}$$

$$\mathbf{L}_g^{ABC} = \begin{bmatrix} \mathbf{L}_g^A & 0 & 0 \\ 0 & \mathbf{L}_g^B & 0 \\ 0 & 0 & \mathbf{L}_g^C \end{bmatrix} \tag{4.31b}$$

The diagonal submatrices are calculated as it was shown in section (4.2.1).

4.3.2 Admittance Calculation.

Similarly to the description presented in the section (4.3.1), equation (4.2) is expressed as follows:

$$-\begin{bmatrix} \frac{d\mathbf{I}_A}{d\xi} \\ \frac{d\mathbf{I}_B}{d\xi} \\ \frac{d\mathbf{I}_C}{d\xi} \end{bmatrix} = \mathbf{Y}_{Modified}^{ABC} \begin{bmatrix} \mathbf{V}_A \\ \mathbf{V}_B \\ \mathbf{V}_C \end{bmatrix} \tag{4.32}$$

where

$$\mathbf{V}_A = \begin{bmatrix} V_{Core}^A \\ V_{Sheath}^A \\ V_{Armor}^A \end{bmatrix}, \mathbf{V}_B = \begin{bmatrix} V_{Core}^B \\ V_{Sheath}^B \\ V_{Armor}^B \end{bmatrix}, \mathbf{V}_C = \begin{bmatrix} V_{Core}^C \\ V_{Sheath}^C \\ V_{Armor}^C \end{bmatrix} \tag{4.33}$$

$$\mathbf{I}_A = \begin{bmatrix} I_{Core}^A \\ I_{Sheath}^A \\ I_{Armor}^A \end{bmatrix}, \mathbf{I}_B = \begin{bmatrix} I_{Core}^B \\ I_{Sheath}^B \\ I_{Armor}^B \end{bmatrix}, \mathbf{I}_C = \begin{bmatrix} I_{Core}^C \\ I_{Sheath}^C \\ I_{Armor}^C \end{bmatrix} \tag{4.34}$$

$$\mathbf{Y}_{Modified}^{ABC} = \mathbf{G}^{ABC} + s\mathbf{C}_g^{ABC} \tag{4.35}$$

and

$$\mathbf{G}^{ABC} = \begin{bmatrix} \mathbf{G}_A & 0 & 0 \\ 0 & \mathbf{G}_B & 0 \\ 0 & 0 & \mathbf{G}_C \end{bmatrix} \tag{4.36}$$

$$\mathbf{C}_g^{ABC} = \begin{bmatrix} \mathbf{C}_g^A & & \\ & \mathbf{C}_g^B & \\ & & \mathbf{C}_g^C \end{bmatrix} \tag{4.37}$$

Matrices $\mathbf{C}_g^{ABC}$ and $\mathbf{G}^{ABC}$ are calculated according to section (4.2.2).

4.4 Application Example

A system of 3-phase cables 2 km long is considered for the following example. Each cable has the geometrical configuration shown in Fig. (4.3). The resistivity of the core, the sheath and the earth is $1.71\text{x}10^{-8}$, $1.38\text{x}10^{-7}$ and 20 Ω-m respectively. The permittivity of the insulation is 3.3 F/m. The relative magnetic permeability of the core, the sheath, the insulation and the earth is 1.

At the sending nodes, the cores of phases A, B and C are energized with a 3-phase sinusoidal source while the sheaths of the 3 phases are left as open circuits. At the end of the cables cores and sheaths are also left as open circuits.

In Fig. (4.4) the transient voltages at the end of cores of phases A, B and C are shown. The transient voltages at the end of the sheaths of each phase are shown in Fig. (4.5). The results are compared with those obtained from a frequency domain method, as shown in Figs. (4.4) and (4.5).

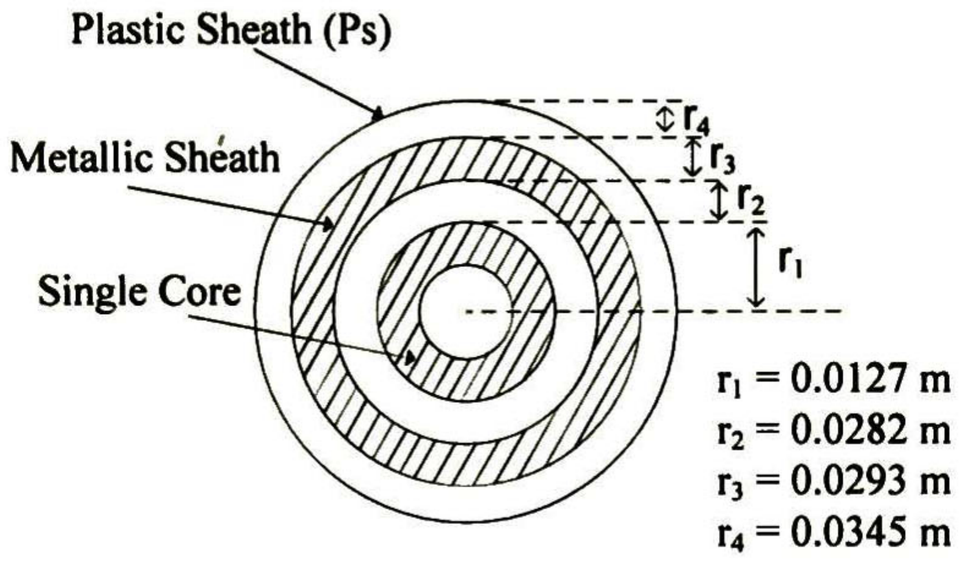

Figure 4.3. Geometrical configuration for a single phase cable without armor.

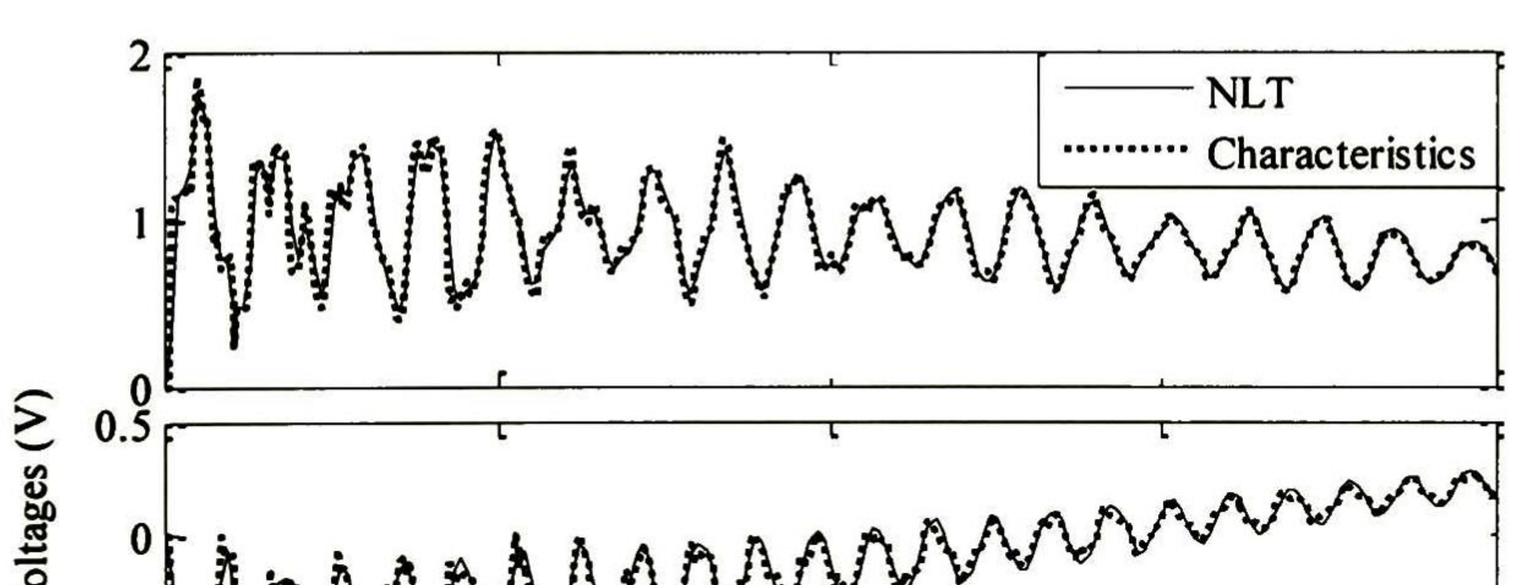

Figure 4.4. Transient voltages at the end of the cores of phases A, B and C.

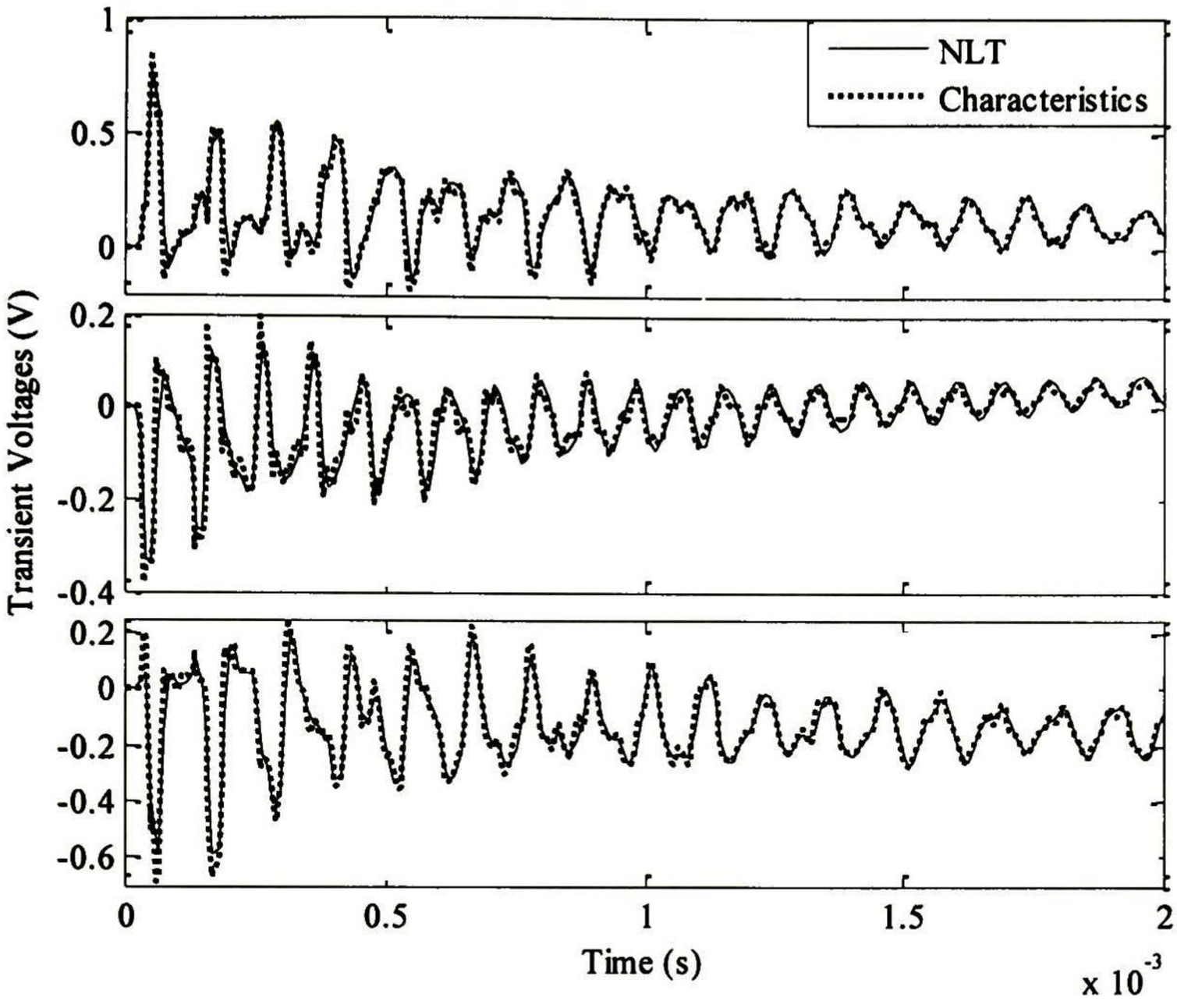

Figure 4.5. Transient voltages at the end of the sheaths of the phases A, B and C.

4.5 Conclusion

In this Chapter the model presented in Chapter 3 was validated for 3-phase cables modeling in transient state. This model decreases the problem with the differences of the modal velocities.

The technique well known as Vector fitting is used for the synthesis of the transient resistance with which the frequency dependence of electrical parameters is included. The R'(s) was fitted with 7 poles for the example.

Results obtained have been compared with those from FDM program (Numerical Laplace Transform).

5 Conclusions and Future Work

5.1 Conclusion

In this thesis, two models for time domain analysis of electromagnetic transients in transmission lines were developed. Both models include the frequency dependence of the electrical parameters by means of the synthesis of the transient resistance. The models are based on the method of characteristics which has been used for the solution of the telegrapher's equations. The techniques convert partial differential equations to ordinary differential equations and then solve the problem using a finite differences scheme. The method of characteristics has been used before in modeling Non-Uniform, Non-Linear and external field excited Transmission Lines. In these cases using this method requires a time-distance discretization mesh.

In the models presented in this work the method of characteristics is reformulated for Uniform Multiconductor Transmission Lines. In these models no discretization mesh is required and Norton equivalent circuits for the line ends are developed. These models possess some important advantages. One of them is that it requires only the synthesis of the transient resistance, while traveling wave models require synthesizing the characteristic admittance and the propagation exponential matrices. The frequency behavior of the propagation exponential matrix presents fast variations and heuristic time delays extraction is required to get accurate fitted rational expansions. In contrast, due to the smoothness of the transient resistance its rational fitting is straightforward, requires only real poles and there is no need of extracting time delays. Another advantage is that only two matrix vector convolutions are required in the Norton model.

The first model is presented in Chapter 2. In order to introduce the basis of the new method a model for multiconductor transmission lines without frequency dependence electrical parameters is first presented. In Section 2.3 the frequency dependence is included by means of a rational approximation of the transient resistance. In this model a linear interpolation method is used to obtain the values of the modal voltages and currents in the propagation-axis, as shown in Appendix A.

The second method is developed in Chapter 3. In contrast with the method presented in Chapter 2, an interpolation method of second order is used to calculate modal voltages, modal currents and convolution terms. Besides, interpolations are made in the time-axis and modal values are interpolated in separated way. This method is used for overhead and underground transmission systems analysis.

Several application examples have been presented to validate the techniques developed in this thesis.

- A 3-phase uniform line in horizontal configuration energized with a sequential closing.

- System with two parallel 3-phase lines in horizontal configuration. In this example the end of the line is considered as open circuit and short circuit.

- System with three parallel 3-phase lines in horizontal and vertical configuration energized with a sequential closing. The ends of all circuits are considers firstly as open circuit and secondly as short circuit.

- Comparison with field measurements of a 3-phase uniform line in horizontal configuration.

- Simulations of transmission lines with non linear loads.

- Simulation of a 3-phase cable system.

The methods presented in this thesis have shown good accuracy in the simulation of a variety of cases. Results obtained with the developed models have been compared with those from the J. Martí model, the ULM, FDM program and field measurements.

5.2 Recommendations for Future Work

The next list shows recommendations for future research work as continuation of the models and techniques reported in this thesis.

- Analysis and modeling of multitransposed lines and cables.

- Development of a program for the analysis of electromagnetic transients in electric networks.

- Implementing the model in a real time transients simulator.

- Application of the developed techniques to the analysis and modeling of other elements of the electric power system, such as transformers and electric machines.

- Application of the proposed methods to the simulation of electronic circuits.

6 References

[1] **A. Greenwood**, "Electrical Transients in Power Systems". Second edition, John Wiley & Sons, Inc. 1991.

[2] **L. A. Siegert**, "Alta Tensión y Sistemas de Transmisión" LIMUSA. México D. F. 1989.

[3] **H. W. Dommel**, Electromagnetic Transient Program (EMTP – Theory Book), Portland, USA, July 1995.

[4] **A. Budner**, "Introduction of Frequency-Dependent Line Parameters into an Electromagnetic Transients Program", IEEE Trans. Power Apparatus and Systems, vol. PAS-89, pp. 88-97, January 1970.

[5] **J. K. Snelson**, "Propagation of Travelling Waves on Transmission Lines-Frequency Dependent Parameters", IEEE Trans. Power Apparatus and Systems, vol. PAS-91, pp. 85-91, January 1972.

[6] **A. Semlyen** and **A. Dabuleanu**, "Fast and Accurate Switching Transient Calculations on Transmission Lines with Ground Return Using Recursive Convolutions", IEEE Trans. Power Apparatus and Systems, vol. PAS-94, March/April 1975.

[7] **J. Martí**, "Accurate Modelling of Frequency-Dependent Transmission Lines in Electromagnetic Transient Simulations", IEEE Trans. Power Apparatus and Systems, vol. PAS-101, no. 1, January 1982.

[8] **L. Martí**, "Simulation of Transients in Underground Cables with Frequency-Dependent Modal Transformation Matrices", IEEE Trans. Power Delivery, vol. 3, no. 3, July 1988.

[9] **B. Gustavsen** and **A. Semlyen**, "Combined Phase Domain and Modal Domain Calculation of Transmission Line Transients Based on Vector Fitting", IEEE Trans. Power Delivery, vol. 13, no. 2, April 1998.

[10] **A. Morched, B. Gustavsen** and **M. Tartibi**, "A Universal Model for Accurate Calculation of Electromagnetic Transients on Overhead Lines and Underground Cables", IEEE Trans. Power Delivery, vol. 14, no. 3, July 1999.

[11] **A. Ambrosio**, "Simulación de Transitorios en Líneas de Transmisión Multiconductoras con Parámetros Dependientes de la Frecuencia Empleando el Método de las Caracteristicas", Tesis de Doctorado, Cinvestav del IPN, Gdl., Jal. 2009.

[12] **J. L. Naredo, P. Moreno, A. C. Soudack** and **José R. Martí**, "Frequency Independent Representation of Transmission Lines for Transient Analysis Through the Method of Characteristic", Athens Power Tech Conferences, Planning Operation and Control. Electric Power System Athens, Greece, September, 1993.

[13] **P. Moreno, P. Gómez, J. L. Naredo** and **J. L. Guardado**, "Frequency Domain Transient Analysis of Electrical Networks Including Non-Linear Conditions", Electrical Power and Energy Systems 27 (2005) 139–146.

[14] **R. Courant, K. Friederichs** and **H. Lewy**, "On Partial Difference Equations of Mathematical Physics", IBM Journal 11, 1967.

[15] **S. J. Day, N. Mullineux** and **J. R. Reed**, "Developments in Obtaining Transient Response Using Fourier Transform, part I: Gibbs Phenomena and Fourier Integrals", Int. J. Elect. Enging. Educ. vol. 3, 1965.

[16] **B. Gustavsen** and **A. Semlyen**, "Rational approximation of frequency domain responses by Vector Fitting", IEEE Trans. Power Delivery, vol. 14, no. 3, pp. 1052-1061, July 1999.

[17] **R. Radulet, A. Timotin, A. Tugulea** and **A. Nica**, "The Transient Response of the Electric lines Based on the Equations with Transient Line-Parameters", *Rev. Roum. Sci. Techn.*, vol. 23, no. 1, pp. 3-19, 1978.

[18] **L. M. Wedepohl, S. E. T. Mohamed**, "Transient Analysis of Multiconductor Transmission Lines with Special Reference to Nonlinear Problems", Proc. IEE, vol. 117, no. 5, pp. 979-988. Mayo 1970.

[19] **P. Moreno, A. Ramírez**, "Implementation of the Numerical Laplace Transform: A Review", IEEE Trans. on Power Delivery, vol. 23, no. 4, pp. 2599-2609, October 2008,.

[20] **J. Mahseredjian, S. Dennetière, L. Dubé, B. Khodabakhchian and L. Gérin-Lajoie**, "On a new approach for the simulation of transients in power systems", Electric Power Systems Research, Vol. 77, Issue 11, September 2007, pp. 1514-1520.

[21] **N. Nagaoka** and **A. Amentani**, "A development of a Generalized Frequency – DomainTransient Program –FTP", IEEE Trans. On Power Delivery, vol. 3, no. 4, pp. 1996-2004, October 1988.

[22] **F. A. Uribe**, "Algorithmic Evaluation of Pollaczek Integral and its Applications to Electromagnetic Transient Analysis of Underground Transmission Systems", Tesis de Doctorado, Cinvestav del IPN, Guadalajara, Jal. 2002.

[23] **M. Davila, J. L. Naredo, P Moreno** and **J. A. Gutierrez**, "The Effects of Non-Uniformities and Frequency Dependence of Line Parameters on Electromagnetic Surge Propagations", Electrical Power and Energy Systems 28 (2006), pp. 151-157.

[24] **A. R. Chávez, P. Moreno** and **J. L. Naredo**, "Fast Transients Analysis of Non-uniform Multiconductor Transmission Lines Excited by Incident Field", IEEE Bologna Power Tech Conference, June 23th-26th, Bologna, Italy 2003.

[25] **F. Castellanos** and **J. R. Martí**, "Full Frequency-Depend Phase –Domain Transmission Line Model", IEEE Transactions on Power System, vol. 12, no. 3, pp. 1331-1339, August 1997.

[26] **B. Gustavsen**, "Time Delay Identification For Transmission Line Modeling", IEEE Trans. Power Delivery, pp. 103-106, 2004.

[27] **B. Gustavsen**, "Validation of Frequency-Dependent Transmission Line Models", IEEE Transactions on Power Delivery, vol. 20, no. 2, April 2005.

[28] **T. Noda, N. Nagaoka** and **A. Ametani**, "Phase Domain Modeling of Frequency – Dependent Transmission Lines by Means of an Arma Model", IEEE Transactions on Power System, vol. 11, no. 1, pp. 401-411, January 1996.

[29] **M. Davila, J. L. Naredo, P Moreno** and **A. Ramírez**, "Practical Implementation of a Transmission Line Model for Transient Analysis Considering Corona and Skin Effects", IEEE Bologna Power Tech Conference, June 23th-26th, Bologna, Italy 2003.

[30] **I. Kocar, J. Mahseredjian** and **G. Olivier**, "Weighting Method for Transient Analysis of Underground Cables" IEEE Transactions on Power Delivery, vol. 23, no. 3, pp. 1629-1635, July 2008.

[31] **B. Gustavsen**, and **J. Mahseredjian**, "Simulation of Internal Overvoltages on Transmission Lines by an Extended Method of Characteristics Approach" IEEE Transactions on Power Delivery, vol. 22, no. 3, pp. 1736-1742, July 2007.

[32] **B. Gustavsen**, and **J. Nordstrom**, "Pole Identification for The Universal Line Model Based on Trace Fitting", IEEE Transactions on Power Delivery, vol. 23, no. 1, pp. 472-479, January 2008.

[33] **Christian Dufour** and **Hoang Le-Huy**, "Highly Accurate Modeling of Frequency-Dependent Balanced Transmission Lines", IEEE Transactions on Power Delivery, vol. 15, no. 2, pp. 610-615, APRIL 2000.

[34] **Abner Ramírez, J. L. Naredo** and **Pablo Moreno**, "Full Frequency-Dependent Line Model for Electromagnetic Transient Simulation Including Lumped and Distributed Sources", IEEE Transactions on Power Delivery, vol. 20, no. 1, pp. 472-479, January 2005.

[35] **H. V. Nguyen, H. W. Dommel** and **J. R. Martí**, "Direct Fast Domain Modeling of Frequency –Dependent Overhead Transmission Line", IEEE Transactions on Power Delivery, vol. 12, no. 3, pp. 472-479, July 1997.

[37] **R. Courant, K. Friedrichs** and **H. Lewy**, "On the Partial Difference Equations of Mathematical Physics", IBM Journal March 1967.

[38] **B. Gustavsen**, "Frequency-Dependent Transmission Line Modeling Utilizing Transposed Conditions", IEEE Transactions on Power Delivery, vol. 17, no. 3, pp. 834-839, July 2002.

[39] **P. Moreno, P. Gómez, M. Davila**, and **J. L. Naredo**, "A Uniform Line Model for Non-Uniform Single-Phase Lines with Frequency Dependent Electrical Parameters", 2006 IEEE PES T&D Conference and Exposition Latin America, Caracas, Venezuela, August 15-18, 2006.

[40] **J. A. Gutierrez, J. L. Naredo** and **P. Moreno**, "Transmission Line Tower Modeling for Lightning Performance Analysis", IEEE Power Engineering Review, July 1999.

Appendix A Transmission Line Electrical Parameters

The electrical parameters permit the description of the currents and voltages along the line. These parameters are the per-unit-length longitudinal or series impedance and the transversal or shunt admittance matrices.

A.1 Longitudinal Impedance Matrix

The total impedance matrix of the transmission line consists of three matrices as follows:

$$\mathbf{Z} = \mathbf{Z}_g + \mathbf{Z}_e + \mathbf{Z}_c \tag{A.1}$$

where $\mathbf{Z}_g$, $\mathbf{Z}_e$, and $\mathbf{Z}_c$ are the geometric impedance matrix, the earth return impedance matrix and the conductors internal impedance matrix, respectively. The geometric impedance takes into account the external electromagnetic field, as if the conductors were ideal, the earth return impedance considers the electromagnetic field that penetrates the soil and the conductors internal impedance models the skin effect.

A.2 Geometric Impedance.

The geometric impedance matrix depends on the geometric configuration and it is defined for a *n*-phase transmission line as follows:

$$\mathbf{Z}_g = \frac{s\mu_0}{2\pi}\begin{bmatrix} \ln\dfrac{D_{11}}{Req_1} & \cdots & \ln\dfrac{D_{1n}}{d_{1n}} \\ \vdots & & \vdots \\ \ln\dfrac{D_{n1}}{d_{n1}} & \cdots & \ln\dfrac{D_{nn}}{Req_n} \end{bmatrix} \tag{A.2}$$

where

$$D_{ij} = \sqrt{(x_i - x_j)^2 + (y_i + y_j)^2} \tag{A.3a}$$

$$d_{ij} = \sqrt{(x_i - x_j)^2 + (y_i - y_j)^2} \tag{A.3b}$$

$$R_{eq,i} = \sqrt[nh]{nh\, r_i\, (r_h)^{nh-1}} \tag{A.3c}$$

where s is the Laplace variable, μ_0 is the free space permeability, (x_i, y_i) are the coordinates of the i*th* phase conductor, *nh* is the number of conductors in a bundle, r_i is the radius of the i*th* phase conductor, r_h is the bundle radius and $R_{eq,i}$ is the equivalent radius of the i*th* phase bundle. Finally, D_{ij} and d_{ij} are computed using the method of images, as shown in Fig. A.1:

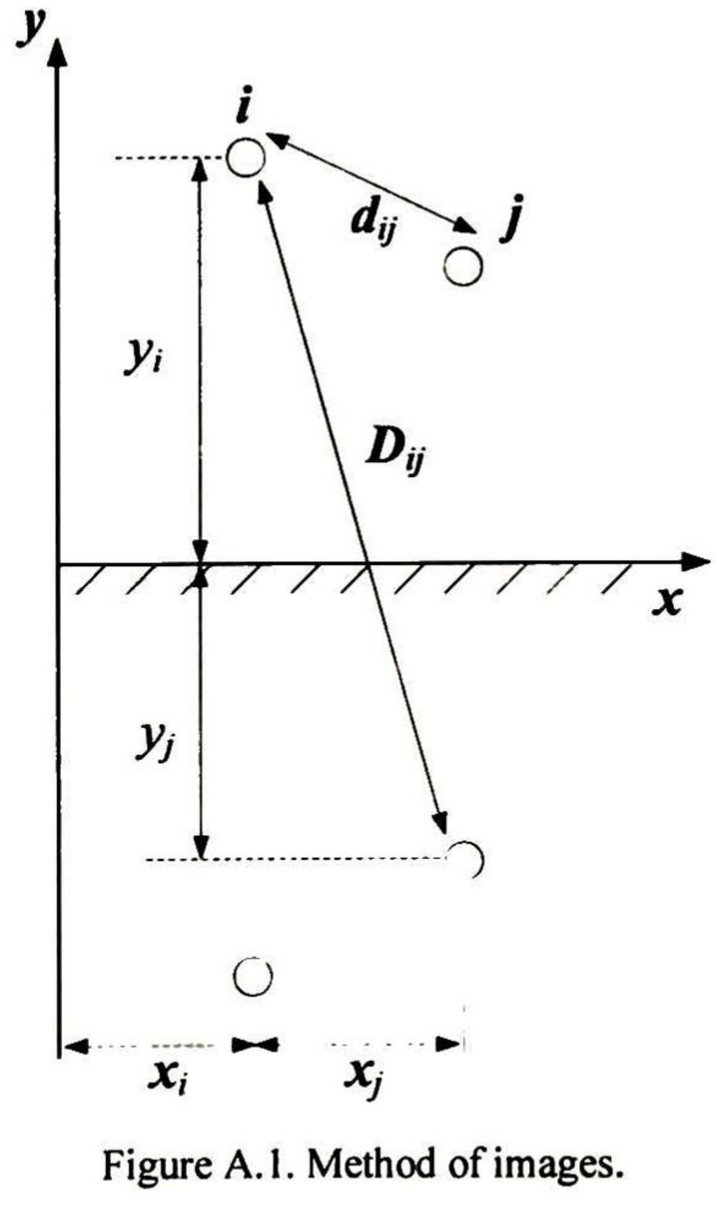

Figure A.1. Method of images.

A.3 Earth Return Impedance.

In order to obtain the earth return impedance the complex image method is used. This method consists of assuming that earth return currents are concentrated in a fictitious area, parallel to the earth plane and defined by the earth surface and a complex penetration depth given by:

$$p = \sqrt{\frac{\rho_e}{s\mu_0\mu_e}} \tag{A.4}$$

where ρ_e is the ground resistivity (Ω/m) and μ_e the ground permeability (H/m). Applying the image method according to Fig A.2, the matrix of earth return impedances is obtained as follows:

$$\mathbf{Z}_e = \frac{s\mu_0}{2\pi}\begin{bmatrix} \ln\dfrac{D'_{11}}{D_{11}} & \cdots & \ln\dfrac{D'_{1n}}{D_{1n}} \\ \vdots & & \vdots \\ \ln\dfrac{D'_{n1}}{D_{n1}} & \cdots & \ln\dfrac{D'_{nn}}{D_{nn}} \end{bmatrix} \tag{A.5}$$

$$D'_{ij} = \sqrt{(y_i + y_j + 2p)^2 + (x_i - x_j)^2} \tag{A.6}$$

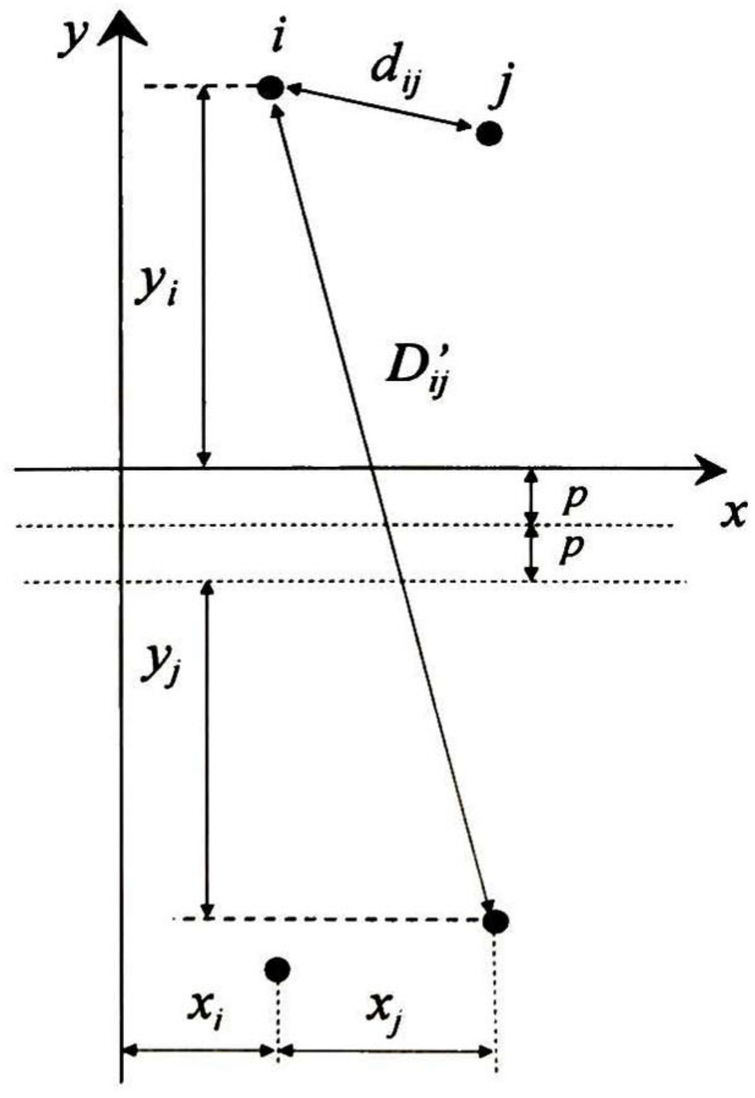

Figure A.2. Method of complex images.

A.4 Conductors Internal Impedance.

The alternating current tends to flow near the conductor surface; the amount of area through which currents flows is a function of the frequency. This phenomenon is well known as "*skin effect*" and produces a complex penetration which is defined by:

$$p_c = \sqrt{\frac{\rho_c}{s\mu_0\mu_c}} \tag{A.7}$$

Using A.7 according to Fig. A.3, the impedance of the i*th* phase conductor can be computed according to the following expression:

$$Z_{c,i} \cong \frac{\sqrt{R_{dc,i} + Z_{hf,i}}}{n} \tag{A.8}$$

where

$$R_{dc,i} = \frac{\rho_{c,i}}{\pi r_i^2} \tag{A.9}$$

$$Z_{hf,i} = \frac{\rho_{c,i}}{2\pi r_i p_c} \tag{A.10}$$

being $R_{dc,i}$ the direct current resistance of the i*th* phase conductor and $Z_{hf,i}$ its high frequency impedance. $\mu_{c,i}$ is the permeability of the i*th* phase conductor (H/m) and $\rho_{c,i}$ its resistivity (Ω/m). Finally, the conductor impedance matrix for the *n* phases of the line is defined as:

$$\mathbf{Z}_c = \begin{bmatrix} Z_{c,1} & 0 & \cdots & 0 \\ 0 & Z_{c,2} & & \vdots \\ \vdots & & \ddots & 0 \\ 0 & \cdots & 0 & Z_{c,n} \end{bmatrix} \tag{A.11}$$

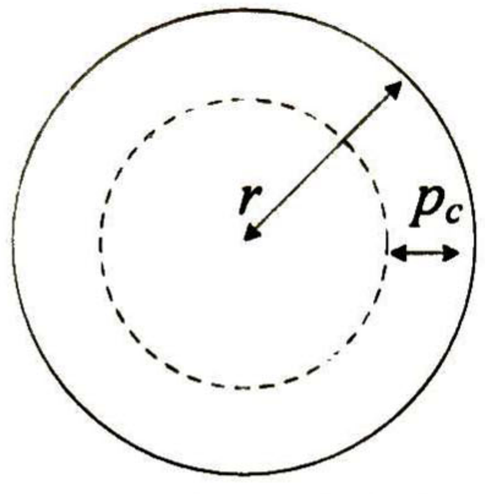

Figure A.3. Complex penetration depth in a conductor.

A.5 Transversal Admittance Matrix.

The shunt or transversal admittance matrix is calculated through the method of the images shown in Fig A.1 as follows:

$$\mathbf{Y} = 2\pi s \varepsilon_0 \begin{bmatrix} \ln \dfrac{D_{11}}{Req_1} & \cdots & \ln \dfrac{D_{1n}}{d_{1n}} \\ \vdots & & \vdots \\ \ln \dfrac{D_{n1}}{d_{n1}} & \cdots & \ln \dfrac{D_{nn}}{Req_n} \end{bmatrix}^{-1} \tag{A.12}$$

where ε_0 the free space permeability.

Appendix B Transient Resistance and Recursive Convolution

B. Synthesis of the Transient Resistance and Recursive Convolution

The frequency dependence of the electrical parameters was included in the model presented in Chapters 2 and 3 by means of the synthesis of the transient resistance matrix, which is defined as a positive and decreasing function as follows:

$$\mathbf{R}' = \left.\frac{\partial \mathbf{V}}{\partial t}\right|_{i=u(t)} \tag{B.1}$$

$\mathbf{R}'$ can be defined as the voltage drop on the line when a step of current is injected. This term appears when the skin effect in the conductor or in the ground is considered in the analysis. The limits of this parameter are:

$$\lim_{t\to\infty}(\mathbf{R}') = \mathbf{R}_{cd} \text{ and } \lim_{t\to 0}(\mathbf{R}') = \infty \tag{B.2a), (B.2b}$$

Consider the well known transmission line longitudinal equation in the frequency domain:

$$\frac{d\mathbf{V}(s)}{d\xi} + s\mathbf{L}_0\mathbf{I}(s) + \mathbf{Z}_C(s)\mathbf{I}(s) + \mathbf{Z}_T(s)\mathbf{I}(s) = \mathbf{0} \tag{B.3}$$

$\mathbf{Z}_C(s)$ and $\mathbf{Z}_T(s)$ are the conductors and the ground return impedances, respectively, $\mathbf{L}_0$ is the geometric inductance and s is the variable of Laplace. From the image in the frequency domain of (2.25) and (B.3) $\mathbf{R}'(s)$ can be defined as:

$$\mathbf{R}'(s) = \frac{\mathbf{Z}_C + \mathbf{Z}_T}{s} \tag{B.4}$$

From (B.4) the transient resistance can be calculated at any frequency or frequency range required.

In order to solve the convolutions in (2.25) and (2.26) the transient resistance needs to be approximated using rational fractions as follows:

$$\mathbf{R}'(s) = \mathbf{H}(s) = \frac{\mathbf{k}_0}{s} + \sum_{i=1}^{n} \mathbf{K}_i (s + p_i)^{-1} + \mathbf{k}_\infty \qquad \text{(B.5)}$$

where $\mathbf{K}_i$ is the residues matrix and p_i are the poles, n is the approximation order and $\mathbf{K}_0 = diag(R_{cd,1}, R_{cd,12} \cdots R_{cd,n})$. Obtaining (B.5) in time domain and substituting the result in the convolution term of (2.25) gives the following:

$$\frac{\partial \mathbf{V}}{\partial \xi} + \mathbf{D}\frac{\partial \mathbf{I}}{\partial t} + \mathbf{R}_{cd}\mathbf{I} + \frac{\hat{c}}{\partial t}\int_0^t \mathbf{h}(t-\tau)\mathbf{I}(\tau)d\tau = \mathbf{0} \qquad \text{(B.6)}$$

where

$$\mathbf{D} = \mathbf{K}_\infty + \mathbf{L}_0 \quad \text{and} \quad \mathbf{h}(t) = \sum_{i=1}^{n} \mathbf{K}_i e^{-p_i t} \qquad \text{(B.7)}$$

Applying the Lebnitz's rule in the convolution term of (B.6) and substituting the result in (B.6) the next expression is obtained:

$$\frac{\partial \mathbf{V}}{\partial \xi} + \mathbf{D}\frac{\partial \mathbf{I}}{\partial t} + \mathbf{R}_X\mathbf{I} + \mathbf{\Psi}(t) = \mathbf{0} \qquad \text{(B.8)}$$

where

$$\mathbf{R}_X = \mathbf{R}_{cd} + \mathbf{h}(0) \qquad \text{(B.9)}$$

$$\mathbf{\Psi}(t) = -\sum_{i=1}^{n} \mathbf{K}_i p_i e^{-p_i t} * \mathbf{I}(\tau) \qquad \text{(B.10)}$$

The equation (B.10) can be expressed in the frequency domain as:

$$\mathbf{\Psi}(s) = -\sum_{i=1}^{n} \frac{\mathbf{K}_i p_i}{s + p_i}\mathbf{I}(s) \qquad \text{(B.11)}$$

The equation (B.11) can be expressed as a first order differential equation in the time domain as follows:

$$\frac{d}{dt}\boldsymbol{\Psi}_i + p_i \boldsymbol{\Psi}_i = \mathbf{K}_i p_i \mathbf{I}(t) \tag{B.12}$$

Applying a finite differences method to (B.12) the next expression for the total convolution is obtained:

$$\boldsymbol{\Psi}(t) = \sum_{i=1}^{n} \boldsymbol{\Psi}_i(t) = \sum_{i=1}^{n} \left[\frac{\boldsymbol{\Psi}_{t-\Delta t}}{1+\Delta t\, p_i} + \frac{\Delta t\, \mathbf{K}_i p_i}{1+\Delta t\, p_i} \mathbf{I}(t) \right] \tag{B.13}$$

Appendix C Interpolation of the Modes

C. Interpolation of Lagrange for the j-*th* Mode

According to Fig. 2 the values V_{mj}^{A}, V_{mj}^{B} and I_{mj}^{A}, I_{mj}^{B} are calculated with the linear interpolation method of Lagrange as follows:

$$V_{mj}^{B} = \alpha_{1j} V_{mj}^{A} + \alpha_{2j} V_{mj}^{B} \tag{C.1}$$

$$V_{mj}^{A} = \alpha_{2j} V_{mj}^{A} + \alpha_{1j} V_{mj}^{B} \tag{C.2}$$

where

$$\alpha_{1j} = \frac{x_j - x_1}{x_0 - x_1} \tag{C.3}$$

$$\alpha_{2j} = \frac{x_j - x_0}{x_1 - x_0} \tag{C.4}$$

$$x_j = \tau Vel_j \tag{C.5}$$

x_0 and x_1 are the distances from points A and B, respectively. x_j is the distance from the respective mode. The modal currents are obtained in the same form. Considering the *n*-modes of the system the interpolated values of the modal voltages and modal currents are expressed in matrix form as follows:

$$\mathbf{V}_m^{B} = \boldsymbol{\alpha}_1 \mathbf{V}_m^{A} + \boldsymbol{\alpha}_2 \mathbf{V}_m^{B}, \quad \mathbf{V}_m^{A} = \boldsymbol{\alpha}_2 \mathbf{V}_m^{A} + \boldsymbol{\alpha}_1 \mathbf{V}_m^{B} \tag{C.6a), C.6b)}$$

$$\mathbf{I}_m^{B} = \boldsymbol{\alpha}_1 \mathbf{I}_m^{A} + \boldsymbol{\alpha}_2 \mathbf{I}_m^{B}, \quad \mathbf{I}_m^{A} = \boldsymbol{\alpha}_2 \mathbf{I}_m^{A} + \boldsymbol{\alpha}_1 \mathbf{I}_m^{B} \tag{C.7a), (C.7b)}$$

where

$$\boldsymbol{\alpha}_1 = \begin{bmatrix} \alpha_{11} & & \\ & \alpha_{12} & \\ & & \alpha_{1j} \end{bmatrix} \quad \boldsymbol{\alpha}_2 = \begin{bmatrix} \alpha_{21} & & \\ & \alpha_{22} & \\ & & \alpha_{2j} \end{bmatrix} \qquad \text{(C.8a), (C.8b)}$$

$$\alpha_{1j} = \frac{\tau Vel_j}{\ell} \cdot \quad \alpha_{2j} = 1 - \frac{\tau Vel_j}{\ell} \qquad \text{(C.9a), (C.9b)}$$

Appendix D Numerical Solution of the Ordinary Differential Equations

Applying the central finite differences method in (2.37a) and (2.37b) according to Fig. (2) and applying equation (B.13) for replacing the convolution terms in the points S and R (ψ_{mj}^{S} . ψ_{mj}^{R}) the next equations are obtained:

$$H_3 V_{mj}^{R} - H_4 V_{mj}^{A} + Z_K I_{mj}^{R} - Z_4 I_{mj}^{A} + \frac{\Delta x_j}{2}\left(\psi_{mj}^{A} + \psi_{mj}^{R'}\right) = 0 \qquad \text{(D.1a)}$$

$$H_3 V_{mj}^{S} - H_4 V_{mj}^{B} - Z_K I_{mj}^{S} + Z_4 I_{mj}^{B} - \frac{\Delta x_j}{2}\left(\psi_{mj}^{B} + \psi_{mj}^{S'}\right) = 0 \qquad \text{(D.1b)}$$

where

$$Z_3 = Z_W + \frac{\Delta x_j \tilde{R}_{Xj}}{2}, \quad Z_4 = Z_W - \frac{\Delta x_j \tilde{R}_{Xj}}{2} \qquad \text{(D.2a), (D.2b)}$$

$$H_3 = 1 - \frac{\Delta x_j Z_{wj} \tilde{G}_j}{2} \qquad H_4 = 1 + \frac{\Delta x_j Z_{wj} \tilde{G}_j}{2} \qquad \text{(D.3a), (D.3b)}$$

$$Z_K = Z_3 - \frac{\Delta t \, \Delta x_j}{2} \sum_{i=1}^{N} \frac{T_v^{-1} K_i p_i T_i}{1 + \Delta t \, p_i} \qquad \text{(D.4)}$$

$$\psi_{mj}^{S'} = -\sum_{i=1}^{N}\left[\frac{\psi_{mj}^{S-\Delta t}}{1 + \Delta t \, p_i}\right], \; \psi_{mj}^{R'} = -\sum_{i=1}^{N}\left[\frac{\psi_{mj}^{R-\Delta t}}{1 + \Delta t \, p_i}\right] \qquad \text{(D.5a), (D.5b)}$$

Variables V_{mj}^{A}, V_{mj}^{B}, I_{mj}^{A}, I_{mj}^{B} and ψ_{mj}^{A}, ψ_{mj}^{B} are calculated with the linear interpolation method of Lagrange as it was shown in section 2.2 and according at the appendix C. Substituting (C.6) and (C.7) in (D.1) and obtaining similar expressions for the convolution terms to (C.6), equations (D.1) in matrix form become:

$$\mathbf{H}_3\mathbf{V}_m^R + \mathbf{Z}_K\mathbf{I}_m^R = \mathbf{V}_{Hm}^A \tag{D.6a}$$

$$\mathbf{H}_3\mathbf{V}_m^S - \mathbf{Z}_K\mathbf{I}_m^S = \mathbf{V}_{Hm}^B \tag{D.6b}$$

where

$$\mathbf{V}_{Hm}^A = \mathbf{H}_4\left(\alpha_2\mathbf{V}_m^A + \alpha_1\mathbf{V}_m^B\right) + \mathbf{Z}_4\left(\alpha_2\mathbf{I}_m^A + \alpha_1\mathbf{I}_m^B\right) - \frac{\Delta x_j}{2}\left(\alpha_2\boldsymbol{\Psi}_m^A + \alpha_1\boldsymbol{\Psi}_m^B\right) - \frac{\Delta x_j}{2}\left(+\boldsymbol{\Psi}_m^{R'}\right) \tag{D.7a}$$

$$\mathbf{V}_{Hm}^B = \mathbf{H}_4\left(\alpha_1\mathbf{V}_m^A + \alpha_2\mathbf{V}_m^B\right) - \mathbf{Z}_4\left(\alpha_1\mathbf{I}_m^A + \alpha_2\mathbf{I}_m^B\right) + \frac{\Delta x_j}{2}\left(\alpha_1\boldsymbol{\Psi}_m^A + \alpha_2\boldsymbol{\Psi}_m^B\right) + \frac{\Delta x_j}{2}\boldsymbol{\Psi}_{mj}^{S'} \tag{D.7b}$$

being $\mathbf{V}_{Hm}^A$ and $\mathbf{V}_{Hm}^B$ the "history terms" delayed a travel time.

Appendix E Published Work

J. C. Escamilla, P. Moreno, José L. Naredo "*A New Model of Multiconductor Transmission Lines for Time Domain Transient Analysis*", Paper submitted to the 14th International Conference on Harmonics and Quality of Power (ICHQP2010) in Bergamo, Italy September 26-29, 2010.

J. C. Escamilla, P. Moreno, E. Cruz "*A New Approach for Modeling Multiconductor Transmission Lines with Constant Electrical Parameters*", North American Power Symposium (NAPS2010) in Texas, USA September 26-28, 2010.

J. C. Escamilla, P. Moreno, P. Gomez "*A New Model for Overhead Lossy Multiconductor Transmission Lines*", Paper in review, IET Generation, Transmission and Distribution.

CENTRO DE INVESTIGACIÓN Y DE ESTUDIOS AVANZADOS DEL I.P.N.
UNIDAD GUADALAJARA

El Jurado designado por la Unidad Guadalajara del Centro de Investigación y de Estudios Avanzados del Instituto Politécnico Nacional aprobó la tesis

Un nuevo enfoque en el Modelado de Líneas de Transmisión Multiconductoras para el Análisis de Transitorios en el Dominio del Tiempo

A New Approach for Modeling Multiconductor Transmission Lines for Time Domain Transients Analysis

del (la) C.

Juan Carlos ESCAMILLA SÁNCHEZ

el día 07 de Diciembre de 2012.

Dr. Pablo Moreno Villalobos
Investigador CINVESTAV 3C
CINVESTAV Unidad Guadalajara

Dr. José Luis Alejandro Naredo Villagrán
Investigador CINVESTAV 3C
CINVESTAV Unidad Guadalajara

Dr. José Raul Loo Yau
Investigador CINVESTAV 3A
CINVESTAV Unidad Guadalajara

Dr. José Alberto Gutiérrez Robles
Profesor Investigador Titular C
Universidad de Guadalajara

Dr. Pablo Gómez Zamorano
Profesor Investigador
IPN